

A Bayesian Approach to The Assessment of Fuel Composition Variability Effects
on Grate-bed Biomass Combustion

Mohammad Hosseini Rahdar

A Thesis
In the Department
of
Building, Civil and Environmental Engineering

Presented in Partial Fulfillment of the Requirements
For the Degree of
Doctor of Philosophy (Building Engineering) at
Concordia University
Montreal, Quebec, Canada

September 2020

© Mohammad Hosseini Rahdar, 2020

CONCORDIA UNIVERSITY
School of Graduate Studies

This is to certify that the thesis prepared

By: Mohammad Hosseini Rahdar

Entitled: A Bayesian Approach to The Assessment of Fuel Composition Variability
Effects on Grate-Bed Biomass Combustion

and submitted in partial fulfillment of the requirements for the degree of

Doctor Of Philosophy (Building Engineering)

complies with the regulations of the University and meets the accepted standards with respect to originality and quality.

Signed by the final examining committee:

_____	Chair
Dr. Rajamohan Ganesan	
_____	External Examiner
Dr. Shahab Sokhansanj	
_____	External to Program
Dr. Hoi Ng	
_____	Examiner
Dr. Fariborz Haghighat	
_____	Examiner
Dr. Chunjiang An	
_____	Thesis Supervisor (s)
Dr. Fuzhan Nasiri	

Dr. Bruno Lee	

Approved by _____

Dr. Ashutosh Bagchi Chair of Department or Graduate Program Director

Sep-23-2020

Date of Defense

Dr. Mourad Debbabi Dean of Gina Cody School of Engineering and Computer
Science

Abstract

A Bayesian approach to the assessment of fuel composition variability effects on grate-bed biomass combustion

Mohammad Hosseini Rahdar, Ph.D.

Concordia University, 2020

Combustion systems are the most energy-intensive facilities in the world. They are responsible for releasing the majority of the greenhouse gases (GHG) and NO_x into the earth's atmosphere. Biomass is the only renewable energy source consisting of fixed carbon elements which can be substituted for fossil fuels in combustion systems. The main distinction between biomass and fossil fuel combustion is fewer pollutant emissions of biomass combustion, as well as, biomass combustion's lower price and simpler storage facility. So far, direct combustion of the solid biomass is the most popular method, both thermally and economically, among all various bioenergy systems, which is due to the price of biofuels process cost. Grate firing technology is of interest to burn solid biomass because it has less sensitivity to feed composition and size, which shows the excellent potential of this technology. However, owing to the intrinsic composition variability of biomass, there are still uncontrolled deflections associated with biomass combustors operations.

This study is an effort to quantify the overall impact of fuel compositions variability on moving bed biomass combustion, which will facilitate the understanding of biomass combustion. Randomly selected biomass pellets were individually investigated via a Thermogravimetric Analysis (TGA) to specify the fuel compositions; moisture, volatile, char, and ash. This data, together with the predefined fuel composition provided by fuel supplier are utilized to train a model using a Bayesian approach to populate our measured data. Simultaneously, a 1D transient numerical model of moving bed biomass combustion is deliberately developed corresponding to the research goals. The model iteratively runs with distributed fuel composition made by the Bayesian data generator and simulates the combustor under uncertain conditions. The comprehensive thermo-economic and environmental analysis of the biomass boiler operated with the three most common biomass types was conducted. Specifically, this includes biomass pellets, wood waste, and municipal solid waste and through this research showed that biomass pellets are the most efficient in terms of thermal operation and financial revenue. An experiment-based approach to the composition uncertainty impact of biomass pellets and bamboo chips on moving bed combustors were also practiced. While a notable heat flux deviation from mean operation conditions was observed for both, the pelletizing helped pellets to limit the level of uncertainty to a satisfying degree. Higher char content can limit the combustion uncertainty

to a strong extent, while the moisture content was found to be the main contributor to the level of uncertainty. As well, NO_x emission arising from biomass combustion fluctuated up to 17% due to composition variability. Finally, combustor operations under more reliable input data via the Bayesian data generator showed a remarkable system deviation from that of predefined input conditions. Overlooking the fuel compositions variability caused an overestimation of heat generation of up to 8.5%. Moreover, a notable amount of unburned biomass particles was sent to an ash bin, which is not in line with biomass harvesting sustainability. To avoid this in the future, the system must be regulated to correspond to the fuel compositions offered by the Bayesian model.

Acknowledgments

I would like to convey appreciation and sincere gratitude to those who supported and encouraged me throughout the completion of this research. First, I acknowledge the outstanding leadership, guidance, understanding and supports received by my co-advisor, Dr. Fuzhan Nasiri. His combined expertise in Energy System Engineering, Reliability Analysis, and Sustainability is exemplary and without him, this thesis could not be started and completed.

Second, I would like to express my particular respect and thanks to my co-advisor Dr. Bruno Lee for his direct help and support, and constructive feedback with which all significant and vital parts of the research were only possible.

I would also like to thank the committee members, Prof. Fariborz Haghighat, Prof. Hoi Dick Ng, Dr. Chunjiang An, Prof. Shahab Sokhansanj for their valuable advice and remarks which directed me through developing the research objectives, findings, and representation. I thank all the *Sustainable Energy & Infrastructure Systems Engineering* (SEISE) team members, past and present, who have enriched the research by their valuable discussions and comments during our weekly meetings. Special appreciation should be presented to colleagues and friends for the support received from: Dr. Mohammad Heidari, Ms. Parisa Ghaneifar, Mr. Mohammad Bitarafan, Ms. Elnaz Ghanbari, Ms. Leila Norouzi, Mr. Soroush Ebadi, Mr. Nima Bonyadi, Ms. Elham NarengiFar, Mr. Ata Hosseini, Ms. Vero Moreno, and Majo Rosero.

I would like to acknowledge the financial support received as Concordia International Tuition Award of Excellence from Concordia University. In addition, I thank NSERC and BMA Ltd. for funding the research on the biomass boiler maintenance planning.

Finally, I would like to extend my heartfelt gratitude to my family, nearest, and dearest people: My mother Zahra Rafiee, My father's soul Kheiroallah, sisters, Mahnaz, Leila, Forough and Elham, my brother Farzad, nephews, Saeid, Mahyar and Mehdi, brothers-in-law Mohammad and Rouzbeh, and my sister-in-law Leila.

List of Publications

This dissertation is formed based on scientific papers written to meet the PhD project objectives set during the research to advance scientific and industrial goals. Most of the details of this study are comprised of the papers below and therefore the submitted manuscript should be aimed only as a summary of the overall research. This study is the outcome of my research as a PhD student at the Department of Building, Civil, and Environmental Engineering, Concordia University, Montreal, Canada, and has resulted in five journal papers and one conference paper listed below:

Journal papers:

Paper 1 A Review of Numerical Modeling and Experimental Analysis of Combustion in Moving Grate Biomass Combustors. Mohammad Hosseini Rahdar, Fuzhan Nasiri, Bruno Lee, *Energy & Fuels*, 2019, 33 (10), 9367–9402

Paper 2 Effect of fuel composition uncertainty on grate firing biomass combustor performance: A Bayesian model averaging approach. Mohammad Hosseini Rahdar, Fuzhan Nasiri, Bruno Lee, *Biomass Conversion and Biorefinery* (2020), 86

Paper 3 Availability-based predictive maintenance scheduling for vibrating-grate biomass boilers. Mohammad Hosseini Rahdar, Fuzhan Nasiri, Bruno Lee, *Safety and Reliability*, 2020, 39 (2), 165-187

Paper 4 Exploring Operation Adaptation of Moving Bed Biomass Boiler Under Different Waste Fuel Conditions. Mohammad Hosseini Rahdar, Fuzhan Nasiri, Bruno Lee. Submitted, *Journal of Cleaner Production*

Paper 5 Uncertainty Quantification of Biomass Composition Variability Effect on Moving Grate Bed Combustion: An Experiment-based Approach. Mohammad Hosseini Rahdar, Bruno Lee, Fuzhan Nasiri, *Energy & Fuels*, 2020, 34 (8), 9697-9708

Conference paper:

Paper 1 Optimal Maintenance Plan for A Vibrating-Grate Biomass Boiler: Availability and Cost Saving Approach, Mohammad Hosseini Rahdar, Fuzhan Nasiri, Bruno Lee. Published, CSCE-Laval (2019)

Table of Contents

List of Figures.....	ix
List of Tables.....	xi
List of Symbols.....	xv
1 Introduction.....	1
1.1 Motivation.....	1
1.2 Problem statement, objectives, and contributions.....	2
1.3 Key assumptions.....	5
2 Literature Review.....	7
2.1 Modeling and numerical simulation.....	7
2.1.1 Classification of the moving grate combustor models.....	8
2.1.2 Degradation sub-processes.....	13
2.1.3 Mathematical modeling specification.....	23
2.1.4 Biomass physical properties.....	24
2.1.5 Overbed modeling.....	28
2.2 Experiments.....	30
2.3 Uncertainty estimation methods.....	34
2.3.1 Probabilistic approach.....	35
2.3.2 Bayesian method.....	36
2.4 Research gaps.....	37
3 Fuel Compositions and Bayesian Method.....	40
3.1 Bayesian method.....	40
3.2 Experiment on biomass fuels.....	41
3.3 Uncertainty estimation.....	44
4 Numerical Modeling of Combustion.....	46
4.1 Background.....	46

4.2	Conversion process.....	48
4.2.1	Drying.....	48
4.2.2	Pyrolysis and decomposition.....	49
4.2.3	Char oxidation and gasification.....	50
4.3	Gas phase reactions.....	53
4.4	Solution algorithm.....	54
5	Results and discussion.....	56
5.1	Model validation.....	56
5.2	Summary of the results.....	57
5.2.1	Comparative analyses of variant types of biomass in grate bed boiler.....	57
5.2.2	Experiment-based analysis of composition variability effects on biomass combustion.....	67
5.2.3	Bayesian approach to composition variability effect on biomass combustion.....	76
5.2.4	An improved predictive maintenance plan for a vibrating-grate biomass boiler.....	83
6	Conclusion and future works.....	94
6.1	Summary.....	94
6.2	Contributions.....	94
6.3	Key Findings.....	95
6.4	Future works.....	97
	Appendix I.....	109
	Appendix II.....	110

List of Figures

Figure 1. Research methodology.....	6
Figure 2. Schematic of a moving grate biomass boiler with the secondary and tertiary feeding air system	7
Figure 3. Modeling approach in the interaction of the bed and overbed for moving grate biomass combustor	8
Figure 4. Continuous medium versus particle resolved approach in the moving grate combustor	12
Figure 5. Biomass particle conversion processes including drying, Devolatilization, and char oxidation	13
Figure 6. Drying kinetic coefficient rate at the vicinity of evaporation temperature	15
Figure 7. Devolatilization constant rate used through different research.....	18
Figure 8. Schematic of char surface reaction of a biomass particle with the free gas stream.....	20
Figure 9. Scheme of the grate bed biomass furnace modeling	30
Figure 10. Schematic of a batch type laboratory-scale biomass furnace	31
Figure 11. Diagram of Bayesian modeling implementation.....	40
Figure 12. TGA device setup for biomass composition experiment.....	42
Figure 13. Prior, likelihood and posterior distribution of (a) moisture content, (b) volatile matter, and (c) char based on Bayesian model	45
Figure 14. Schematic of the moving grate biomass combustor with the reacting fuel bed.....	46
Figure 15. Modeling perception in terms of continuous medium approach in a moving grate combustor; (a) heat transfer mechanisms within the bed, (b) process simulation in walking column	47
Figure 16. A simplified biomass bed conversion perspective.....	48
Figure 17. Devolatilization and char reaction mechanisms	49
Figure 18. Solution algorithm of biomass combustion integrated with uncertainty model in terms of composition variability.....	55
Figure 19. Validation of the model versus the experiments; (a) Ref [68], (b) [234].....	56
Figure 20. Contour of solid temperature for combustion of: (a) biomass pellets, (b) wood waste, (c) RDF	60
Figure 21. Mass loss (dashed-line) and temperature evolution (solid line) profiles of the three fuels	61
Figure 22. Volumetric concentration of emitting gases from fuel bed	61
Figure 23. Life cycle cost contribution for 30 kW biomass boiler; C_c : capital cost, C_{el} : electricity cost, C_{mun} : maintenance+unseen cost, C_f : fuel cost.....	64
Figure 24. System boundary for the LCA implementation	65
Figure 25. Proportion of three key contributors to the greenhouse gases for each feeding fuel	66
Figure 26. Ignition speed versus different amount of air flow rate for bamboo and wood pellet	68
Figure 27. Solid temperature evolution versus composition variability over the fuel bed conversion process	69
Figure 28. Distribution of heat production under fuel composition variability	70
Figure 29. Effect of fuel composition variability on the heat generation for bamboo chips and wood pellet combustion	70
Figure 30. Effect of fuel composition uncertainty on the flame temperature, mass conversion rate, and ignition rate ..	71
Figure 31. Straight correlation of ignition rate and heat generation in the biomass combustion.....	72
Figure 32. Mole fraction of outflowing gas species from biomass bed conversion.....	73

Figure 33. Nitrogen precursors yield over the biomass combustion in the moving grate bed boiler; (a) NH ₃ and HCN (b) NO generation	75
Figure 34. Temperature contour of the biomass fuel bed in (a) 1 st scenario (b) 2 nd scenario	77
Figure 35. Bed surface temperature evolution over the fuel bed conversion process	78
Figure 36. Molar mass of emitting gases from particle conversion for first and second scenarios	78
Figure 37. Produced heat fluctuation respect to fuel composition uncertainty in biomass boiler	79
Figure 38. correlation between fuel compositions variability and ignition rate, conversion rate and flame temperature	80
Figure 39. Heat generation from biomass combustion in the grate-firing combustor for various scenarios	81
Figure 40. GHG contributors' breakdown for each scenario	83
Figure 41. System configuration and instrument diagram of a 750 kW vibrating grate biomass boiler	85
Figure 42. The model overview and interface of tools	85
Figure 43. The fault tree analysis of serious incident of the vibrating biomass boiler	89
Figure 44. Optimization algorithm including two separate loops (Bottom-loop and Top-loop) for maintenance scheduling	91
Figure 45. List of components based upon the maintenance effect corresponding to the fault tree analysis	91
Figure 46. Optimal maintenance plan of the biomass boiler components	93

List of Tables

Table 1. Objectives, methodology and solution platform of biomass combustors modeling in literature	9
Table 2. Model classification of current literature in terms of different modeling approaches	10
Table 3. Classification of bed modeling based on the resolution scale	11
Table 4. Kinetic rate coefficient and activation energy of drying rate Arrhenius model	15
Table 5. Devolatilization rate coefficients for the Arrhenius model.....	18
Table 6. Kinetic and diffusion factors of char reaction rate	21
Table 7. Summary of shrinkage model and corresponding factors	23
Table 8. Description of general conservation equation coefficients for each sort of equation.....	23
Table 9. Specific heat capacity employed for various biomass fuel	26
Table 10. Effective thermal conductivity models for biomass fuels	27
Table 11. Overall governing equation; gas and solid phases	28
Table 12. Homogeneous gas phase reactions originated from fuel bed conversion.....	29
Table 13. Classification of experimental works according to measurement usage	31
Table 14. Experimental works on the grate type biomass combustion system; objectives and results	33
Table 15. Temperature evolution progress in the TGA experiment	42
Table 16. Measured compositions (Moisture, volatile, carbon and ash).....	43
Table 17. Declared primary biomass pellet characteristics by supplier	44
Table 18. Mean and standard deviation for moisture, volatiles and char composition	45
Table 19. Arrhenius kinetic rate of devolatilization and char combustion	49
Table 20. Reaction heat of evaporation, pyrolysis, and char oxidation	51
Table 21. Arrhenius kinetic rate of devolatilization and char combustion	52
Table 22. Conservation equations regarding the solid and gas phase of fuel packed bed conversion	52
Table 23. Fuel properties and stoichiometric air-fuel ratio	58
Table 24. Primary air distribution of biomass combustor for different fuels	59
Table 25. Operational characteristics of the heating system for each fuel	62
Table 26. List of breakdown costs for biomass boiler heating system.....	63
Table 27. Economic analysis conclusion for the system under different fuel conditions	64
Table 28. Input data for LCA respecting biomass pellet, wood waste and RDF individually	65
Table 29. Results of life cycle impact analysis for the heating system fed with proposed fuels	66
Table 30. Statistical analysis of bamboo chips and wood pellets	67
Table 31. Reactions used in modeling of NO _x precursor formation	74
Table 32. Scenarios of system performance evaluation	76
Table 33. Input data for LCA analysis; first, second biomass scenario and coal-fueled case.....	81
Table 34. LCA results of proposed scenarios based upon characterization indicator.....	82
Table 35. failure modes and potential failure effects of asset components	86

Table 35. Components characteristics regarding failure distribution and maintenance time 109

Thesis Outline

This dissertation is a compilation of scientific articles based on the PhD project objectives that were set to proceed with scientific and industrial goals. The main body of the thesis comprises 6 chapters, which are described below.

Chapter 1

Introduction: This chapter presents the motivation, problem statement, and objective of this PhD research on fuel composition variability effect on moving grate biomass combustors.

Chapter 2

Literature review: This chapter aims to provide a better understanding of the moving grate biomass combustors from aspects of modeling and experiment, and in the last part uncertainty analysis methods are introduced. The chapter discusses the recent research progress, gaps, and new ideas for future work.

Chapter 3

Fuel composition and Bayesian method: This chapter aims to quantify the fuel compositions variability taking the advantages of the Bayesian probabilistic method. A description of the uncertainties method is given with a focus on the Bayesian method. In a laboratory, a set of randomly selected fuel particles are tested to gather the particle compositions data, and in the combination of measured data and declared values by fuel supplier, the Bayesian model is formed. Thanks to our Bayesian model, the uncertainty interval of fuel compositions is provided and can be applied in the numerical model.

Chapter 4

Numerical modeling of combustion: This chapter describes the numerical model for moving grate biomass combustion. First, the boundary of the intended system is defined followed by chosen mathematical models of conversion sub-processes; drying, devolatilization, and char combustion. Initial and boundary conditions of the bed are deliberately described. Finally, the combustion model is integrated with fuel composition uncertainty, and the solution algorithm is introduced.

Chapter 5

Results and discussion: In this chapter, after validation of the model, the results of the research are presented in three sections. In the first section, the model is employed to evaluate the biomass boiler's operation under the three most common fuels from thermal, economic, and environmental views. In the next section, the variability of fuel composition is measured via the TGA experiment, and the relevant standard deviation is governed in the model to gauge combustion uncertainty for two different biomass fuels; bamboo chips and biomass pellets. In the last section, the developed Bayesian model is applied in order to take advantage of prior fuel data in addition to the measured data so that the operational system deflection from the theoretical one is addressed.

Chapter 6

Conclusion and future works: The main conclusions of this research are highlighted here together with achievement and contribution by this study. Some possible improvements in this work as well as potential research areas in this field are recommended for future works.

List of Symbols

Nomenclature

A_i	pre-exponential factor (s^{-1})
A_{sp}	particle surface area (m^2)
Bi	Biot number
C_p	specific heat ($J\ kg^{-1}\ K^{-1}$)
C_m	moisture concentration ($kg\ m^{-3}$)
d	equivalent diameter (m)
D	diffusivity of the species in the mixture ($m^2\ s^{-1}$)
E_i	activation energy ($J\ mol^{-1}$)
f	Shrinkage factor (-)
h	convection coefficient ($W\ m^{-2}\ K^{-1}$)
H	enthalpy ($J\ kg^{-1}$)
h_m	mass transfer constant ($m\ s^{-1}$)
k	kinetic rate (s^{-1})
k_d	diffusion kinetic rate (s^{-1})
k_r	chemical kinetic rate (s^{-1})
LH	latent heat ($J\ kg^{-1}$)
M_C	carbon molecular weight ($kg\ kmol^{-1}$)
\dot{m}	Mass flow rate ($kg\ m^{-3}\ s^{-1}$)
p	Probability (-)
P_{O_2}	Oxygen partial pressure (pa)
R	ideal gas constant ($J\ K^{-1}\ mol^{-1}$)
S	source term ($W\ m^{-3}$)
S_p	particle surface (m^2)
Sh	Sherwood number (-)
t	time (s)
T_{evap}	evaporation temperature (K)
T_g	gas temperature (K)

T_s	solid temperature (K)
v_g	gas velocity (m s^{-1})
Y	mass fraction (kg/kg)

Greek symbols

ϕ	bed void fraction (-)
ρ	density (kg m^{-3})
ϵ	particle porosity (-)
Ω_c	stoichiometric coefficient of the char oxidation (-)
σ	Stefan Boltzmann coefficient ($\text{W.m}^{-2} \text{K}^{-4}$)
λ	thermal conductivity ($\text{W.m}^{-1} \text{K}^{-1}$)
ω	emissivity

Subscripts

C	carbon
dry	drying
g	gas
$mois$	moisture
s	solid
V	volatile
vol	volatile
0	initial state
Y	Mass fraction

1 INTRODUCTION

This chapter presents the motivation, problem statement, and objective of this PhD research on the effects of fuel composition variability on moving bed biomass combustors.

1.1 Motivation

Today, due to climate change threats and the insecurity of energy supplies worldwide many types of research projects are defined to diversify energy supply resources and to create more sustainable and efficient energy systems. It is imperative to take advantage of renewable energies to support growing global energy demands, as well as, to limit threats that our global environment currently faces. Combustion systems are of the most energy-intensive systems, which are the largest source of pollutant emissions in the industry. Among all types of renewable energy, biomass, in different forms (solid, liquid or gas), is the only renewable energy with a source of fixed carbon elements that can be substituted for fossil fuels in the combustion systems [1]. The key difference of biomass combustion against fossil fuel combustion is identified as the fewer pollutant emissions from biomass, besides its lower price and simpler storage method in the case of solid fuels. Recall that the carbon emissions are released as much as they are absorbed by the sourcing plants [2,3]. This is a significant reason for conducting more research within the scope of biomass conversion that could considerably help to move away from using the combustion systems, and move toward more sustainable energy supplies. Nevertheless, the thermochemical conversion of biomass in contrasted with traditional fossil fuels especially gases and liquids, and deals with ambiguous processes, e.g., pyrolysis and char combustion [4,5]. Despite a lot of development in the biofuel industry, the direct combustion of biomass particles is still regarded as having commonly high biofuel processing costs [6–10]. Currently, there are different types of biomass incinerators, namely fixed-grate, moving grate, pulverized blast, and fluidized-bed furnace [11]. Grate firing technology is of interest to burn solid biomass because of its decreased sensitivity to feed composition and the demanded size of particles [12–14]. Despite the lower combustion efficiency of the grate-firing biomass furnaces compared to the fluidized bed type, there is greater adaptability to (1) the various fuel types; (2) the possibility to be manufactured on a smaller scale; (3) less complexity in terms of the engineering and maintenance; and (4) the lower capital cost. In addition, the market appeal for these types of systems has been rising. Likewise, this technology is increasingly approaching the district heating system due to the fact that it can be economically manufactured from small-scale to large-scale, as well as fuel that can be simply stored and locally supplied.

Growing market claims toward biomass fuels due to the policy set on fossil fuel consumption and that of emission restrictions forces engineers to increasingly work on the optimization of the fixed-bed biomass

combustors which can deploy different sorts of particles such as chips, pellets, logs, and municipal solid waste. Although the moving grate biomass combustion technologies are already running in different industries, they have not yet been accounted for as a fully developed technology due to some performance deficiencies, such as low combustion efficiency, contaminant emissions, and combustion instability. Uncontrolled deflection of grate-firing biomass combustors from the design operating point is one of the most problematic issues associated with these systems to date. Generally, the experimental and numerical methods are approached in order to study the modification of biomass combustors. The experimental methods are expensive and they have some physical restrictions, while numerical modeling is a less expensive and more flexible practice that can effectively save time. Still, this needs experimental results for validation [15]. Taking both accuracy and the cost of practice into the account, numerical modeling of the fuel bed is the most reliable way to quantify deflections of the biomass combustion properties under variable initial and boundary conditions.

1.2 Problem statement, objectives, and contributions

As previously mentioned, there are some areas for grate-firing biomass combustors that have not been thoroughly examined. In order to drive the direct biomass combustion technologies towards a more well-developed industry, it is important to minimize system unreliability to a great extent. An in-depth examination of the literature reveals that grate biomass furnaces suffer from fluctuating and lagging operations that have originated from the uncontrolled deviation in functional characteristics of the system and fuel feeding properties. One problematic feature of the proposed systems that have not been addressed so far is the feeding of the fuel compositions variability. Overlooking the uncertainty in feeding compositions results in fluctuating operation and consequently a greater source of deficiency in the system. Furthermore, the sensitivity analysis of fuel compositions cannot always be valid and can create misleading results since changing one biomass composition means a change in other compositions. Therefore, an uncertainty analysis is needed. Up until now, fuel composition variability is almost always discounted for in the biomass combustion analyses, while it has been quantified for some other modes of fuel combustion, e.g., biogas and nuclear combustion. Thanks to the fuel elements sampling devices such as the TGA device, the uncertainties of raw fuels fed to the system are more accountable.

This research, firstly, quantifies the effect of biomass compositions variability on combustion properties. Next, operation adaptation for a small biomass boiler under different biomass fuel conditions is presented, and the economic, environmental consequence of fuel switching is pinpointed. Lastly, a preventive maintenance plan is proposed for a more efficient maintenance program of a vibrating grate biomass boiler. To conduct this, we will employ different tools and finally, integrate them in such a way to provide the

intended research aims. Figure 1 shows the flowchart of the governed tools and their relevant interlinks in order to deliver the proposed objective of the research.

Based on the stated objective in this research, the following contributions will be expected:

- A comprehensive literature review study on modeling and an experiment of the moving bed biomass combustors, as well as on the uncertainty methods.

Approach: After forming the subdivisions of this review work, Google Scholar and Scopus were applied to obtain the documents based on keywords. For paper management aims and to keep track of them, a citation software called Mendeley was utilized. Based upon the subdivisions, several folders were made and in each of them, the related papers were stored. About 500 documents were collected by this searching method. The first action for filtering the articles was reading the abstract. Therefore, some of the irrelevant ones were detected and eliminated. Creating the main summary of the importance of these papers helped to avoid an overlap of reading later on in the research process. The filtering in this step decreased the papers to approximately 250. Finally, by reading through the selected articles for each subdivision, the consecutive parts of the current manuscript were created.

- Delivering a novel methodology that counts fuel compositions variability into the biomass combustion properties.

Approach: To quantify the biomass particle compositions uncertainty, a sufficient amount of fuel composition sampling was required. Since the TGA experiment was time-consuming, a limited amount of 30 biomass pellets was examined based on the fact that T-distribution, which is used for small data, becomes quite similar to Gaussian distribution for 25 samples above. Having pre-defined fuel composition values provided by the fuel supplier, which were not necessarily equal or close to the measured values, allowed us to take advantage of the Bayesian method to reliably populate the data to a great extent. In an iterative way, a massive data set was formed and distribution of moisture, volatiles, char, and ash content was made.

- Synchronizing moving bed biomass combustors using a developed combustion model in such a way to avoid incomplete fuel conversion.

Approach: a 1D transient numerical model of moving bed biomass combustion was built up employing the most appropriate mathematical models for moisture evaporation, devolatilization, and char burnout. Although the geometry of the bed is in 2D, due to the negligible gradient of reactions in the horizontal direction, a 1D walking column approach was taken in this research. The model can simulate the

combustion process for every kind of biomass fuel in detail so that the system can be easily synchronized under each certain fuel condition.

- Investigating the effect of biomass composition variation on system outputs for preprocessed and non-preprocessed fuel.

Approach: The biomass combustion model and uncertainty model are the tools needed for this purpose, yet an implementation platform is required to join these tools. In doing so, through a Python routine code an iterative solution script was written so that in each cycle of fuel conversion, new compositions were randomly selected. When a desirable amount of data was collected and stored in a data frame, the system operation susceptibility to composition variation was investigated.

- Analysis of economic and environmental impacts of biomass boiler utilization.

Approach: A small-scale 25kW biomass boiler was used for the economical examination. Net Present Value (NPV), Annual Cost (AC) and Internal Rate of Return (IRR) indices were used to gauge the relative economical privilege of three various fuels; biomass pellets, wood waste, and refuse-derived fuel (RDF). All details of boiler costs were considered, and the cost of biomass generated heat was compared with the rate of the US electricity grid. In the course of environmental analysis, SimaPro software, which is a well-known and robust life cycle analysis (LCA) tool was employed, and the North American database was applied. The LCA input data was provided from the model output, earlier literature, and from some logistic data.

- Proposing an optimal maintenance plan for vibrating-grate biomass boilers.

Approach: First, the critical components of the system were identified and classified. Using Failure Modes, Effects Analysis (FMEA), the criticality ranking of parts was determined. Since time-dependent failure rates were needed for mathematical calculation, Weibull regression was mapped over the constant failure data, and shape and intensity parameters were obtained. With the help of Fault Tree Analysis (FTA), a Reliability, Availability, Maintainability, Supportability, and implicitly Cost (RAMS+C) approach was practiced to analyze the proposed asset. Finally, a maintenance planning algorithm was proposed to reduce the maintenance cost while keeping the asset availability in the desired range.

The rest of the thesis is structured as follows: Chapter 2 presents the comprehensive literature review on the fixed bed biomass boilers in viewpoints of numerical and experimental analysis as well as uncertainty methods. Chapter 3, provides the Bayesian uncertainty model along with the fuel particles experiment for biomass compositions uncertainty estimation. Chapter 4 presents the numerical model for biomass fuel combustion in a moving bed combustor along with an integrated solution algorithm. In chapter 5, a paper-

based summary of results is presented and important conclusions from this research are discussed. And finally, chapter 6 concludes a summary of the study, contributions, and key findings followed by recommendations for future works.

1.3 Key assumptions

The following principal assumptions are made during this research:

- The reaction in the bed only occurs along the vertical direction.

Justification: Because of the low moving speed of solid fuel on the grate, primary air flow keeps the combustion front limited to the air flow direction. Therefore, the assumption of one-dimensional reaction instead of two-dimensional is quite valid.

- No air infiltration is accounted for in combustion properties calculation.

Justification: In practice, since the combustion chamber is not sealed in moving bed combustors, they are associated with air infiltration that causes the heat loss in combustors. In this way, the local climate of the operating system site can change the calculation results to a high degree. In this study, however, local climate condition is neglected for the sake of focusing on the effect of biomass composition variability on the system.

- Water vapor is not condensed inside the boiler.

Justification: when fuel moisture evaporates inside the combustor, water vapor absorbs some heat by means of latent heat. If the temperature of a part of the combustion chamber is less than water saturation temperature, this heat can be recovered inside the chamber, otherwise, the water vapor leaves the furnace stack. As there is not any zone in the proposed combustor with the temperature lower than the water saturation temperature, water vapor is not condensed inside the boiler.

- Ash content does not involve combustion modeling.

Justification: Ash content is an inorganic compound of biomass that remains at the end of combustion. It can get melted at a temperature around 1400 °C, yet this temperature never reaches in moving bed. In this study, ash content variability would be considered like other fuel compositions as they must be adding up to one, however, it will remain neutral throughout the combustion process.

- Biomass property variability is only associated with the composition.

Justification: Although the assumption of uniform size and constant porosity for biomass particles is not completely valid, the focus of this study is on fuel composition uncertainty. Therefore, to quantify

the effect of fuel composition variability on combustion properties, other aspects of uncertainty are overlooked.

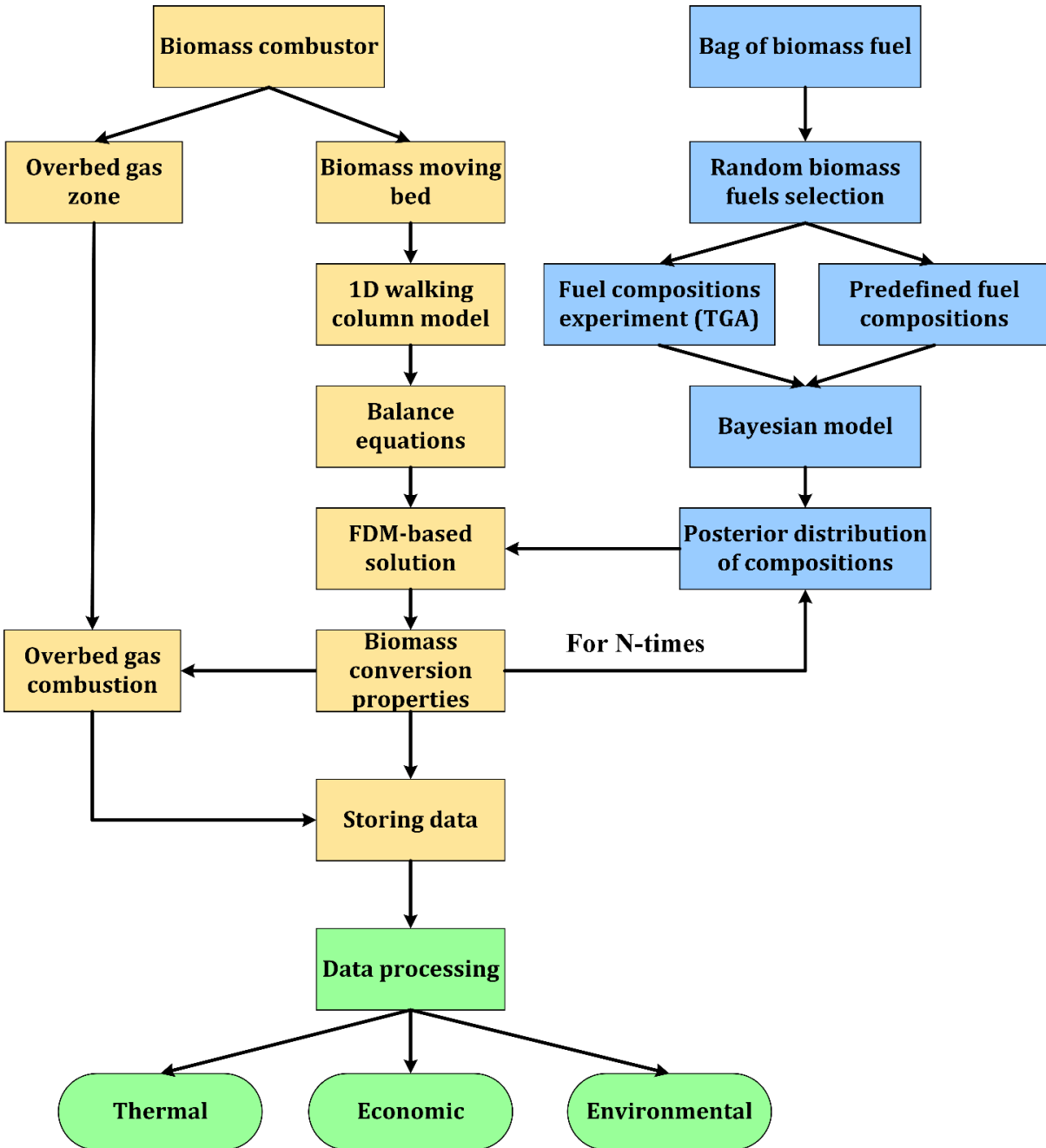


Figure 1. Research methodology

2 LITERATURE REVIEW

This chapter aims to provide a better understanding of the moving grate biomass combustors from aspects of modeling and experiment, and in the last part uncertainty analysis methods are introduced. The chapter discusses the recent research progress, gaps, and new ideas for future work.

A version of this chapter was published as: “Hosseini Rahdar, M.; Nasiri, F.; Lee, B. A Review of Numerical Modeling and Experimental Analysis of Combustion in Moving Grate Biomass Combustors. Energy & Fuels 2019”

2.1 Modeling and numerical simulation

Moving grate biomass combustors are the most typical sort of biomass combustion system worldwide. From the modeling viewpoint, combustion in a moving grate biomass furnace can be divided into two parts: solid fuel bed, and overbed gas combustion. As can be observed in Figure 2, the bed is a place for feed conversion, and this conversion highly depends on fuel quality and the primary air which flows underneath of the grate.

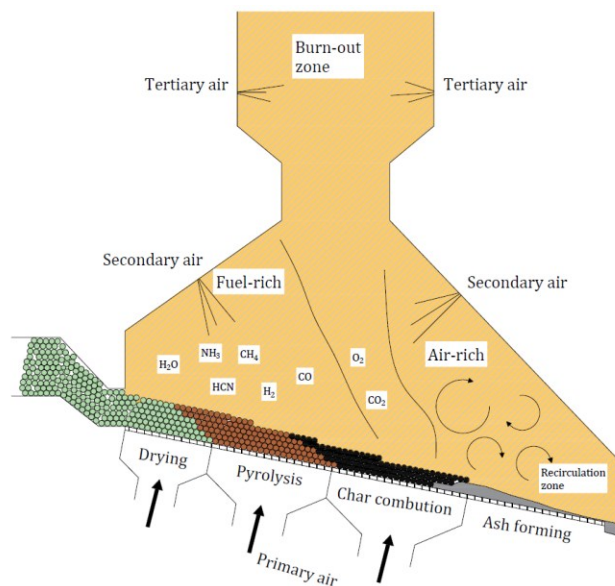


Figure 2. Schematic of a moving grate biomass boiler with the secondary and tertiary feeding air system

Here the fuel bed has the same functionality as the gas burner in the natural gas combustors. The fuel conversion inside the bed deals with various mechanisms consists of heat conduction between fuels and also between fuels and grate, heat convection between fuels and air, heat radiation from furnace walls to the fuels as well as between fuel particles, and mass transfer between solid and gas phase. more details about the fuel bed will be given in the next sections. On the other hand, overbed region (the yellow area in Figure 2) deals with the homogeneous gas reactions taking the secondary air and sometimes tertiary air to make the

combustion process complete. These two region interacts with each other continuously such that the species concentration, gas flow temperature and velocity from the fuel bed are received by overbed region as the boundary condition. Inversely, the radiation flux from the overbed region wall is contemplated as the bed boundary condition. Figure 3 schematically illustrates the interaction between the furnace bed and overbed zone.

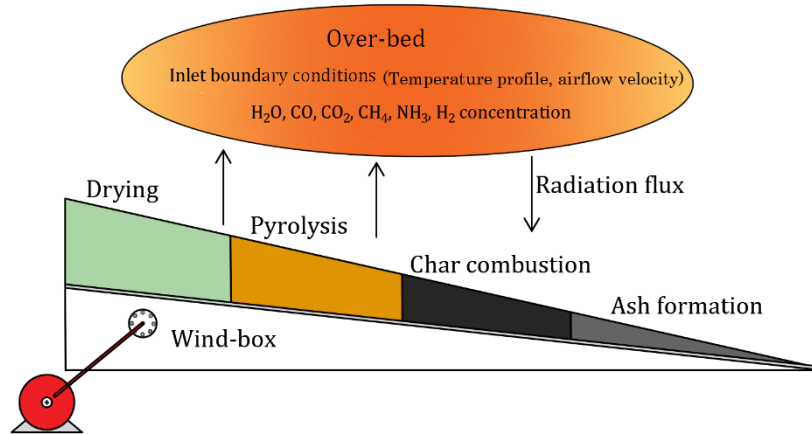


Figure 3. Modeling approach in the interaction of the bed and overbed for moving grate biomass combustor

2.1.1 Classification of the moving grate combustor models

Combustion of the grate firing biomass furnaces is generally modeled based upon the thermochemical reactions inside the fuel bed and the overbed [16,17]. These two zones are vigorously connected via the gaseous species released from fuel bed to the overbed and radiation flux from overbed walls to the fuel particles in the bed surface as is visualized in Figure 3. Combustion in the overbed region includes homogeneous gas reactions with turbulent flow regime which is predominantly responsible for pollutants emitted to the atmosphere. As the numerical modeling of the gas phase combustion has been documented well in the literature [18–20], the study here focuses on the fuel bed conversion. The numerical modeling of gas phase combustion will be briefly addressed in the last part of this section.

So many studies have been fulfilled on the biomass conversion evaluation in the fuel bed in order to understand the conversion process more precisely. It is not unrealistic if one says that the fuel bed conversion is the most key part of the whole biomass furnace modeling respect to this fact that without the precise results of bed model, it is unlikely to obtain credible outcomes from the overbed simulation. All complete/incomplete combustion in overbed and inside the bed, the formation of NO_x, SO_x, PM and CO, combustion efficiency and instability are influenced by the biomass conversion attitude inside the bed.

Take a delicate look at the papers in Table 1, the models can be grouped into three different approaches. The first approach which is a traditional approach integrates the bed and overbed zone in a single zone and

simulates the process of solid fuel conversion in a porous zone at the boundary of the furnace geometry along with the gas phase reaction simultaneously. This approach can be entirely modeled within commercial software such as Fluent or OpenFOAM. This method so-called porous media (traditional) is a numerical model which although is a non-expensive method, is not proper for sensitivity analysis of bed characteristics [21–25].

The second approach addresses the bed conversion on the measurement basis of the combustion system as a function of location in the fuel bed. Subsequently, the temperature and velocity of gases, as well as the species concentration inflowing the overbed, can be determined in terms of mass and heat balances between the fuel and primary air [26–37]. Although the experience-based method performance is highly prevailing in the analysis of the grate biomass boilers, it is an expensive practice by which it is not able to deliver the sensitivity analysis in order to evaluate the bed conversion process.

Table 1. Objectives, methodology and solution platform of biomass combustors modeling in literature

Modeling scale	Main objective	Methodology	Bed model numerical solution	Gas phase numerical solution	Ref
Single particle	To provide accurate drying and pyrolysis sub-models	Heat-mass balance around biomass particle	Compiled C-code in ANSYS Fluent	-	[38]
Single particle	To identify pyrolysis regime depends on external temperature, particle size and thermal wave regime	1D modeling of wet wood slab as porous solid using conservation equations	Second-order finite difference using Fortran code	-	[39]
Single particle	To investigate effect of ash fusion and particle size on burnout rate and char conversion rate	Single particle 1D modeling considering independent drying, pyrolysis, and char conversion	Fully implicit difference method using tridiagonal matrix method in MATLAB	-	[40]
Fixed bed	To evaluate impact of different packing factors on gasification	Biomass gasification modelled in a fixed bed for solid and gas phase separately	C++ subroutine through user defined functions (udfs)	ANSYS-Fluent simulation	[41]
Moving bed	To optimize the combustion process in biomass steam generator via air distribution modification	A commercial software was used to simulate the combustion process of gas phase	Based on experiments within the fuel bed	ANSYS-Fluent simulation	[22]
Moving bed	To assess using recycled flue gas in bed and overbed on boiler performance	Decoupled models; Empirical 1D model for conversion of waste wood and 3D numerical simulation for gas	Second-order upwind scheme implemented in MATLAB	3D steady CFD simulation on ANSYS-Fluent	[42]
Fixed bed	To study effect of various chemical compositions on combustion characteristics	Coupled interface of solid conversion model in UDF platform and gas phase model by commercial software	User defined subroutine of bed conservation equations	3D CFD model by AVL Fire	[43]
Single particle	To compare different evaporation models for different particle shapes	Heat-mass balance around single biomass particle	Transient conservation equations discretized based on numerical methods	-	[44]

The last approach in this category is the independent fuel bed model which simulates feeding conversion on top of the grate independent from the overbed zone. Then, the solution of the model will terminate the temperature, species concentration and the flow velocity, which embark on the gas combustion domain. The independent bed modeling is unique from the viewpoint of its capability to study the sensitivity of the feed conversion behavior to the particle size, moisture, density, effective thermal conductivity and specific heat value, primary air flow rate, the rate of heat and mass transfer [45–56].

According to Table 2, which classifies literature within the three modeling approaches together with their objectives and methodology, more researchers recently approach independent modeling. This can be attributed to the fact that the independent model contributes to bed modeling to some details that the experiments cannot reach in spite of the high practice cost .

In order to model the bed conversion independently, mass, energy, and species equations for the solid phase and the same equations plus the momentum equation for gas phase must be solved for the biomass feed, albeit comparison between literature shows discrepancies in equation’s terms. This can be explained by this fact that due to the complexity of the fuel bed, there always assumptions are engaged with the modeling or sometimes because of the certain objectives of the studies. In course of moving grate bed, it has often been assumed that the bed model to be a 1D unsteady model [45,57–59] such that a narrow fuel column is solved as a fixed bed conversion and then the effect of moving on the bed is contemplated by the elapsed time from bed entrance to the bed terminal. This approach can be fair taking low thermal gradient in the horizontal direction within the bed, while in more precise practices a 2D model reflects the horizontal heat transfer into the simulation [60–65]. From literature, the independent models can be classified according to the degree of bed homogeneity/inhomogeneity assumption to three principal classes encompassing: single-particle, continuous medium, and resolved particle as sorted out in Table 3.

Table 2. Model classification of current literature in terms of different modeling approaches

	Objective	Methodology	Ref
<u>Traditional method</u>	Present a 2D simulation to evaluate local value and shrinkage inside the bed	Fortran subroutines coupled with AVL Fire	[66]
	Analyze effect of various water temperature of domestic biomass boiler on the combustion variables	Mass and energy equation were coded in C-code and coupled to ANSYSFluent	[67]
	Providing a numerical aided design of a new wood log firedstove	An empirical model for wood log combustion was provided and numerical model for gas phase	[15]
	A 3D model of fixed bed reactor to analyze effect of different air flowrate	The bed was modelled as a porous zone within UDF was introduced to numerical code	[68]

	Studying heat-up, drying and pyrolysis of packed bed of large single particle and then deem packed bed as a finite number of particles	Conservation equations were discretized by FVM approach and coded into UDF	[69]
<u>Experience-based method</u>	Four different secondary air configurations and various primary air distribution were inspected to eliminate slagging problems and reduce emissions	Incinerator bed was measured to find temperature profile and species concentration as boundary conditions for ANSYS Fluent to simulate whole combustor	[23]
	Different baffle configurations inside the radiation shaft were investigated to eliminate existing recirculation zone	Based on experimental measurements, a mathematical model was developed using Fluent	[22]
	Improving thermal and environmental boiler performance by secondary air injection modification	A sample of fuel was screened and analyzed to specify heating value and chemical composition	[24]
<u>Independent method</u>	Potential of NO _x reduction and flue gas recirculation on combustion process was investigated	Bed was modelled with equilibrium calculation method (ECM) and boundary profiles was given to free board	[70]
	2D pyrolysis numerical model was developed to determine kinetic of wood particles pyrolysis in packed bed reactor	Three modes of heat transfer between particles were considered and governing equations were solved in FVM	[71]
	Mathematical model in terms of particle and reactor scale was made to consider details effects inside the bed	A Jacobian structure was used for solving the governing equation into BzzMath library	[72]

Table 3. Classification of bed modeling based on the resolution scale

Homogeneity degree	Governing equations	Dimensionality 0D/1D/2D/3D	Experiment	Model type		Sub-process			Emission	Ref
				Standalone	Porous zone	Drying	Pyrolysis	Char oxidation		
Single-particle	Mass/ Energy	1D	✓	✓	×	✓	✓	✓	×	[73]
	Energy	1D	×	✓	×	✓	✓	✓	×	[74]
	Species/ Energy	0D	×	✓	×	×	×	✓	×	[75]
Continuous medium	Species/ Energy	1D	✓	✓	×	×	✓	✓	×	[76]
	Mass/Energy/Species	3D	✓	×	✓	✓	✓	✓	×	[77]
	Mass/Energy/Species	3D	✓	×	✓	✓	✓	✓	×	[78]
Resolved particle	Mass/Energy/Species	1D	×	✓	×	✓	✓	✓	×	[72]
	Species/ Energy	2D	×	✓	×	×	✓	×	×	[71]
	Mass/Energy/Species	1D	✓	✓	×	✓	✓	×	×	[69]

2.1.1.1 Single-particle model

Although the biomass furnace bed is a solid-gas phase reacting zone, a homogeneous bed model presumes the biomass packed bed to be a single phase so that air and solid particles' thermal properties are aggregated into one equation or on the other words, both phase is assumed to have an equal temperature. Chemical reaction mechanism dominates the conversion in this method and the results of the single biomass particle model extend to the whole bed [4,40,41,46,75,79–92]. In course of the bed modeling of the grate bed

combustors, this method would not provide the precise outcomes as in reality the particles inside the bed have different boundary conditions, while this model can perform much better for fluidized bed modeling.

2.1.1.2 Continuous medium model

This simulation approach treats the biomass packed bed on a macro-scale that reckons the particles in the bed cell as a unified medium with same thermal and chemical properties regardless of the various shape and size of the particle in the bed, the identical shapes are employed for the particle with high aspect ratio [93]. In fact, this assumption is much fair for thermally thin particles. The temperature and element concentration gradient inside the particle is neglected together with conduction terms in both the solid and gas phase. It is supposed that reaction heat is generated throughout the solid phase and the heat transfer coefficient plays the role of heat carrier between two phases. In some articles [94,95] the continuous medium packed bed was put into the practice to model the large particles combustion process. This macroscopic approach of modeling against the microscopic approach of single-particle modeling does not need of precise arrangement of interface boundaries. It also prescribes conversion processes through continuous media with reference to differentiable parameters which facilitates the mathematical analysis. It is necessary to be noted that these benefits are at the expense of sacrificing the detailed microscopic information [63,77,78,96–98].

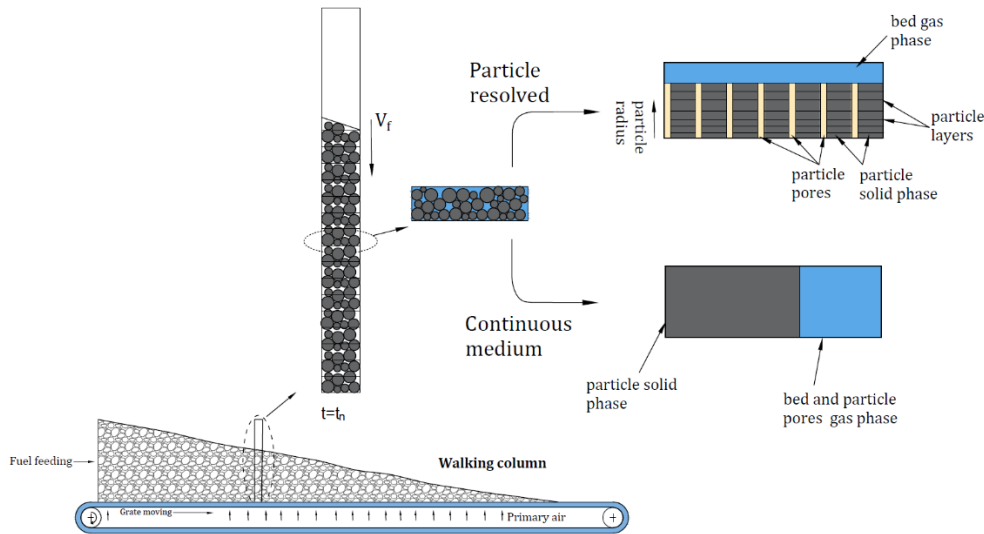


Figure 4. Continuous medium versus particle resolved approach in the moving grate combustor

2.1.1.3 Particle resolved model

This modeling method can count the internal gradient of the temperature and species concentration for large particles, though is applicable for the fine particle as well [99]. Unlike the continuous medium model, as shown in Figure 4, the resolved packed bed model incorporates gradient of diffusivity and heat conduction

inside the particle within the calculation of particle conversion. In fact, this method first uses a micro-scale particle method (single-particle model) and subsequently use the results into a macro-scale such that a more precise model is obtained at the expense of high computational cost. The particle resolved model abstracts a certain bunch of particles into a cell regardless of whether intra-particle heat and mass transfer are negligible or not and serves up a more accurate perception of the fuel bed conversion [59,99–104]. This model is rationally approached since the thermally thick particles are considered within the bed. Based on the literature [104], using the Biot number is a key to recognize there thermal gradient should be taken for the particle or not.

$$Bi = \frac{\alpha d_p}{k} \tag{1}$$

Where k is solid thermal conductivity, α is the heat transfer coefficient and finally, d_p implies the particle diameter. This correlation evinces it is only particle diameter as an effectual factor in Bi value. It is proven that for particles with d_p greater than 35 mm namely thermally thick particles, the temperature gradient can be over 400 °C evolved at the reaction front. Simultaneously, the conversion processes including drying, devolatilization, and char oxidation overlap each other along the length and height of the bed. For particles with Bi less than 2, the thermally thin particle is reckoned, which skips over the temperature gradient inside the particles.

2.1.2 Degradation sub-processes

Fuel conversion inside the moving grate bed can be rationally distinguished in three different sub-processes so-called evaporation, pyrolysis (devolatilization) and char oxidation. As Figure 5 depicts, the drying and pyrolysis processes are endothermic while the char oxidation is regarded as an exothermic reaction. During the fuel conversion, these sub-processes overlap each other and sometimes harm the others, e.g., efflux of volatile matters are impediments against the O_2 diffusion to the char surface. More details are provided in the next sections for each sub-processes.

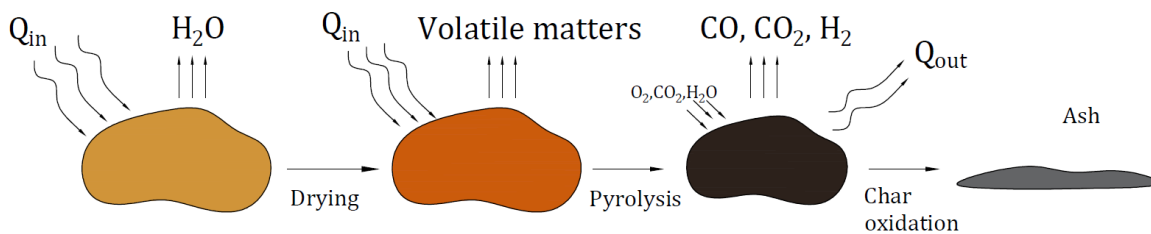


Figure 5. Biomass particle conversion processes including drying, Devolatilization, and char oxidation

2.1.2.1 Evaporation

Undoubtedly, the moisture content has a severe influence on the different aspects of biomass combustion such as ignition rate, combustion efficiency, and pollutant emissions. The flame front temperature decreased by wetter fuels and it can shift the stoichiometric combustion to a fuel-lean condition. Moreover, higher moisture content resulted in lower CO and the other unburned gaseous elements, albeit a higher amount of O₂ in overbed is achieved. The types of moisture in the woody biomass fuel can be categorized through three forms:

Liquid water occupies within void space of particle and is approximated to compose more than 30% of the total water in the particle. To evaporate this type of moisture, energy equal to the latent heat of evaporation (ΔH_{evap}) is required. *Bound water* is adsorbed to the particle cell walls and takes lower than 30% of total water. The moisture leaves the particle by means of diffusion and required energy to evaporate this bound water is equivalent to adsorption heat along with latent heat of the water. *Water vapour* is considered as a result of liquid and bound water evaporation and is in equilibrium with liquid water and always is ignored due to the negligible amount compared to the other two. The particle temperature rises during the combustion process and water vapour pressure grows within the void spaces. As a result of richer water vapour, diffusion dominates the outflowing of vapour and subsequently, saturation pressure of the water vapour surpasses the external pressure and vapour effluxes via convection. As water vapour concentration drops in particle pores, the rest of the liquid water evaporates to fill the lean pores and when the whole liquid water is over, then the bound water tends to evaporate. Here the three most common mathematical drying models are presented [105].

Arrhenius law model

This model undertakes a first-order kinetic reaction rate to simulate the drying reaction used in lots of surveys owing to convenient implementation and numerical stability [51,59,106,107]. The model assumes that water temperature and moisture mass fraction restrict the evaporation rate, and it is independent of saturation water vapour [39]. Drying rate is generally presented as follows:

$$r_{dry} = k_{dry} \rho_{moisture} \quad [kg/m^3s]; \quad k_{dry} = A_v \exp\left(-E_v/RT_s\right) \quad [1/s] \quad (2)$$

In drying rate coefficient (k_{dry}) the terms A_v and E_v are pre-exponential factor and activation energy respectively. These factors can be counted quite different values for a wide range of fuels in the different experimental conditions as it is apparent in Figure 6 that shows drying rate profiles for variant experiments.

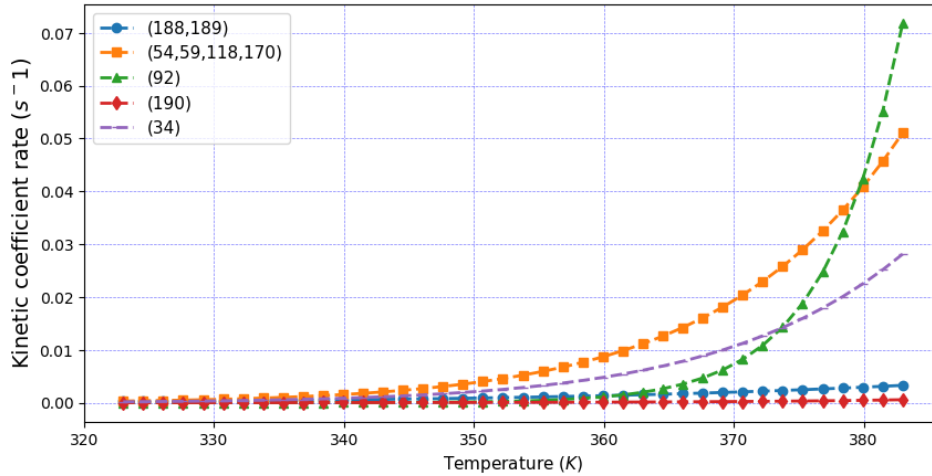


Figure 6. Drying kinetic coefficient rate at the vicinity of evaporation temperature

However, it is controversially argued that this method supposes drying in temperature less than 100 °C and the given kinetic data is hardly adapted to condition different from that where the data were derived. Bates and Ghoniem [108] modified the Arrhenius model by means of setting up the drying rate by 0 for temperature lower than the boiling temperature and making the boiling temperature dependence on the local moisture content. With respect to these adjustments, the Arrhenius model performance is significantly improved, taking this fact into account that the Arrhenius model is very easy to be mathematically implemented. Table 4 summaries some kinetic rate coefficients from literature.

Table 4. Kinetic rate coefficient and activation energy of drying rate Arrhenius model

A (1/s)	E_v (j/mol)	Ref	Fuel type
4.5×10^3	45,000	[108,109]	Woody biomass
5.13×10^{10}	88,000	[39,44,87,110]	Wood
1.6×10^{27}	207,850	[51]	Wood
1.43×10^4	88.6×10^6	[106]	Pinewood
2.822×10^{10}	87,995	[107]	Straw
7×10^4	83,000	[111]	Woody biomass
5.6×10^8	88,000	[112]	Wood

Constant temperature thermal model

According to the thermal drying model which has been considerably approached in articles [99,113–120], the drying occurs since the particle temperature reaches the evaporation temperature (T_{evap}), typically set by 100 °C. Above this temperature, it is supposed that all heat absorbed to fuel, is consumed to evaporate the moisture no matter what sort of water exists. Indeed, it is imagined that all moisture inside the particle is

free water. The model is formulated based on the energy balance at T_{evap} in reaction front layer of the fuel bed which behaves like a heat sink, wherefore it is occasionally called *Heat Sink* model, and heat transfer mechanism controls the drying rate. Some postulate this reaction front to be a very thin layer and separates the bed/particle to dried and wet parts. However, this approach exposes invalidity in the case of thick drying front although it is easy to implement for one-dimensional models. Another approach to drying zone is to engage conditional energy equation associated with the boiling temperature so that for temperature higher than the conditional one, the temporal term of energy conservation is set to zero and the drying rate is calculated respecting the heat flow divergence. This approach is not computationally efficient owing to steep discontinuities in the solution of the governing equation [121]. As the practical matter, evaporation and overheating occur simultaneously, so in order to reflect this fact into the model, some literature added a parameter (τ) to seize only a fraction of heat transfer into the particle for evaporation [63,77,78,122].

$$\begin{cases} \dot{\omega}'_{moisture} = \tau \frac{\rho_p C_p}{LH_{moisture}} \frac{\partial T_s}{\partial t}, & T_s \geq T_{evap} \\ 0 & otherwise \end{cases} \quad (3)$$

Where, $LH_{moisture}$ is water latent heat (around 2,260 kJ/kg), and ρ_p is the moisture density of the particle.

Equilibrium model

The equilibrium model is based on the thermodynamic equilibrium between liquid water and water vapour. Therefore, it can be concluded that the drying rate has a direct correlation to the difference between the concentration of water liquid in the particle surface and current vapour in the particle which is justifiable for low temperature drying. The model is dominated by diffusion mechanism at temperature up to water boiling point and is dependent not only on the heat transfer but also on the mass transfer as it was presented in Ref. [123]. Since the temperature surpasses the boiling point, the equilibrium model would change to the thermal model.

$$r_{evap} = S_p h_m (C_{m,s} - C_{m,g}), \text{ when } T_s < 100 \text{ }^\circ\text{C} \quad (4)$$

$$r_{evap} = Q_{cr} / H_{evap}; \quad T_s \geq 100 \text{ }^\circ\text{C} \quad (5)$$

Where, S_p is particle surface (m^2), h_m is the mass transfer coefficient between the solid and gas phase (m/s), $C_{m,s}$, $C_{m,g}$ are the concentration of liquid moisture and vapour (kg/m^3) respectively, T_s as solid temperature (K), H_{evap} is evaporation latent heat (J/kg) and Q_{cr} is heat flux to the particle by radiation and convection sources (W):

$$Q_{cr} = S_p h_c (T_g - T_s) + \varepsilon_s \sigma_b S_p (T_{env}^4 - T_s^4) \quad (6)$$

Where h_c is convective heat transfer coefficient ($W/m^2 K$), T_g is gas temperature (K) and T_{env} is the furnace temperature (K). The moisture mass transfer coefficient in the biomass particle can be assigned as follows[124]:

$$h_{m,vap} = \frac{3.66D_{eff,H2O}}{d_{pore}} \quad (7)$$

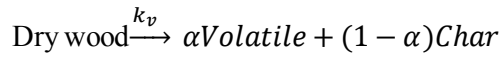
$$D_{eff,H2O} = \exp(-9.9 - \frac{4300}{T} + 9.8Y_m) \quad (8)$$

2.1.2.2 Pyrolysis (devolatilization)

Followed by the drying process, devolatilization of volatile matters which comprise the highest volumetric percentage of the biomass fuels starts at a certain temperature depending on the type and characteristics of fuels. Among all devolatilization models three of them namely single-step pyrolysis model, competitive parallel reactions pyrolysis model and secondary tar reaction pyrolysis model are most frequently exercised. Some other schemes, for instance, Ranzi scheme and Broido-Shafizadeh scheme, are omitted to be discussed in this work.

Single-step model

This model simply presumes that dry biomass fuel converts to gases and char in one step reaction which follows the energy balance such that the radiation heat transfer replaces convection as the limiting mode. The volatile elements are supposed to be C_mH_n , CO, CO₂, H₂, CH₄, CH_xO_y [45] and the product rate constant as a function of temperature is modeled by the Arrhenius law equation.



$$\text{Volatile} = \gamma_1 \text{CO} + \gamma_2 \text{CO}_2 + \gamma_3 \text{H}_2 + \gamma_4 \text{CH}_4 + \gamma_5 C_m H_n + \gamma_6 \text{tar}(CH_x O_y)$$

where k_v denotes pyrolysis reaction rate, and α is a mass fraction or stoichiometric coefficient, and the estimated ultimate volatile can be presented as $\rho_{v,\infty} = \alpha \rho_{sd,0}$ where, $\rho_{sd,0}$ is the initial volatile density in dry biomass and it is determined in the ultimate analysis of fuel.

$$\frac{d\rho_v}{dt} = k_v (\rho_{v,\infty} - \rho_v) \quad \left[\frac{kg}{m^3 s} \right] \quad ; \quad k_v = A_v \exp(-E_v/RT_s) \quad (9)$$

$$\alpha \text{Volatiles} = \sum_{i=1}^6 \gamma_i \text{Volatile}_i \quad (10)$$

This is a simple method from the implementation viewpoint and was employed in much earlier research [45,125,126]. However, the main weakness of the model is the inability of the recognition of the product rate of each species and therefore, the species portion must be estimated beforehand.

Competitive parallel reactions model

The three independent reactions model including permanent gases, tar and char are deployed to model the dry fuel degradation. The summation of mass fraction of the corresponding products must be unit at every time, and this is one and only relation among all three reactions. This parallel model is regarded as a robust and flexible model that was developed for the first time by Shafizadeh and Chin [127]. The volatile species in the parallel model are supposed the same as the one-step model and the composition of released gases are specified based on the experimental tests.

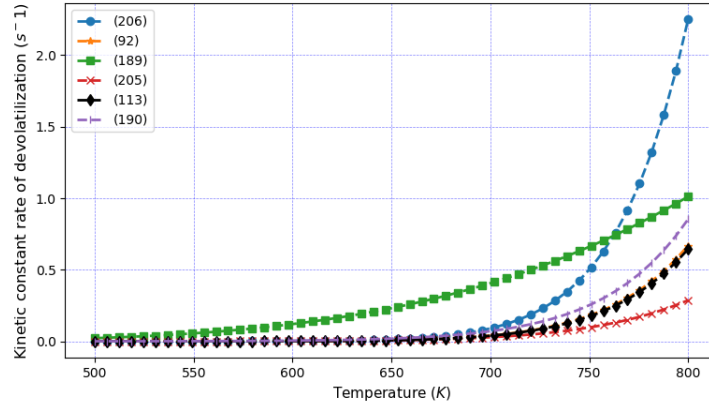


Figure 7. Devolatilization constant rate used through different research

The very common approaches in this model were introduced in terms of three parallel reactions [61,68,82,114,128–130] consisting of gas, tar and char production, and the pyrolysis rate was represented via the sum of all three reaction rates. The residence time of the released elements is assumed to be short so that no meaningful reaction (particularly secondary pyrolysis reaction) occurs in this modeling approach. Figure 7 illustrates profiles of kinetic rate coefficients respect to devolatilization used in literature. The figure reveals that for some fuels, pyrolysis arises at a higher temperature than the other fuels depend on different chemical bound within the fuels, and also the experiments setting and measurement.

$$\frac{d\rho_{dry}(t)}{dt} = -\rho_{dry,0} \sum_{i=1}^3 A_i \exp\left(-\frac{E_i}{RT}\right) \quad [kg/m^3s] \quad (11)$$

The pre-exponential factor and activation energy of Arrhenius equations for devolatilization sub-processes used in literature with the corresponding fuel type are reported in Table 5.

Table 5. Devolatilization rate coefficients for the Arrhenius model

Fuel	Kinetic rate	A	E	Ref	Fuel	Kinetic rate	A	E	Ref
Pine wood	Gas+Tar+Char	1.4×10^{10}	150,000	[131]	Wood pellet	Gas	111×10^9	177×10^3	[61]
Wood	Gas	1.3×10^8	140298	[51]		Tar	9.28×10^9	149×10^3	

	Tar	2.2×10^8	133098			Char	30.5×10^9	125×10^3
	Char	1.1×10^7	121401		Beech	Gas	1.3×10^8	140,000 [82]
Torrefied	Gas	602	42,500	[109]		Tar	2×10^8	133,000
	Char	8,000	130,000			Char	1.08×10^7	121,000
Wood pellet	Gas	1.44×10^4	88,600	[128]	Wood	Gas	8.607×10^5	88,600 [132]
	Tar	4.13×10^6	112,700			Tar	2.475×10^8	112,700
	Char	7.38×10^5	106,500			Char	4.426×10^7	106,500
Pine wood	Cellulose	2×10^9	146,000	[112]				
	Hemicellulose	7×10^4	83,000					

Secondary tar reaction pyrolysis model

Taking the assumption of the long residence time of primary volatile matters through the bed region, the secondary tar reaction was developed by Shafizadeh [133], and Thurner and Mann [132] based on adding this reaction to three primary parallel reactions model. The tar cracking yields are supposed to be light gases (CO and CO₂) and char. Chan et al. [134] postulated the secondary gases and tars as the primary tar cracking outcome, while the main hindrance of this assumption referred to the calculation of the stoichiometric coefficient of this secondary reaction. The more common assumption of the secondary tar reaction yields supposes that the tar converts to gases and char by means of the tar cracking and repolymerisation [135], while k_5 was reckoned forty times slower than k_4 .

$$\frac{d\rho_{dry}(t)}{dt} = -\rho_{dry,0}(k_{v,1} + k_{v,3} + k_{v,4} + k_{v,5}) \quad \left[\frac{kg}{m^3 s} \right] \quad (12)$$

To sum up, the single-step model is not enough accurate for reliable modeling and can be used only as an approximation. On the other hand, the three-parallel reaction model and tar cracking model describe the process much better in the cost of a moderate increase in computational cost. In the course of the tar cracking model, data for the secondary tar reaction is not widely available for every biomass fuel, and this is regarded as this model issue. Since the data for tar cracking is not available, the three parallel reaction model is the most preferable.

2.1.2.3 Char burnout

Contrary to the pyrolysis reaction, the char conversion is a heterogeneous reaction between the solid and gaseous reactants for which both kinetic of reaction and mass transfer are needed to be paid attention. Char is constituted mainly of carbon, over 90%, and a few amounts of oxygen, nitrogen, hydrogen [136]. The classical approach of char conversion postulated the reaction to be uniformly distributed through the particle

so that no temperature and species gradient are taken inside the solid fuel which is more sufficient for conversion at low temperature. The char combustion is referred to the reaction between char and oxygen, while once the char reacts with other gaseous reactants such as carbon dioxide and water vapour, and hydrogen, it is simply termed char gasification. In addition to the classical approach, char conversion can be categorized into surface reaction model by which reaction takes place fast, and particle zone model which is relatively slower. The surface reaction model happens at the particle surface since the reactants reach the surface and advances towards the particle center therefore, the conversion rate is proportional to the corresponding surface area. In the course of the zone model, the reaction occurs inside the particle and progresses through the particle so that it is proportional to the surface area inside the pores. The char oxidation and gasification reactions are assumed as follows:



The first reaction is much faster than the gasification of char however since the oxygen is consumed by carbon the other reactants will be influential [137,138]. Laurendeau [139] narrated the process to start by diffusion of heat and mass agents surrounding the fuel surface, and consequently, these agents diffuse into the porous zone of the particle and react with char surfaces that involve internal and external particle surface. Finally, the gaseous products transport from the fuel surface toward the overbed.

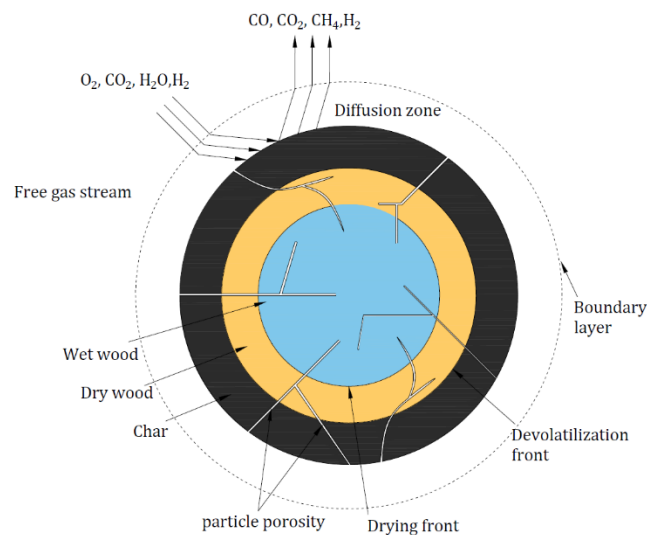


Figure 8. Schematic of char surface reaction of a biomass particle with the free gas stream

The term Ω signifies stoichiometric ratio of char combustion which would be often determined via the ratio, $r_c = \text{CO}/\text{CO}_2$ at which for some of them, it is rational up to a particle temperature threshold. For instance, in the model applied by Yang et al. [140], the r_c is valid for temperature between 730 to 1170 K. Many authors only considered the char combustion reaction in their investigations regardless of gasification reactions effects on the modeling consequences due to the tiny fraction of these equations in char conversion [45,60,68,107,109,111,114,141]. Furthermore, in some other works, the gasification reaction of char with hydrogen was omitted for the negligible reaction rate than the other two gasification reactions [97,106,142,143]. A schematic of the char particle reacting with the free gas stream around the particle is shown in Figure 8.

$$\frac{d\rho_{ch}}{dt} = - \sum_{i=1}^4 A_p P_{O_2} \left(\frac{1}{k_{r,i}} + \frac{1}{k_{d,i}} \right) \rho_i \quad (13)$$

$$k_{r,i} = A_{v,i} \exp(-E_{v,i}/RT_s) \quad (14)$$

k_r and k_d are the chemical kinetic and diffusion rate coefficients respectively, A_p is the volumetric area of char particle, P_{O_2} the oxygen partial pressure at the char surface. The char reaction rate data derived from the literature are sorted in Table 6.

Table 6. Kinetic and diffusion factors of char reaction rate

Ref	Char reactions	Reaction rate	CO/CO ₂	Fuel
[109]	R1	$k = 0.39 \exp(-47,500/RT_s)$	-	Wood
[61,144,145]	R1	$k = 1.715 \cdot T_s \cdot \exp(-9,000/T_s)$	-	Wood pellet
	R2	$k = 3.42 \cdot T_s \cdot \exp(-15,600/T_s)$		
	R3	$k = 5.7114 \cdot T_s \cdot \exp(-15,600/T_s)$		
[45]	R1	$k = 8,620 \exp(-15,900/T_s)$	$12 \exp(-3,300/T_s)$	Straw
[146]	R1	$k = 860 \cdot p_{o_2} \cdot \exp(-18,000/T_s)$	-	-
	R2	$k = 10,400 \cdot p_{co_2} \cdot \exp(-178,000/T_s)$		
[51,59]	R1	$r_{h,1} = (1 - \alpha) \Omega \frac{C_{O_2}}{1/k_{r1} + 1/h_m}$	-	Wood
	R2	$r_{h,2} = \frac{C_{CO_2}}{1/k_{r2} + 1/h_m}$		
	R3	$r_{h,3} = \frac{C_{H_2O}}{1/k_{r3} + 1/h_m}$		
	R4	$r_{h,4} = \frac{C_{H_2}}{1/k_{r4} + 1/h_m}$		

[114]	R1	$k = 301 \exp(-149,380/T_s)$	-	Wood
[111]	R1	$k_{global} = \frac{1}{1/k_r + 1/k_d}$	$2500 \exp(-6,420/T_s)$	Pine wood
[106]	R1	$k = 1.63 \times 10^{11} \cdot T^{-1.5} \cdot \exp(-3,430/T_s)$	-	Pine wood
	R2	$k = 2.78 \times 10^3 \exp(-1,510/T_s)$		
	R3	$k = 3.552 \times 10^{11} \exp(-15,700/T_s)$		

2.1.2.4 Porosity and shrinkage model

The particle and bed porosity are distinguished by means of the internal pores of particle and void space in the fuel bed respectively. While the conversion process proceeds toward the end of the grate, the particle mass is consumed and the particle porosity increases. The volumetric shrinkage of the particle is tracked within the conversion process to identify the bed porosity which influences the bed height [86]. The mass loss rate in the drying process is various depending on remained moisture content, and results in more particle porosity, whereas the bed porosity almost remains constant. The bed porosity can be regarded as a function of particle mass fraction change and the shrinkage factor, f :

$$\epsilon = \epsilon_0 + (1 - \epsilon_0) \sum_i f_i (Y_{i,0} - Y_i) \quad [-] \quad (15)$$

Where ϵ_0 is initial bed porosity, $Y_{i,0}$ initial mass fraction of i -th solid particle in the cell, f_i shrinkage factor of i -th cell which can vary in the range of 0 to 1, where the value 0 means no bed porosity change, and value 1 means the bed porosity changes by the whole particle volume. Some simplified models disregarded the particle shrinkage throughout drying and devolatilization [147–151], nevertheless, this hypothesis is far from reality when Thunman et al. [152] concluded 20 to 50% particle shrinkage in pyrolysis process, and Johansson et al. [51] observed 10% particle volume shrinkage during drying for a fuel with 50% moisture content. A general form of particle shrinkage model by counting all sub-processes including drying, pyrolysis and char conversion is mentioned as follows:

$$\frac{V}{V_0} = 1 - a_1(M_0 - M) - a_2(VM_0 - VM) - a_3(C_0 - C) \quad (16)$$

Where a_1 , a_2 and a_3 imply shrinkage factor of drying, pyrolysis and char oxidation respectively. For more detail of the proposed models in the literature, Table 7 is referred to. In another approach which could be held as an implicit method, the particle mass consumption inside the grid is observed until a porosity of 100% in the grid is achieved. This means the whole mass in the grid has reacted and converted to the gas phase. In this way, bed shrinkage is taken into the account in the model while biomass conversion proceeds [46,153].

Table 7. Summary of shrinkage model and corresponding factors

Model approach	Shrinkage model	Shrinkage factors	Ref
Single-particle	$\theta = 1 + (1 - \theta_m) \left(\frac{\rho_m}{\rho_{m0}} - 1 \right) + (\theta_m - \theta_v) \left(\frac{\rho_{bm}}{\rho_{bm0}} - 1 \right) + (\theta_v - \theta_c) \left(\frac{\rho_c}{\rho_{c0}} - 1 \right)$	$\theta_m = 0.9, \theta_v = 0.75, \theta_c = 0$	[142]
Single-particle	$\frac{V_s}{V_{s0}} = \frac{(\rho_w + \rho_c + \rho_r)}{\rho_{w0}}$	-	[148,149]
Single-particle	$V = V_s + V_g$	$\alpha = 0.3, \beta = 0, \gamma = 0.3$	[147]
Fixed pack bed	$1 - \varepsilon = f_{sh}^{1-n} (1 - \varepsilon_0)$	$f_{sh} = \frac{V_s}{V_{s0}}$	[86]
Fixed pack bed	$\frac{V_p}{V_{p0}} = 1 - \theta_{dry} \frac{Y_{M0}}{Y_{m,\theta}} \left(1 - \frac{Y_M}{Y_{M0}} \right) - \theta_{dev} \left(1 - \frac{Y_v}{Y_{v0}} \right) - \theta_{comb} \left(1 - \frac{Y_c}{Y_{c0}} \right)$	-	[51,56]
Fixed pack bed	$\frac{V_{cv}}{V_{cv0}} = f_{sh}$	$f_{sh} = f_{sh,min} + \eta(1 - f_{sh,min})$ $\eta = \frac{M_w}{M_{w0}}$	[50]
Fixed pack bed	$\frac{V}{V_0} = 1 - a_1 \times (M_0 - M) - a_2 \times (VM_0 - VM) - a_3 \times (C_0 - C)$	$a_1 = a_2 = a_3 = 0.8$	[57,104]
Single-particle	-	$f(\phi) = 1 + 1.5(1 - \phi)$	[103]
Moving bed	$\frac{\partial V_{sh}}{\partial t} = f_{sh} \frac{1}{(1 - \varepsilon_0)} \frac{\partial V}{\partial t}$	$f_{sh} = 0.4$	[154]

2.1.3 Mathematical modeling specification

The moving grate biomass furnace consists of solid-gas phase zone on the grate, and mathematical modeling of the bed and overbed are assigned to articulate the complex thermochemical conversion inside the bed as well as turbulence, oxidization, heat and mass reaction, and so on at the overbed zone. In general form, the conservation form of governing equations for independent variable φ as a porous media is formulated by:

$$\frac{\partial(\varepsilon\rho\varphi)}{\partial t} + \frac{\partial(\varepsilon\rho v\varphi)}{\partial x} = \frac{\partial}{\partial x} \left(\Gamma \frac{\partial\varphi}{\partial x} \right) + S_\varphi \quad (17)$$

In LHS, the first term is the temporal term and the second one is convection term and on the other hand, diffusion and source terms in RHS, respectively. All transient equations consist of mass, momentum, species and energy equations follow this structure of partial differential equation (PDE), and respect to the grate firing biomass boiler, φ , Γ and S_φ are determined as in Table 8.

Table 8. Description of general conservation equation coefficients for each sort of equation

Equation	φ	Γ	S_φ
----------	-----------	----------	-------------

Mass	1	0	r [$\text{kg}/\text{m}^3.\text{s}$]
			Heterogeneous reaction rate
Momentum	V [m/s]	μ [$\text{kg}/\text{m}.\text{s}$]	0
		Kinematic viscosity	
Energy	H [J/kg]	λ_{eff}/c_p [$\text{kg}/\text{m}.\text{s}$]	\dot{q} [W/m^3]
	Specific enthalpy	Effective thermal conductivity over specific heat capacity	Summation of Heat transfer rate
Species	Y_i	$\epsilon\rho D_i$ [$\text{kg}/\text{m}.\text{s}$]	r_i [$\text{kg}/\text{m}^3.\text{s}$]
	Mass fraction of each species	Bulk density times dispersion coefficient	Production/consumption rate of

The above equations are valid for both solid and gas phase just by reflecting each phase's properties into the parameters. The above mathematical description is in terms of the 1D model in a transient form which can suitably correspond to 2D steady-state model for grate firing boilers as shown in Figure 4. This method so-called walking column method is a very proficient approach as it makes the calculation practice much easier while only a negligible error appears against the steady-state 2D model. This negligible error between 1D and 2D models can be explicated by this fact that the reaction front inside the packed bed predominantly moves in direction of the air flow. Despite the structure of the general form of the governing equation, the conservation equations can be composed in many different forms based upon the author's view. The solution of conservation equations for the fuel bed extremely depends on the boundary conditions around the particles. Since the solid biomass fuels are generated from natural sources without any chemical process (at least in most of the cases), therefore the fuel quality uncertainties become an important objective of study. This could be the main reason behind of existing sheer number of biomass sub-models kinetic reactions which significantly impacts the main model behavior such that choosing a non-compatible sub-model can deviate the main model toward the wrong side.

2.1.4 Biomass physical properties

The radiation and conversion mechanisms are deemed as the most dominant factors at the boundaries to affect particles temperature growth [151,155–159]. Constant uniform radiative flux was adjusted to dictate heat flux to particles in some articles [151,160,161] while some used a simple approach of determinate background temperature [39,114,162]. In some literature, more sophisticated assumption of both convection and radiation flux concerning surrounding gas and flame temperature at the top boundary of biomass particles bed was taken [59,163,164]. The heat flux intensity can influence the char density at the boundary and inside the particle, so that the high heat flux results in the lower char density at boundary than inside, and moreover, it results in more tar in pyrolysis products [151]. During drying of the biomass particles, a

layer of steam covers the exterior surface so that it absorbs part of radiation and consequently cools down the surface temperature partially. This cooling effect was neglected in the majority of literature, excluding many few cases [165]. Even though consideration of radiation flux directly from combustion flame is a step toward reality, still the fluctuation and instability of the flame result in some uncertainties in radiation flux determination. One of the important parameters among boundary conditions which can change radiation flux absorbed by particles is particle emissivity. Different values for emissivity were determined in literature. for example, Refs. [98,143,166] set by 0.85 and Refs. [45,141] in value of 0.9 and Refs. [154,167,168] assigned 0.8. It must be noted that emissivity of the particle changes during the conversion process from fresh particle to char, based on the fuel composition and it tends to increase as the conversion process proceeds. No clear principle can be found in the aforementioned works respect to specifying the emissivity coefficient. It could be concluded that it is adjusted to enforce the model to reach a better agreement with experiments, and there still is observed obscurity in chosen values. It must be noted that during char burning, as the ash layer is formed on the char surface, the emissivity declines and have a meaningful effect on the conversion [89]. This ash layer has a dual mechanism as it decreases heat loss from particle surface by means of decreasing in emissivity as well as by adding more resistance to O₂ diffusion, therefore, brings the particle temperature down.

The heat and mass transfer coefficients were assumed fixed values in some works [151,155,169], while in more exact models [169–171], they supposed these coefficients as a function of other factors such as specific heat capacity (c_p), effective thermal conductivity (λ_{eff}), mass dispersion coefficient (D_i). From the initiation of fuel drying, up to the end of pyrolysis, the gases continuously efflux from the particle border resulting in a convective impediment which means a reduction in the heat transfer coefficient. The heat and mass transfer coefficients regarding these outflowing gases were corrected by means of Stefan correlation which acquired the effect of gases mass flow into the formulation [142,172]:

$$h_c = \frac{\dot{m}_g c_{p_g}}{\exp\left(\frac{\dot{m}_g c_{p_g}}{h_{c_0}}\right) - 1}, h_{c_0} = \frac{Nu k_g}{d_{ch}} \quad (18)$$

$$h_m = \frac{\dot{m}_g / \rho_g}{\exp\left(\frac{\dot{m}_g}{\rho_g h_{m_0}}\right) - 1}, h_{m_0} = \frac{Sh D_{AB}}{d_{ch}} \quad (19)$$

Where d_{ch} is characteristic particle length such as spherical particle diameter, Nu is the Nusselt number and Sh is Sherwood number, $\dot{m}_g = \rho_g u_g A_P$ is outlet gases mass flow rate, A_P is the particle surface area, and 0 means initial state. D_{AB} is the diffusion coefficient from element A to B environment which strongly depends on temperature and pressure of flow gas as represented in Eq. 20.

$$D_{AB} = \frac{0.00143T^{1.75}}{PM_{AB}^{0.5}[(v)_A^{1/3}+(v)_B^{1/3}]^2} \quad [\text{W/ m K}] \quad (20)$$

Where P is pressure, M_{AB} is molecular weights of A and B, g/mol, and v atomic diffusion volumes. This formulation is correct while radiation dominates the heat transfer mechanism. However, if convection overcomes the heat transfer, the correlations should be modified and it can decelerate the biomass devolatilization up to 20% [110]. It must be noticed that the diffusion coefficient is experimentally determined at a reference temperature (e.g., 273K or 297K) and needs to be updated for different physical environments as Eq. 21 [98,173–176].

$$D_{AB} = D_{AB,ref} \left(\frac{T_g}{T_{ref}}\right)^{1.75} \quad [\text{W/ m K}] \quad (21)$$

2.1.4.1 Specific heat capacity

Identification of the biomass specific heat capacity involves lots of challenges due to a variety of fuel compositions together with this fact that primary specific heat capacity changes during the conversion process. Despite this fact, some works supposed the specific heat capacity of fuel to last consistent during conversion [114,177–179] while some authors assumed a linear variant of specific heat capacity in terms of temperature or combination of fresh fuel and char specific heat [45,98,142,154]. For instance, authors of Refs. [151,180] presumed a weighted-average specific heat capacity based on fresh fuel and char as follows:

$$c_{p,s} = \eta c_{p,f} + (1 - \eta) c_{p,c} \quad [\text{kJ/kg K}] \quad (22)$$

where, $c_{p,f}$ is fresh fuel specific heat capacity and $c_{p,c}$ is char specific heat capacity. For the gas phase, with respect to the different gaseous species such as moisture, air, pyrolysis gases, a fraction of the specific heat of each element is considered base on Eq. (23):

$$c_{p,g} = \sum_{i=1}^N c_{p,i} X_i \quad [\text{kJ/kg K}] \quad (23)$$

where X_i is the volume fraction of each element. A list of specific heat capacity used in different literature can be found in Table 9.

Table 9. Specific heat capacity employed for various biomass fuel

Ref	Biomass type	Formula (J.kg ⁻¹ .K ⁻¹)	Ref	Biomass type	Formula (J.kg ⁻¹ .K ⁻¹)
[39,181]	Basswood	$c_W = 3.867(T - 273.2) + 103.1$	[182]	Wood	$c_{p,W} = 1200 + 2.45(T_s - 273)$
		$c_{p,c} = 1390 + 0.36T$	[183]	Softwood	$c_{p,W} = 231.6 + 3.69T_s$
		$c_{p,vol} = 2400$			$c_{p,c} = -795.28 + 5.98T - 3.8 \cdot 10^{-3}T^2$

		$c_{p,M} = 4180$	[98]	wood	$c_{p,M}=4200$
[69]	Beech wood	$c_p = 2551.3$			$c_{p,W}=103.1+3.87 T_s$
[114,178]	Wood	$c_{p,M}=4200$			$c_{p,C}=1390+0.36 T_s$
		$c_{p,W}=1380$	[154]	Wood char	$c_{p,S}=X_C c_{p,C} + X_A c_{p,A}$
		$c_{p,vol} = 1100$			$c_{p,C}=2300$
		$c_{p,C}=1250$			$c_{p,A}=754+0.586(T_s - 273)$
[179]	Wood	$c_{p,0}=1670$	[45]	straw	$c_p=977.75 \ln(T_s)-4144.4$
		$c_{p,C}=1000$			

2.1.4.2 Effective thermal conductivity

In biomass conversion, the thermal conductivity of the fuel is recognized as a variable depending on temperature, composition, density, and direction of heat transfer to the fuel particles. Thermal conductivity of char was determined constant in many research since the pure carbon is assumed to remain in char reaction [39,184]. Two different techniques are frequently employed to model effective thermal conductivity. In first Technique which was developed by Wakao and Kagueli [185], a fixed bed combustor is proposed to obtain thermal conductivity which ignores the effect of gas flow while the conduction correction factor α , is valued 0.1 and 0.5 for axial and radial conduction flux respectively.

The second technique is more sophisticated which develops effective thermal conductivity in terms of an adjusted summation of all elements of solid particles including water, volatile materials and char plus the contribution of particle mixing and radiation flux. Table 10 classifies some of the effective thermal conductivity models through the literature.

Table 10. Effective thermal conductivity models for biomass fuels

Formula (W.m ⁻¹ .K ⁻¹)	Ref	Formula (W.m ⁻¹ .K ⁻¹)	Ref
First Technique		Second Technique	
$k_{eff} = k_{eff,0} + 0.5.Pr.Re.k_f$	[186]	$k_{eff} = (1 - \epsilon_b)(Y_m k_m + Y_W k_W + Y_C k_C) + \frac{16\sigma\epsilon_b}{3R} T_s^3$	[98]
$k_{eff,0} = \eta.(k_f + h_{rv}\Delta l) + \frac{(1-\eta)\Delta l}{1/(k_f/l_v + h_{rs}) + l_s/k_s}$		$\lambda_{eff} = \lambda_s + \lambda_{rad}$	[122]
$k_e = k_e^o + (k_e)_i$	[187]	$\lambda_s = \epsilon_p \lambda_g + \sum_k Y_k \lambda_k, \lambda_{rad} = 4\epsilon\sigma_b \omega d_p T_s^3$	
$k_{eff} = \frac{\eta C^t}{\pi D}$	[188]	$\lambda_s = (1 - \phi)(\rho_s/4511)^{3.5} T_s^{0.5} + 2.27 \times 10^{-7} d_p \left(\frac{\epsilon}{2 - \phi}\right) T_s^3 + \lambda_{mix}$	[63]
		$\lambda_{eff} = \lambda_{cond} + \lambda_{rad}$	[39]
		$\lambda_{rad} = \epsilon/(1 - \epsilon)\sigma\phi_p d_p 4T^3$	
		$\lambda_{cond} = \lambda_M + \eta\lambda_W + (1 - \eta)\lambda_C$	

$$k_{eff} = G(B + CM) + A; \quad [189]$$

$$k_{wood} = 0.1941\rho_w + 0.0186 \quad [184]$$

$$k_{char} = 0.105$$

$$k_{eff} = 0.8k + 0.5d_h c_p \rho U / \varepsilon \quad [49]$$

$$k_{eff} = k_{eff,0} + 0.5PrRek_f \quad [60]$$

An expanded form of the governing equations for feed conversion inside the bed is given in Table 11. Quite often the momentum equation of solid phase is overlooked from the equation set owing to the almost stationary state of particles inside the bed. Furthermore, the solid phase species equation is spontaneously solved while the solid mass equation gets resolved.

Table 11. Overall governing equation; gas and solid phases

Transient equations for gas phase		
Mass	$\frac{\partial}{\partial t}(\phi\rho_g) + \nabla \cdot (\phi\rho_g v_g) = S_{react}$	(24)
Momentum	$\frac{\partial}{\partial t}(\phi\rho_g v_g) + \nabla \cdot (\phi\rho_g v_g v_g) = -\nabla p_g + F(\bar{v}_g)$	(25)
Energy	$\frac{\partial}{\partial t}(\phi\rho_g c_{p,g} T_g) + \nabla \cdot (\phi\rho_g v_g c_{p,g} T_g) = \nabla \cdot (\lambda_g \nabla T_g) + hS(T_s - T_g) + S_{s,g}$	(26)
Species	$\frac{\partial}{\partial t}(\phi\rho_g Y_i) + \nabla \cdot (\phi\rho_g v_g Y_i) = \nabla \cdot (\phi\rho_g D_{g,i} \nabla Y_i) + \phi S_{s,i}$	(27)
Transient equations for solid phase		
Mass	$\frac{\partial}{\partial t}(\rho_s) = -S_{react}$	(28)
Energy	$\frac{\partial}{\partial t}(\rho_s c_{p,s} T_s) = \nabla \cdot (\lambda_{eff} \nabla T_s) + hS(T_g - T_s) + S_{s,s} + S_{rad}$	(29)
Momentum	$\frac{\partial}{\partial t}((1 - \phi)\rho_s v_s) + \nabla \cdot ((1 - \phi)\rho_s v_s v_s) = -\nabla \cdot \sigma - \nabla \cdot \tau + \rho_s g + A$	(30)
Species	$\frac{\partial}{\partial t}((1 - \phi)\rho_s Y_{is}) + \nabla \cdot ((1 - \phi)\rho_s Y_{is} v_s) = -S_{react,i}$	(31)

2.1.5 Overbed modeling

In contrast to the complicated aspects of biomass conversion modeling in the fuel bed, the overbed homogeneous zone is well documented. Since the gaseous species are released from the biomass conversion, they react with the oxygen originated from secondary air and partially primary air as well. Here as the mixing rate is slower than the gaseous combustion, it becomes an important factor in combustion performance. The most of gas-phase numerical modeling in the moving grate biomass combustors focuses on the gases mixing

and optimization [16,30,35,190–194]. From the literature, the majority of the reactions between released gases from bed with oxygen within the overbed zone are reported in Table 12.

Table 12. Homogeneous gas phase reactions originated from fuel bed conversion

#	Reaction	Ref											
		[78,166,195]	[196]	[197,198]	[199,200]	[51]	[59]	[201]	[202]	[16,61,77]	[123]	[110]	[203]
1	$C_6H_6 + \frac{9}{2}O_2 \rightarrow 6CO + 3H_2O$	✓							✓	✓	✓		
2	$CH_4 + \frac{3}{2}O_2 \rightarrow CO + 2H_2O$	✓	✓	✓	✓	✓	✓	✓	✓	✓	✓		✓
3	$H_2 + \frac{1}{2}O_2 \rightarrow H_2O$	✓	✓	✓	✓	✓	✓	✓	✓	✓		✓	✓
4	$CO + \frac{1}{2}O_2 \rightarrow CO_2$	✓	✓	✓	✓	✓	✓	✓	✓	✓	✓	✓	✓
5	$CO_2 \rightarrow CO + \frac{1}{2}O_2$	✓							✓				
6	$0.006C_6H_{6.2}O_{0.2} + 2.9O_2 \rightarrow 6CO + 3.1H_2O$		✓										
7	$C_lH_mO_n + (\frac{l}{2} + \frac{m}{4} - \frac{n}{2})O_2 \rightarrow lCO + \frac{m}{2}H_2O$			✓									
8	$C_6H_{6.2}O_{0.2} + 2.8O_2 \rightarrow 3CO + 3.1H_2$					✓						✓	
9	$CO + H_2O \rightarrow H_2 + CO_2$					✓				✓			✓
10	$H_2 + CO_2 \rightarrow CO + H_2O$					✓				✓			✓
11	$NH_3 + NO \rightarrow N_2 + H_2O + \frac{1}{2}H_2$								✓				
12	$NH_3 + O_2 \rightarrow NO + H_2O + \frac{1}{2}H_2$								✓				
13	$C_2H_4 + 2O_2 \rightarrow 2CO + 2H_2O$										✓		✓

It is a typical approach in the numerical modeling of the overbed combustion to create a three-dimensional model of the overbed zone in a CAD (computer-aided design) software on the real scale and mesh the geometry. The gas temperature profile, gas flow profile, and mass fraction of gaseous species calculated from fuel bed model are considered the boundary condition at the bedside. The other boundary conditions will be the secondary air properties such as air flow rate, temperature, pressure besides the furnace wall temperature and material. Then, the proper solvers regarding the turbulence, combustion, radiation, and NO_x model must be governed. The conceptual modeling method of the complete biomass combustor domain is illustrated in Figure 9.

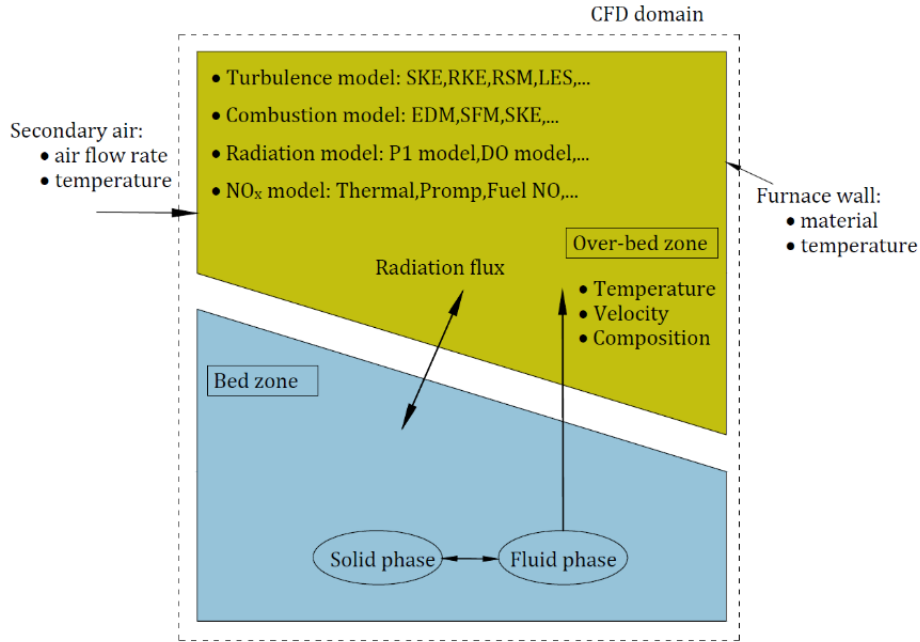


Figure 9. Scheme of the grate bed biomass furnace modeling

2.2 Experiments

Apart from combustion modeling of moving grate biomass combustors, the experimental efforts on these facilities play a vital role within this research area. These experiments are carried out in order to attain data to be used for three different purposes as shown in Table 13. The first application of the data is to validate the numerical modeling accuracy, depending upon the modeling objectives, these measured data can vary. Quite often, temperature and species concentration in some points through the bed, furnace and flue gas are recorded to see the error margin of models [17,52,97,110,204]. This is a very common approach for validation of moving bed models to use fixed column reactor data since distance along a grate corresponds to the time on the fixed column reactor. A wood chip cylindrical reactor was considered and temperature at various heights of bed and overbed with fuel mass consumption was recorded during the combustion process [128]. Ryu et al. [205] applied a developed FLIC code [206] for fixed bed combustion simulation. An experimental setup arranged to measure the temperature at 11 spots, more concentrated inside the bed, together with an ADC MGA3000 gas analyzer to record the CO/CO₂/O₂ concentration just above the bed. A typical configuration of lab-scaled fixed bed biomass reactor is displayed in Figure 10. In general, this apparatus is equipped with air flowmeter to regulate the primary and in a few cases secondary air attached with an adjustable valve to increase the accuracy of the flow rate. The air enters the stationary grate which supports the fresh fuel placed on the grate.

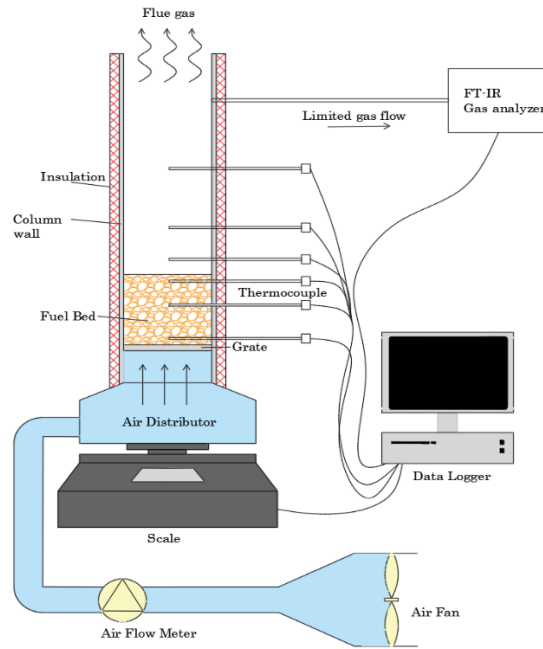


Figure 10. Schematic of a batch type laboratory-scale biomass furnace

Depend on the experiment's objectives, the system is equipped with the thermocouples and gas measuring sensors that are connected to a computer as a data logger to record the values as the function of time. To measure the mass loss during the test, it is a common idea to put the apparatus on the scale to record the fuel weight reduction. On the other hand, pure experimental surveys individually investigate the combustion system from viewpoints of conversion and thermal performance as well as pollutant emissions released in the atmosphere. Mathematical analysis of some phenomena regarding combustion in the fuel bed is still deemed challenging e.g., channeling effect. Hence, the experimental works interestingly come to attention to reliably analyze such daunting phenomena [73,207–209]. Cepic et al. [210] investigated wheat straw combustion in a fixed bed reactor for two different air flow rates to analyze the ignition front speed and burning rate behavior at various combustion conditions. The K-type thermocouples measure the inside bed temperature at different height levels, so the speed of the combustion front can be specified in this order.

Table 13. Classification of experimental works according to measurement usage

Purpose	Combustion system	Measurement				Ref
		Temperature	Volatiles	Emission	Other	
Model validation						
	Wheat straw vibrating grate	✓	O ₂ , CH ₄ , CO ₂ , H ₂	NO, NH ₃ , CO	×	[117]
	Woodchips cylindrical	✓	×	×	Total mass of the bed	[97]
	Single-particle Pyrex reactor	✓	C _x H _y , CO ₂	CO	Axial shrinkage, tar yield	[151]

Wood chip reciprocating boiler	✓	O ₂ , CO ₂	NO _x , SO ₂ , CO	×	[197]
Wood pellet stationary sloping grate	✓	O ₂	NO, CO	Water flowrate in boiler wall plus inlet and outlet temperature	[196]
System evaluation					
Lab-scale furnace	×	×	×	Equivalent flame diameter	[211]
Reciprocating grate furnace	✓	O ₂ , CH ₄ , CO ₂	NO, CO	×	[212]
Single particle combustor	✓	O ₂	×	Combustion camera recorded	[73]
Lab-scale pellet boiler	✓	O ₂ , CH ₄ , CO ₂	CO, NO _x , PM ₁	Primary and secondary air flow	[213]
Lab-scale cylindrical reactor	✓	O ₂ , C _x H _y , CO ₂	CO	Total mass	[209]
Overbed boundary condition					
Straw grate boiler	✓	O ₂ , C _x H _y , CO ₂ ,	CO, NO, SO ₂	Air flow velocity	[214]
MSW sloping grate boiler	✓	O ₂ , CO ₂	CO, NO _x , SO ₂	Air flow velocity	[22,23]
Wood sloping grate boiler	✓	CH ₄ , CO ₂ , H ₂ O	CO, NO, NH ₃	×	[37]

The single wheat straw pellet was inspected to find how different sizes, shapes, primary air temperature, and velocity can influence on thermal and emission aspects within a combustor in a work by El-Sayed and Khairy [215]. Prior to the experiments, a TGA test was performed to obtain the conversion rate characteristics of the test sample under the ambient temperature by 1000 °C and heating rate by 30 K min⁻¹. Two heaters powered 1.0 kW along the primary air inlet duct were mounted to adjust the primary air temperature, and a mechanical scale with an accuracy of 0.1 gm measured the mass loss during tests. In addition, K-type thermocouples were employed and fixed on pellet surface and inside the particle along with IMR 3000P gas analyzer to measure gas species concentration (CO, CO₂, and O₂), while the reactor external surface was insulated with ceramic-fiber material covered by galvanized steel sheet.

Moreover, measurement into the bed can be directly employed as the boundary conditions of the overbed simulation so that bed modeling can be avoided in such cases [21–24]. Stubenberger et al. [28] studied NO_x precursors released during different woody biomass conversion in a lab-scaled batch reactor with measurement in a packed bed. They concluded that under air-rich conditions, NO was more dominant element, while under fuel-rich conditions, NH₃ was the most important precursor. The experiment setup was equipped with two channels to facilitate the species concentration measurement consisting of H₂O, CH₄, CO, CO₂, C₂H₆, C₂H₄, C₂H₂, NO, HCN, N₂O and NH₃ over the bed and several thermocouples within the packed

bed to build up a user-defined function (UDF) as the boundary condition for the overbed zone modeling. For more recent experimental literature, Table 14 is referred.

Table 14. Experimental works on the grate type biomass combustion system; objectives and results

Objectives	Achievements	Ref.
Effect of oxygen excess ratio and exhaust gas ratio (EGR) was studied	EGR is positive for thermal performance and contaminant emissions at low excess air (10-20%)	[190]
Effect of Sodium carboxymethyl cellulose (CMC) on the PM emissions	-In general, adding CMC, increases the PM emission -Addition of CMC to biomass fuels enhances the pellets qualities -PM emissions of rice husk reduced by adding 5 wt% of CMC	[216]
Analyze the release of the NO _x precursors for different fuels in a fixed bed reactor	-NH ₃ /HCN ratio increases for fuels with a higher nitrogen content -NO release decreases with higher nitrogen content	[217]
Inspect impact of excess air (up to $\lambda = 2$) and velocity and cold flue gas recirculation on reaction rate	-higher excess air and velocity leads to higher reaction rate -Cold flue gas can decrease the peak temperature in the combustion chamber, and prevent ash melting -Cold flue gas decreases the reaction rate	[207]
Study the behavior of volatile matters and char residue using the images obtained from flame diameter and average luminous intensity	-Two burning phases including enveloped faint volatile combustion, stable bright char combustion were observed -Two peak points in flame size profile was observed due to the hemicellulose and cellulose devolatilization -Estimated char combustion time to the volatile combustion time increases with the ratio of fixed carbon to volatile matter	[211]
Investigate the role of temperature on the K/Cl/S transformation and fine particle formation during combustion temperature range of 1000-1300°C	-With temperature growth from 1000 to 1300°C concentration of fine particle reduces by about 50% -A certain amount of sulfur in PM ₁ is observed at 1000°C, while it disappears above 1100°C	[218]
Study the feasibility of internal flue gas recirculation technique (IFGRT) on minimizing the NO _x emission while maintaining high thermal efficiency	IFGRT can reduce NO formation through thermal, NNH and N ₂ O routes, as well as reburning mechanism	[70]
Examine behaviour of selected alkali-metals during combustion	-For woody particles, intensive radical CH, OH emissions were observed due to their nature -At low flame temperature 750°C, emission signal from selected metal ions is too weak in order to use for analysis -Sodium and calcium intense radiation occurs at the beginning of combustion from ignition to until pyrolysis stop	[219]
Study effect of feedstock properties and temperature on the PM emission	-For PM ₁ , vaporization-condensation of the alkali compound is the main formation pathway -For PM ₁₋₁₀ , (1) direct transform of CA-/Mg- and Si-rich particles with heterogeneous condensation (2) formation of silicates and phosphates -From temperature from 1073 to 1473 K, total PM ₁₀ decreases and PM _{0.1} increases	[220]

2.3 Uncertainty estimation methods

Uncertainty in various courses can be described in different ways, however, uncertainty is typically the lack of exact awareness, regardless of what is driving factor of this inaccuracy [221]. With a quick look at the biomass conversion steps, the uncertainty is ordinarily observed on every step of the combustion process and analysis. The source of these uncertainties includes broad factors from the randomness of input data with respect to fuel intrinsic variability, sampling and system performance up to the mathematical equations of the kinetic reactions and solution methods. Hence, the uncertainty model should provide a realistic frame of the available knowledge and the possible shortcomings in the modeling results. Uncertainty is mainly represented as the probability distribution that reveals how probably each of the possible outcomes might occur. In literature, overlapping in definitions and classifications of uncertainties are widely observed [221–223], but regarding the engineering problem modeling, they can be generalized and categorized basically into two categories in accordance with belonging nature: stochastic uncertainty, someone might say inherent randomness; and epistemic uncertainty caused by the deficient knowledge which might be removed to some extent by means of more efforts in those particular areas in opposite to the first type which is commonly intractable. As long as the above category is acceptable, the uncertainty stem is presented as following [224]:

1. *Inherent randomness.* Despite we might be aware of the process and the initial conditions, still no one can guarantee what will show up as the outcomes exactly. This sort of randomness can be interpreted as nature inherent, and hopefully can quite often be quantified and manageable within the probabilistic models.

2. *Measurement error.* As it is obvious from the name, it mirrors the uncertainty caused by the measured value of a parameter. To estimate for this type of uncertainty, statistical methods along with several measured samples are required, here the related uncertainty is accountable in probabilistic models.

3. *Systematic error.* it basically originates from a biased sampling in measurements and is not easy to evaluate, therefore, it might be cumulated in the models.

4. *Natural variation.* This type of uncertainty belongs to the change in the natural conditions of the system and so do the parameters. To quantify the uncertainty caused by the parameters, the possible range and its possibilities of the unknown parameter need to be estimated.

5. *Model uncertainty.* Owing to the differences between the natural system and models which are the abstract of reality, this sort of uncertainty will arise. These differences include ignorance of some less critical variables and interactions within the natural system, and moreover, the functions often induce an abstract of real processes. In addition, insufficient knowledge in the proposed course can magnify this uncertainty. The

accounting procedure of the model parameters is carried out in the same way of natural variation, whereas the model structure uncertainty is truly a challenging task to be exercised.

6. *Subjective judgment.* This kind of uncertainty occurs since the data are scarce or error inclined, the interpretation becomes less accurate than the natural system, and as a result, more uncertainty will be generated. In reality, distinguishing the system uncertainties into the mentioned category deals with too many difficulties, however, knowing the various sources of uncertainty can aid the modeler to rationalize and play with these uncertainties.

All of the numerical models of the grate firing biomass furnaces are almost deterministic, resulting in only a single output value respect to each variable, regardless of the uncertainty span or the anticipated variation around this single value. However, what if we know this single value would be never guaranteed by the model, in reality, owing to the different uncertainty mentioned above. Therefore, needs to use the uncertainty methods to take the output variable range into the account becomes crucial. The uncertainty modeling techniques have been increasingly developed in recent decades and they cover a wide range of techniques consist of probabilistic approaches, possibilistic approaches, hybrid possibilistic-probabilistic approaches, optimization approaches, etc. Each of these techniques can be of interest depend on the problem objectives. Owing to the type of our research problem and available measured data, as well as the robustness of probabilistic methods, the focus will be on this method in the following.

2.3.1 Probabilistic approach

This approach is basically assumed that the probability density function (PDF) of the input variables are known. Hence, according to this assumption, the most proper PDF, e.g., Weibull and normal PDF, which fits the uncertain input variable, is selected to model the input variable instead of fixed values.

2.3.1.1 Numerical methods

This method includes different type of Mont Carlo Simulations (MCS), which is of the most frequent and precise stochastic approaches by which it is employed since the system is highly complex and nonlinear. This can be attributed to the fact that this method is system-size independent. In general, the MCS follows the iterative procedure as follows:

Phase 1: set MCS counter c to 1

Phase 2: generate a random sample for the vector X by means of the PDF of each input variable x_i

Phase 3: calculate y_c using PDF as $y_c = f(X)$

Phase 4: calculate the expected value of y as $E(y) = \frac{\sum_c y_c}{c}$

Phase 5: calculate the variance of y , $\sigma(y) = E(Y^2) - E^2(Y)$

Phase 6: if stopping criteria is met go to the end, otherwise, set counter $c=c+1$

The MCS method is a very powerful method that supports all probability functions and it is relatively easy to implement when the problem is non-differentiable and complex. On the other hand, the count of simulation will increase as the degree of freedom of the solution space rises, which means more than thousands of simulation and millions of computational iterations, and is pondered as the weakness of the MCS method as well.

2.3.1.2 Analytical methods

This approach models the system and its inputs by means of the mathematical equations such as PDFs and fitting the given data to a mathematical expression. The main idea behind the analytical approach is to carry out the algebra with PDFs of the random input variables. This approach would be more attractive since the complexity of the system is presumed from the small scale up to the middle scale.

2.3.2 Bayesian method

A more comprehensive method to tackle with uncertainty is Bayesian model averaging (BMA) by which provides us to take advantage of results to replace the specifications in terms of posterior distributions with the coefficients and models. The main advantage of the BMA model is to use the prior belief or data about the purpose parameters in the uncertainty estimation. BMA became superior in statistics within the mid-90s and proceeded in the courses, e.g. economic, biology, ecology, and public health. Here could be said that BMA is particularly useful among three individual contexts. BMA is recognized rather informative since one wants to evaluate the evidence through two or more competitive measures of the same concept especially when there would be considerable uncertainty amongst the input variables. The second application is when there is uncertainty through the control variables, BMA can be applied to assess the robustness of the estimation in a more systematic way. Lastly, BMA might be used to estimate the impacts of large numbers of the possible predictor of an influential dependent variable. The Bayesian theory provides the probability of an event given the probability of another event that has already happened, and is mathematically presented as follows:

$$P(y|X) = \frac{P(X|y) P(y)}{P(X)}$$

Where y is class variable and X is observed feature vector of size n which can be described as:

$$X = (x_1, x_2, x_3, \dots, x_n)$$

Now, with an assumption of independency between elements of X, we can expand the formula:

$$P(y|x_1, \dots, x_n) = \frac{P(x_1|y)P(x_2|y) \dots P(x_n|y) P(y)}{P(x_1)P(x_2) \dots P(x_n)}$$

$$P(y|x_1, \dots, x_n) = \frac{P(y) \prod_{i=1}^n P(x_i|y)}{P(x_1)P(x_2) \dots P(x_n)}$$

$$P(y|x_1, \dots, x_n) = \frac{P(y) \prod_{i=1}^n P(x_i|y)}{\sum P(y) \prod_{i=1}^n P(x_i|y)}$$

$$P(y|x_1, \dots, x_n) \propto P(y) \prod_{i=1}^n P(x_i|y)$$

Recently, Bayesian model has been widely deployed to address uncertainty in input variables and measurement, input model, etc. A BMA method was utilized to map the input variables uncertainty on the future energy projection model [225]. The authors mentioned that quantification of uncertainty assists in predicting the potential energy scenarios and lets an investigation of possible consequences as progressed by energy scenarios in a highly uncertain economic, political, and environmental system. To avoid missing uncertainty associated with flood inundation, Liu and Merwade [226] applied BMA to combine ensemble predictions from variant hydraulic models to create a robust distributional prediction. It was pointed out that although BMA does not always outperform the best model in the ensemble, it predicts better than the ensemble mean prediction and provides the reliable deterministic flood stage projection. Yen et al. [227] applied the normally distributed random noise to the input parameters of a watershed process modeling to investigate whether the uncertainty model can perform better. It was concluded that using these random noises cannot guarantee the uncertainty model improvement, and should be carefully considered. More theoretical discussion on the Bayesian uncertainty method can be found somewhere [228,229].

2.4 Research gaps

From the literature review, the following conclusions and gaps were derived which can be helpful for system diagnosis and modification, and the attention could be paid to them in future studies.

1. From the review of the literature, it can be concluded that the properties of biomass fuels in the forms of wood chips, pellets, straw, etc. can vary to a significant extent. Fuel shape, size, and composition variability likely to have a further impact on combustion stability and efficiency. It is thus recommended to consider these fuel variabilities into the combustion uncertainty.

2. The solid particles column in the packed bed continuously moves during the conversion due to the particle collapse and bed shrinkage. These collapses significantly influence the local conversion rate in the bed, which should be taken into account to increase the accuracy of models.
3. Heat generation from radiative heat transfer mechanism in the bed was recognized a considerable amount based on earlier research especially since the moisture evaporates. Here the particle size has the prominent role to play on the absorption of this radiation heat which accelerates drying and devolatilization of biomass particles. By virtue of modeling complexity respecting the different particle sizes in the packed bed, most models assume the same particle size over the grate and consequently, they ignore this radiative effect variation through the models.
4. Mapping of biomass particle combustion properly to mathematical model involves many challenges which of key parameters are thermophysical properties, e.g., specific heat capacity, effective thermal conductivity, mass dispersion, etc. These factors must be chosen suitably in order to generate a relatively precise model. Nevertheless, these thermophysical properties may not be credible from many aspects like an incompatibility between the extracted lab-based model and the purposed modeling condition resulting in a meaningful error in some works. Also, the given lab-based models are valid in a certain temperature range while it could be in contradiction with the current model condition.
5. Thanks to data science development within many different research areas in recent years, the application of data science should be vigorously developed in biomass combustion studies. For example, a high-speed infrared imaging tool is able to deliver the pure and accurate data during the biomass combustion, and these data could be analyzed and learned using machine and deep learning techniques to construct data-driven models.
6. Apart from the thermochemical properties of biomass conversion, some geometrical characteristics of moving grate combustors are still not well recognized. Among all, grate hole arrangement and angle, grate to secondary air nozzles span adjustment, and the combustion chamber shape are recommended to be studied by a numerical simulation tool from aspects of the mixing rate, pollutant emission, and thermal performance.
7. In the past decade, research has mainly focused on analysis of the biomass combustor performance from thermal, chemical and pollutant viewpoints and valuable accomplishments have been reported. However, economic analysis of biomass furnace applications such as replacing a fossil fuel boiler with a biomass boiler or modification of an existing biomass system has been almost disregarded to a large extent. A 3E (energy-economic-environment) analysis of a grate firing boiler using ships or hospitals wastes to produce heat and power instead of storage and disposal of them would be a future research area. This can particularly resolve the great issue of carrying the garbage by ships during a

long journey on seas. By using such a system not only they can get rid of the garbage but also it would be a great energy resource instead.

In what follows in this thesis, items 1, 2, 4, and 7 will be addressed and discussed. A numerical model regarding biomass combustion on the moving bed furnace will be developed so that to facilitate the research objectives. Mathematical terms and coefficients will have opted for the best match with the experiment. Then, fuel composition variability quantified with Bayesian analysis will be deployed in the combustion model. An economic analysis of using the biomass boiler for the heating purpose will be completely examined. LCA of replacement of coal combustor with biomass-fueled one will show the environmental consequences of biomass use.

3 FUEL COMPOSITIONS AND BAYESIAN METHOD

This chapter aims to quantify the fuel compositions variability taking the advantages of the Bayesian probabilistic method. A description of the uncertainties method is given with a focus on the Bayesian method. In a laboratory, a set of randomly selected fuel particles are tested to gather the particle compositions data, and in the combination of measured data and declared values by fuel supplier, the Bayesian model is formed. Thanks to our Bayesian model, the uncertainty interval of fuel compositions is provided and can be applied in the numerical model.

A version of this chapter was published as: " Hosseini Rahdar, M.; Nasiri, F.; Lee, B. Effect of Fuel Composition Uncertainty on Grate Firing Biomass Combustor Performance: A Bayesian Model Averaging Approach. Biomass Conversion and Biorefinery 2020. "

3.1 Bayesian method

The Bayesian analysis uses the probability statements to specify the unknown parameters within the statistical model. It relies on the assumption that all model parameters are random values based on prior knowledge. The Bayes' theorem is used to build up the posterior distribution of the model parameters which is updated from the prior knowledge of model parameters and the observed data about the parameters. Then, the formed posterior distribution is used to obtain data such as posterior mean, medians, uncertainty intervals, etc. Moreover, every statistical test on the model parameters can be represented in terms of a probability distribution based upon the obtained posterior distribution function. Hence, the posterior expression is a function of two important terms so-called prior and likelihood distribution.

Bayesian model perfectly fits the statistical problems with two data set. For the current study as there is a data set for predefined fuel composition values and another one for sampled fuel composition, Bayesian is an ideal choice in place of other common uncertainty estimator model such as Monte Carlo simulation.

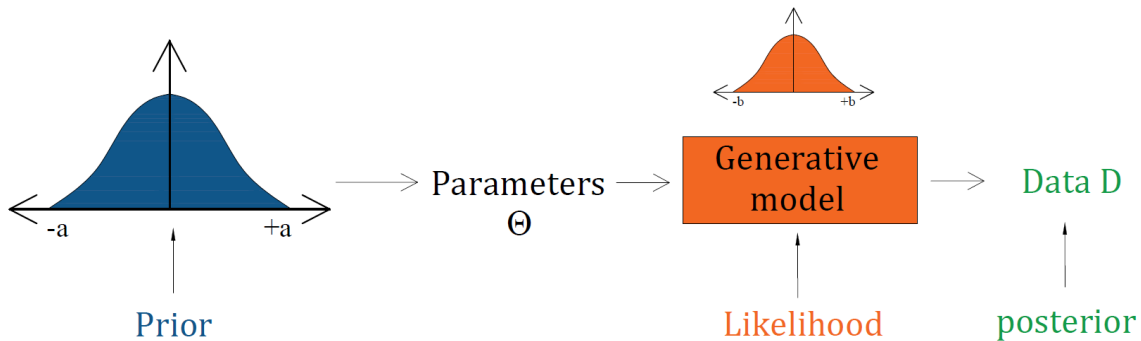


Figure 11. Diagram of Bayesian modeling implementation

The general form of conditional Bayesian probability rule is as follows:

$$p(B|A) = \frac{p(A|B)p(B)}{\sum p(A|B)p(B)} \quad (32)$$

where A and B are both random variables. $p(B)$ gives probability of variable from prior distribution and $p(A|B)$ gives the probability of the chosen variable from prior distribution in likelihood distribution. From Figure 11, the process begins with the formation of prior and likelihood distribution based upon our prior and measured data. Next, a value for the purposed variable is randomly picked from the prior distribution and then, is mapped in the likelihood distribution. This process repeats for tons of times to provide a big amount of data and using the Eq. 32), the posterior distribution can be created. This posterior model, which is highly dependent on the number of measured data to some extent, then it can deliver uncertainty interval and the high probably expected value of fuel composition.

3.2 Experiment on biomass fuels

For examining the fuel composition uncertainty, 30 samples of the Switchgrass pellet were randomly picked from the different pellet bags. The experiments were carried out on a TGA lab thermobalance, which can heat up to 1800 K with heating rate range between 0.01 to 50 °C/min. The pellet samples on the weight of 33×10^{-6} kg was finely ground and put on the platinum crucible of the TGA apparatus according to ASTM E870 (Figure 12).



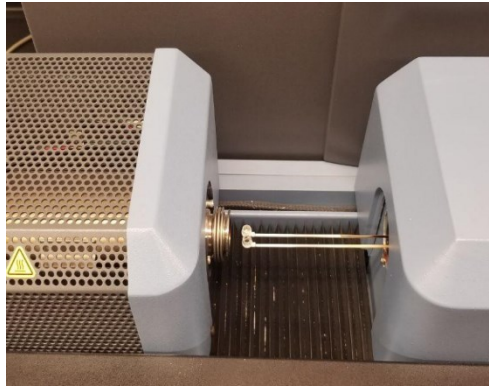


Figure 12. TGA device setup for biomass composition experiment

The amount of 12 mg of ground fuel is placed on crucible. The experiment was initiated under the inert environment of the nitrogen with a rate of 50 mL/min to avoid the ground fuels from oxidation in order to specify the moisture and volatile matter concentration. In the end, the experiments were terminated via dry air flow 50 mL/min to determine the ash content so as in this way, the fixed carbon can be easily defined by subtracting moisture, volatile and ash weight percentage from 100. The rate of temperature change in each step was determined as scan rate in Table 15.

Table 15. Temperature evolution progress in the TGA experiment

Step	1	2	3	4	5	6	7	8	9	10	11	12	13
T _{start} (K)	303	343	363	378	378	418	418	773	773	873	873	873	973
T _{end} (K)	343	363	378	378	418	418	773	773	873	873	873	973	973
Scan rate (K/min)	30	15	2	0	10	0	10	0	20	0	0	20	0
Time (s)	80	80	450	1800	240	600	2130	3600	300	600	2400	300	600
Reactant	N ₂	Air	Air	Air									

Referring to Table 15, the steps 1 to 4 were implemented to obtain the moisture content followed by the steps 5 to 10 regarding the volatile matter determination, and finally, the ash content of biomass particles was achieved through the steps 11 to 13. Indeed, within these steps, the other thermal properties of the fuel can be specified which are out of the scope of this section. During the experiments, the samples were weighted in the crucible as they are uniformly spread to diminish the measurement error in addition to the ignorance of the particle thermal gradient owing to the fine particle size.

Table 16. Measured compositions (Moisture, volatile, carbon and ash)

Sample #	Measured data			
	M%	V%	C%	Ash%
1	8.5	65.98	22.52	3
2	9	69.44	19.05	2.51
3	11	63.09	21.39	4.52
4	10.55	66.34	20.52	2.59
5	11.51	63.92	18.57	6
6	13.11	63.37	21.52	2
7	12	60.88	23.59	3.53
8	14	62.41	17.59	6
9	9.55	66.95	20	3.5
10	13.32	61.6	19.57	5.51
11	12.01	62.33	19.25	6.41
12	11.87	64.8	20.41	2.92
13	13.2	59.24	21.12	6.44
14	12.24	60.1	21.34	6.32
15	11.21	66.85	18.97	2.97
16	10.87	64.9	19.28	4.95
17	10.12	63.95	20.17	5.76
18	10.98	64.6	21.11	3.31
19	9.81	62.73	21.34	6.12
20	12.05	65.6	20.43	1.92
21	11.36	61.2	20.61	6.83
22	12.14	63.78	19.71	4.37
23	13.15	65.32	18.99	2.54
24	11.36	62.57	20.54	5.53
25	12.17	61.4	21.32	5.11
26	10.25	62.08	20.97	6.7
27	11.09	64.53	19.87	4.51
28	10.98	63.33	21.87	3.82
29	11.37	67.61	18.77	2.25
30	10.58	65.35	20.39	3.68

The ground sample was heated up on 378 K in the nitrogen environment once a constant weight was obtained. The lost weight was considered as moisture content (M%) which can be achieved through the

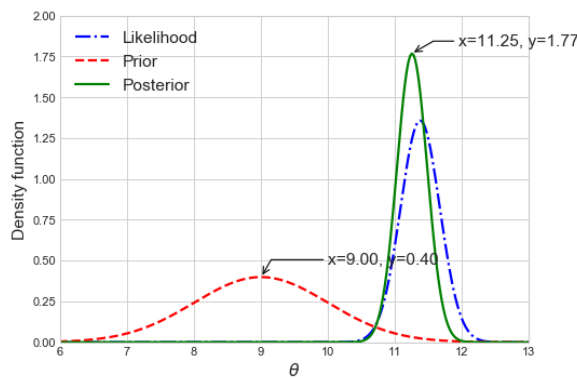
following relation: $100 \times \frac{(m_1 - m_2)}{m_1}$, where m_1 is initial fuel weight and m_2 the constant weight of sample at 378 K. Similarly, volatile matter (V%) was determined using sample weight difference on the steps 5 and 10 in the nitrogen atmosphere using the formula: $100 \times \frac{(m_2 - m_3)}{m_1}$, where the m_3 means the fuel mass by 873 K. The remaining inorganic mass after complete combustion was measured as the ash weight (m_4), so the ash content (Ash%) was calculated via $100 \times \frac{(m_4)}{m_1}$. Consequently, the fixed carbon (FC) was calculated using $FC = 100 - (M\% + V\% + \text{Ash}\%)$. The measurement results of samples are shown in Table 16, based on the composition content including moisture, volatile, char, and ash. In the next section, these data will be utilized to address the fuel composition uncertainty.

Table 17. Declared primary biomass pellet characteristics by supplier

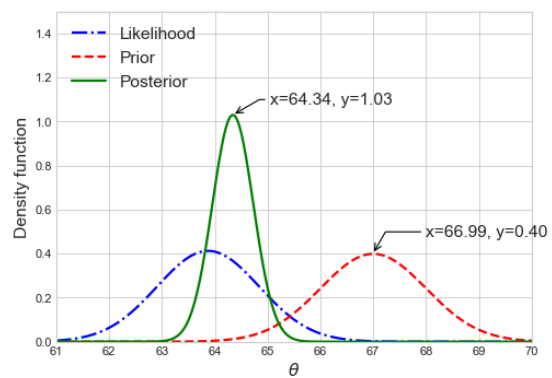
Moisture (%)	Volatile (%)	Fixed carbon (%)	Ash (%)	HHV
9	67	22	2	18.72
C (%)	H (%)	O (%)	N (%)	S (%)
44.49	5.25	42.4	1.28	0.29

3.3 Uncertainty estimation

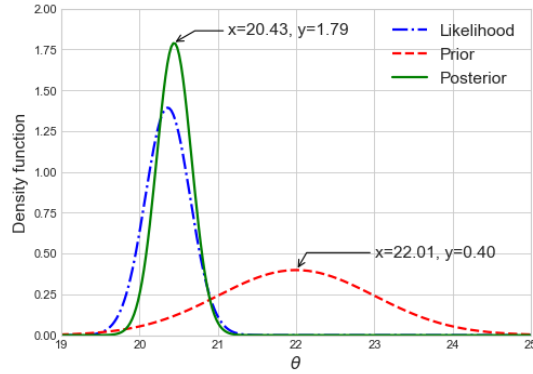
On the BMA method basis, the prior and measured data are employed to achieve a credible interval of uncertainty for each fuel composition separately. Here the prior function is obtained according to prior given data from fuel supplier which reported in Table 17. Since no fuel characteristic deviation was reported by the supplier, it is supposed as one percent for each composition. Then, the likelihood function will be counted using the measured data, Table 16, and a posterior function will be presented by Eq. (32).



(a)



(b)



(c)

Figure 13. Prior, likelihood and posterior distribution of (a) moisture content, (b) volatile matter, and (c) char based on Bayesian model

The standard deviation interval of each composition, which is used to phase in the possible range of compositions values, is estimated using the Bayesian analysis. These intervals are governed in combustion model as the fuel composition inputs which results in an output range instead of the spot results. Table 18 sorts out the mean value and that of the standard deviation for the moisture, volatile, and char content in fuel samples derived from obtained posterior function. The prior, likelihood and posterior curves for each fuel composition are visualized through Figure 13.

Table 18. Mean and standard deviation for moisture, volatiles and char composition

Composition	Mean	Standard deviation
Moisture	11.25	0.25
Volatiles	64.34	0.45
Char	20.43	0.30
Ash	3.98	0.25

4 NUMERICAL MODELING OF COMBUSTION

This chapter describes the numerical model for moving grate biomass combustion. First, the boundary of the intended system is defined followed by chosen mathematical models of conversion sub-processes; drying, devolatilization and char combustion. Initial and boundary conditions of bed are deliberately described. Finally, the combustion model is integrated with fuel composition uncertainty, and the solution algorithm is introduced.

4.1 Background

A comprehensive combustion modeling of an industrial biomass furnace consists of reaction processes into the packed-bed and the overbed region. The bed conversion process which occurs on the moving grate is a daunting phenomenon due to the heterogeneous reactions and nature of solid biomass fuels accompanied by the intensive heat and mass transfer in the solid and gas phase. Contrarily, within the overbed zone, homogeneous reaction of gas species occurs, and simulation of the process deals with less complexity than the bed zone conversion. The schematic configuration of the moving grate biomass furnace is illustrated in Figure 14. This research mainly focuses on the modeling of solid-gas phase bed conversion although the gas reaction properties in the overbed zone are fairly considered in order to quantify the effect of biomass compositions variability on furnace outputs.

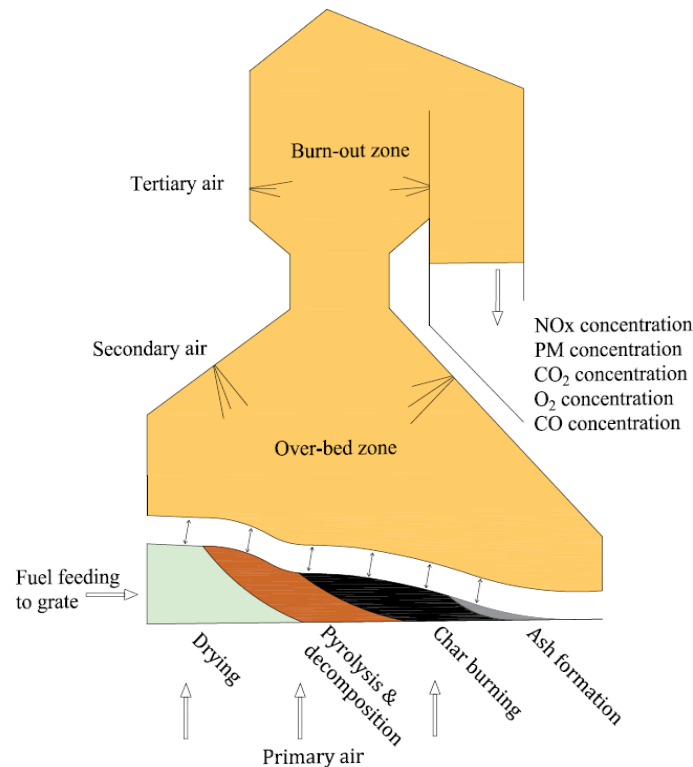


Figure 14. Schematic of the moving grate biomass combustor with the reacting fuel bed

A one-dimensional transient model so-called walking column method is deemed for simulation of fuel bed conversion. Three heat transfer mechanisms consisting of radiation, convection and conduction, drive the conversion process while it is accelerated by chemical reactions inside the particles from a certain step. The radiation mechanism dominates the conversion for the particles on the bed surface until the moment of char combustion initiation, and from this moment the chemical reaction of carbon sways the process. A thin layer of reaction zone maintains on the bed top, and it quickly propagates to the grate surface when the char combustion is triggered for the surface particles. For the thick layer of fuels under the reaction zone, conduction and conversion mechanisms dominantly control the heat transfer so that convection is the controlling mechanism at the drying phase whereas conduction sways heat transfer at the rest of the process. Figure 15(a) demonstrates the existing heat transfer mechanisms inside the bed in which the radiation between particles is overlooked in the model. Since the surrounding particles in the bed are in the close temperature, ignorance of mechanism 3 would not cause a meaningful dispersion.

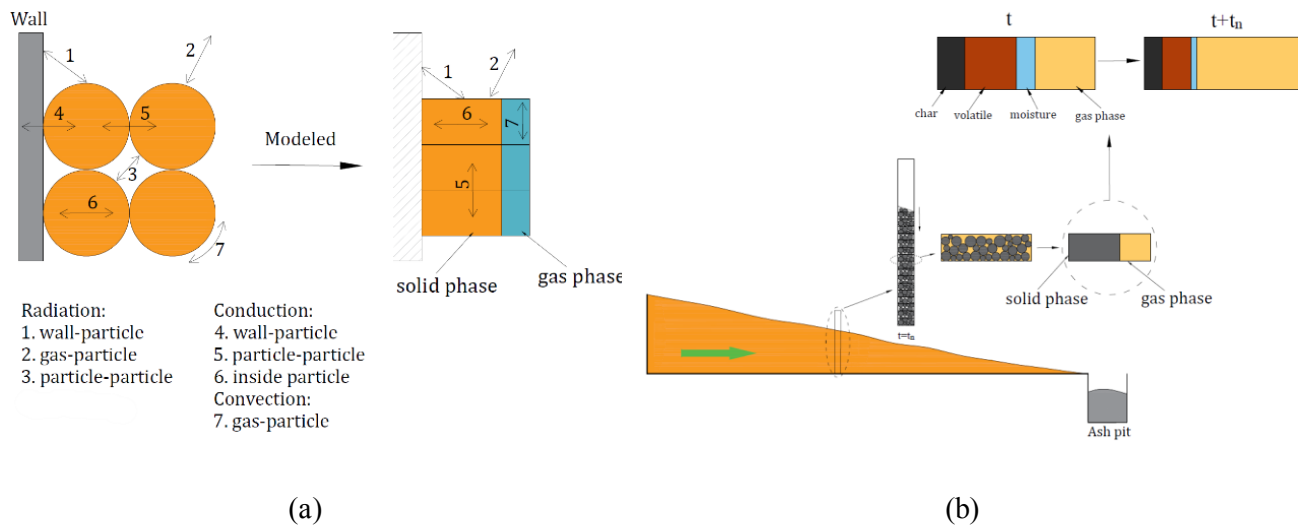


Figure 15. Modeling perception in terms of continuous medium approach in a moving grate combustor; (a) heat transfer mechanisms within the bed, (b) process simulation in walking column

In the system-scale, however, a narrow walking column is analyzed in 1D vertical space and the other direction is mapped out via time. Figure 15(b) portrays how the walking column is split to small cells, and each cell is simulated via approach presented in Figure 15(a). The solid phase of cells including moisture, volatiles, and char is converted to gases over time until all mass turns in gas. Following assumption have been made for the bed combustion modeling:

- The reaction in the bed only occurs along the vertical direction and horizontal gradient is negligible, so the assumption of one-dimensional modeling is credible.

- The fuel ignitor is installed in the overbed zone and the reaction front develops toward the grate.
- The fuel properties along the width direction of the bed are propagated uniformly so modeling in that direction is out of interest.
- The gas behaves such as ideal gases.
- The gas-phase species are presumed to be CO, CO₂, O₂, H₂, H₂O, CH₄, C₆H₆, NH₃, HCN and N₂.
- The particles are thermally thin.
- The solid phase momentum is negligible.

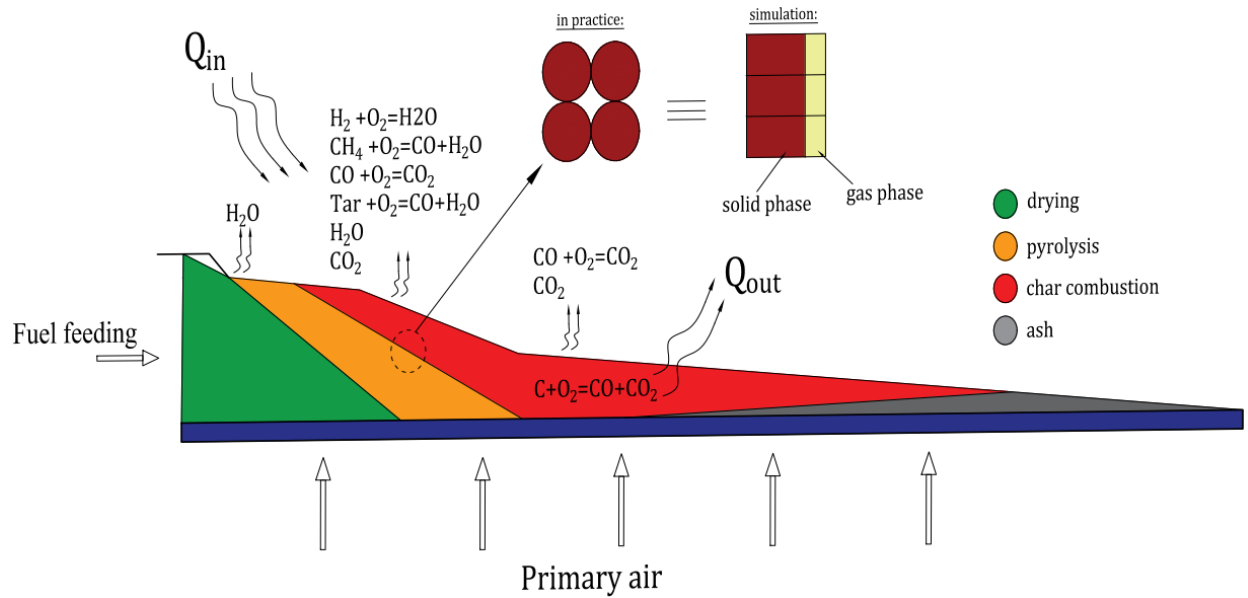


Figure 16. A simplified biomass bed conversion perspective

4.2 Conversion process

4.2.1 Drying

Drying is an endothermic process occurring in the vicinity of the boiling point dominantly under the diffusion mechanism (Figure 16). The heat balance model is selected to simulate the drying process in this work due to its ability to follow the trend of evaporation process. The effect of overheat is addressed in this model by adding coefficient of 0.5 so that only a part of the heat is exploited to evaporate the existing moisture and the rest will increase particle temperature [122].

$$\frac{d\rho_M}{dt} = \begin{cases} -0.5 \frac{\rho_p C_p (T_s - T_{evap})}{LH \Delta t}, & T_s \geq T_{evap} \\ 0 & \text{Otherwise} \end{cases} \quad (33)$$

4.2.2 Pyrolysis and decomposition

Since the volatile matters compose most of the biomass content, the devolatilization step is important among the whole conversion process. The experiments have revealed that the pyrolysis is a wide series of interlinked reactions in which only one kinetic expression is not able to sufficiently model the behavior of these reactions. Here the pyrolysis is modeled using the three parallel reactions approach. Then, the total mass loss of particles during the pyrolysis reaction is the summation of all three reactions. At the end of the pyrolysis reaction, the particle will convert to the char but, it is not the only source of existing char in this step but, some part of tar converts to char as well as (Figure 17).

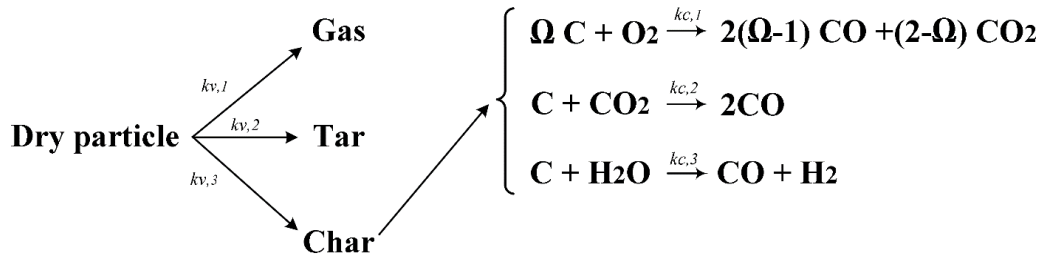


Figure 17. Devolatilization and char reaction mechanisms

Referring to the general formula in Eq. (11), the devolatilization rate is obtained via summation of Arrhenius terms given in Table 19. Based on the pyrolysis rate, mass fraction converting to the char is calculated using the Eq. (41).

Table 19. Arrhenius kinetic rate of devolatilization and char combustion

#	Kinetic reaction model	
$k_{V,1}$	$1.44 \times 10^4 \exp(-88.6 \times 10^3 / RT_s)$	(34)
$k_{V,2}$	$4.13 \times 10^6 \exp(-112.7 \times 10^3 / RT_s)$	(35)
$k_{V,3}$	$7.38 \times 10^5 \exp(-106.5 \times 10^3 / RT_s)$	(36)
$k_{C,1}$	$4 \times 10^3 \exp(-8 \times 10^4 / RT_s)$	(37)
$k_{C,2}$	$3.6 \times 10^4 \exp(-1.76 \times 10^8 / RT_s)$	(38)
$k_{C,3}$	$3.42 \exp(-1.297 \times 10^8 / RT_s)$	(39)
Ω_c	$\frac{2(1 + 4.3 \exp(-3390/T_s))}{2 + 4.3 \exp(-3390/T_s)}$	(40)

To determine the amount of volatile species released from the reacting biomass particle, mass fraction of each particular element is deemed according to the experimental results [230]. The corresponding source term of the gas phase species is known by means of Eq. (42) when the mass fraction of them was obtained.

In course of tar, it is assumed to be benzene with chemical formula C_6H_6 and LHV 26 MJ/kg [231], in addition, heat reaction of pyrolysis is approximated to take 300 kJ/kg [232].

$$Y_{V,c} = \frac{k_{V,3}}{\sum_{i=1}^3 k_{V,i}} \quad (41)$$

$$S_{V,k} = -Y_{V,k} \frac{d\rho_{dry}}{dt} \quad (42)$$

4.2.3 Char oxidation and gasification

Since the volatile matters escape from particle mass, the char is formed which instantly begins to react with oxygen on the mass surface resulting mainly in CO and CO₂ as depicted in Figure 16. Despite the char contains a small amount of oxygen, hydrogen, and nitrogen, it is assumed that the char is pure carbon by which this simplification is in the sacrifice of very small dispersion. During the char burnout, the density of the char is presumed to remain constant over the whole particle volume. In this work, the heterogeneous reaction of char with the gaseous is considered to occur by means of three parallel reactions and the reaction of char with the hydrogen is easily neglected for simplicity. Please refer to Figure 17 for the intended reactions, and as it is obvious in the reactions, CO and CO₂ are the major reaction products. Kinetic rate of these three reactions is sorted in Table 19 along with the stoichiometric coefficient of the char oxidation. The effective char conversion rate relies on the chemical reaction rate and on the diffusion rate to the particle surface as well. This simplified model ignores the decaying effect of gasification while it moves toward the fuel interior which this simplification has a tiny deviation compare to the intrinsic model. As the pyrolysis and char reaction overlap in thermally thick particle, in this course, the volatile emission decays the diffusion of the reactants to the particle, and therefore, the parameter f_b is assigned to address this.

$$\frac{d\rho_{C,j}}{dt} = -f_b M_C \Omega_C k_{eff,C,j} \quad (43)$$

$$k_{eff,C,j} = A_{sp} \frac{k_{C,j} h_{m,i}}{k_{C,j} + h_{m,i}} C_i \quad (44)$$

$$f_b = 1 - \frac{\rho_s}{\rho_{s,0}} \quad (45)$$

$$S_{C,kj} = \Omega_{k,j} \frac{M_k}{M_C} \frac{d\rho_{C,j}}{dt} \quad (46)$$

where j is count for char reactions, i is reactant O_2 , CO_2 , and H_2O , C_i means the molar concentration of the reactant, $S_{C,kj}$ is the gas phase source term corresponding to the char consumption, M_k and M_C are molecular weight of the species and carbon, respectively. The mass transfer coefficient h_m can be calculated in associated with the diffusion coefficient as follows:

$$h_m = \frac{ShD_f}{d} \quad (47)$$

$$D_f = 3.49d \left(\frac{T_m}{1600} \right)^{1.75} \quad (48)$$

where Sh , D_f , d are the Sherwood number, diffusion coefficient (cm^2/s), and particle diameter (cm) respectively. The Sherwood number which is the ratio of the convective mass transfer over the mass diffusivity represents the effectiveness of the mass convection at the surface and is a function of Reynolds (Re) and Schmidt (Sc) number as well.

Moreover, the reaction heat associated with each endothermic and exothermic conversion reaction including drying, pyrolysis and the char oxidation is given in Table 20, and consequently, the total heat source of conversion can be obtained as follows:

$$S_{Q,s} = \sum_{\rho_s} \Delta H_{r,j} \frac{\partial \rho_{s,j}}{\partial t}, j = \text{drying, pyrolysis, char burning} \quad (49)$$

Table 20. Reaction heat of evaporation, pyrolysis, and char oxidation

Reaction heat	Value
H_{mois}	-2.2465×10^6
H_{V1-3}	-3×10^5
H_{C1}	-14.3833×10^6
H_{C2}	-10.95×10^6
H_{C3}	$(2(\Omega_C - 1)9.8 \times 10^6 + (2 - \Omega_C)33.1 \times 10^6)/\Omega_C$

Lumping the above coefficients and sub-models into the governing equation mentioned in Table 11 forms the system of partial differential equations which simulates the conversion of solid fuels inside the bed. Through these equations, S_{reac} is drying/devolatilization/char combustion rate, S_g is set to zero, $S_{g,i}$ is generation/consumption rate of gaseous species, S_s means heat absorption/generation during drying/devolatilization/char combustion processes, ϕ the bed void fraction, Y_i is species mass fraction. Table 21 displays the other gas and solid fuel characteristic functions and coefficients employed in the governing equations in this work.

Table 21. Arrhenius kinetic rate of devolatilization and char combustion

Property	Value	Ref.
Gas heat capacity, $C_{p,g}$	$(0.99 + 1.22 \times 10^{-4}T_g - 5.68 \times 10^3 T_g^{-2}) \times 10^3$	[153]
Gas viscosity, ν_g (m/s)	0.15	[98]
Gas thermal conductivity, λ_g	$4.8 \times 10^{-4}T_g^{0.717}$	[98]
Solid heat capacity, $C_{p,s}$	$\sum_k Y_k C_{p,k}$, k=drying, pyrolysis, char burning	[122]
Effective solid conductivity, λ_{eff}	$\sum_k Y_k \lambda_k$, k=drying, pyrolysis, char burning	[122]
Bed void fraction, ϕ	0.42	[122]
Emissivity, ω	0.85	[122]
diffusion coefficient, m ² /s	D_{H_2O-air}	0.219 [233]
	D_{H_2-air}	0.611 [233]
	D_{CO_2-air}	0.138 [233]
	D_{CO-air}	0.162 [233]
	D_{CH_4-air}	0.196 [233]
	D_{O_2-air}	0.178 [233]
	$D_{C_6H_6-air}$	0.119 [233]
Updating term	$D_{AB} = D_{AB,ref} \left(\frac{T_g}{T_{ref}}\right)^{1.75}$	[234]
shrinkage	$\frac{V}{V_0} = 1 - a_1(M_0 - M) - a_2(VM_0 - VM) - a_3(C_0 - C)$	[142]
	$a_1 = 0.1, a_2 = 0.15, a_3 = 0.75$	

Table 22. Conservation equations regarding the solid and gas phase of fuel packed bed conversion

Gas-phase governing equations	
Mass	$\frac{\partial}{\partial t}(\phi \rho_g) + \nabla(\phi \rho_g v_g) = S_{mois} + S_{vol} + S_{char}$
Momentum	$\frac{\partial}{\partial t}(\phi \rho_g v_g) + \nabla(\phi \rho_g v_g v_g) = -\nabla P_g + F(\bar{v}_g)$

$$\text{Energy} \quad \frac{\partial}{\partial t}(\phi \rho_g c_{p,g} T_g) + \nabla(\phi \rho_g v_g c_{p,g} T_g) = \nabla(\lambda_g \nabla T_g) + hS(T_s - T_g) + S_g$$

$$\text{Species} \quad \frac{\partial}{\partial t}(\phi \rho_g Y_i) + \nabla(\phi \rho_g v_g Y_i) = \nabla(\phi \rho_g D_{g,i} \nabla Y_i) + \phi S_{g,i}$$

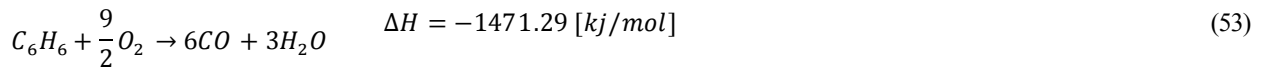
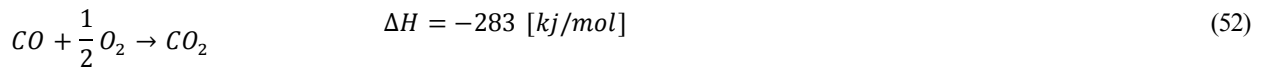
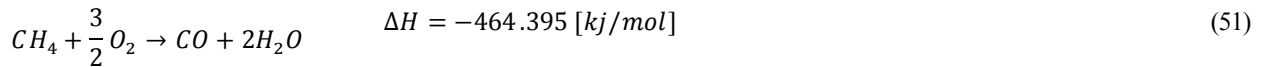
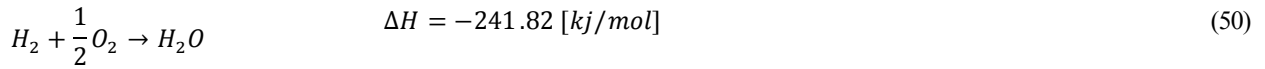
Solid-phase governing equations

$$\text{Mass} \quad \frac{\partial}{\partial t}((1 - \phi) \rho_s) = -S_{mois} - S_{vol} - S_{char}$$

$$\text{Energy} \quad \frac{\partial}{\partial t}((1 - \phi) \rho_s c_{p,s} T_s) = \nabla(\lambda_{eff} \nabla T_s) + hS(T_g - T_s) + S_s + S_{rad}$$

4.3 Gas phase reactions

Outflowing gas species from solid fuel conversion are presumed to be CO, CO₂, CH₄, H₂, H₂O, C₆H₆, NH₃ and HCN which some react with oxygen mainly in the overbed zone. Homogeneous gas-phase reactions [201] together with the corresponding enthalpy of reaction are presented in Eqs. (50-53). The overbed gas-phase reactions along with the char combustion reaction inside the bed eventually form the source of heat generation in the combustion chamber. It must be noted that the share of primary and secondary air from total air flow is 40% and 60% respectively.



Useful output heat of the combustor can be calculated using Eq. (6) where N_f is mole of fuel, $h_{s,f}$ sensible enthalpy of fuel, $h_{s,i}$ sensible enthalpy of each products, h_{fg} latent heat of water vapor, and q_{loss} is heat leakage [235]. It is assumed that flue gases leave the stack at the temperature 400 K.

$$q = h_{s,f} + HHV + \frac{N_{air}}{N_f} h_{s,air} - \sum_{i=1}^I \frac{N_i}{N_f} h_{s,i} - \frac{N_{H_2O}}{N_f} h_{fg} - \frac{q_{loss}}{\dot{N}_f} \quad (54)$$

4.4 Solution algorithm

Eventually, the governing equations of the solid and gas phase from Table 22 are handled to mathematically portray biomass conversion in the moving bed. The solution algorithm for numerical model of combustion considering the uncertainties in biomass composition is presented in Figure 18. The model is implemented in the Python software, where the conservation equations are discretized using finite difference methods (FDMs).

FDM is a well-documented method which suitably fits the simple geometries. A fully implicit scheme BTCS is picked to resolve the energy equation for solid phase (heat equation), upwind scheme for gas-phase mass and momentum equations using backward difference in time and central difference in space and finally, an upwind scheme for gas-phase energy and species equations (advection-diffusion equation) using backward difference in time, forward difference in first-order derivative term and central difference for second-order derivative term. Although the selected schemes are unconditionally stable, the accuracy of the solution will be protected by choosing the proper step size. Varied time steps (10^{-2} to 10^{-3} s) were picked along with 100 grid cells to simulate the conversion process in the bed. As most elements of the time-space matrix were zero, a sparse matrix method was used to speed up the solution procedure.

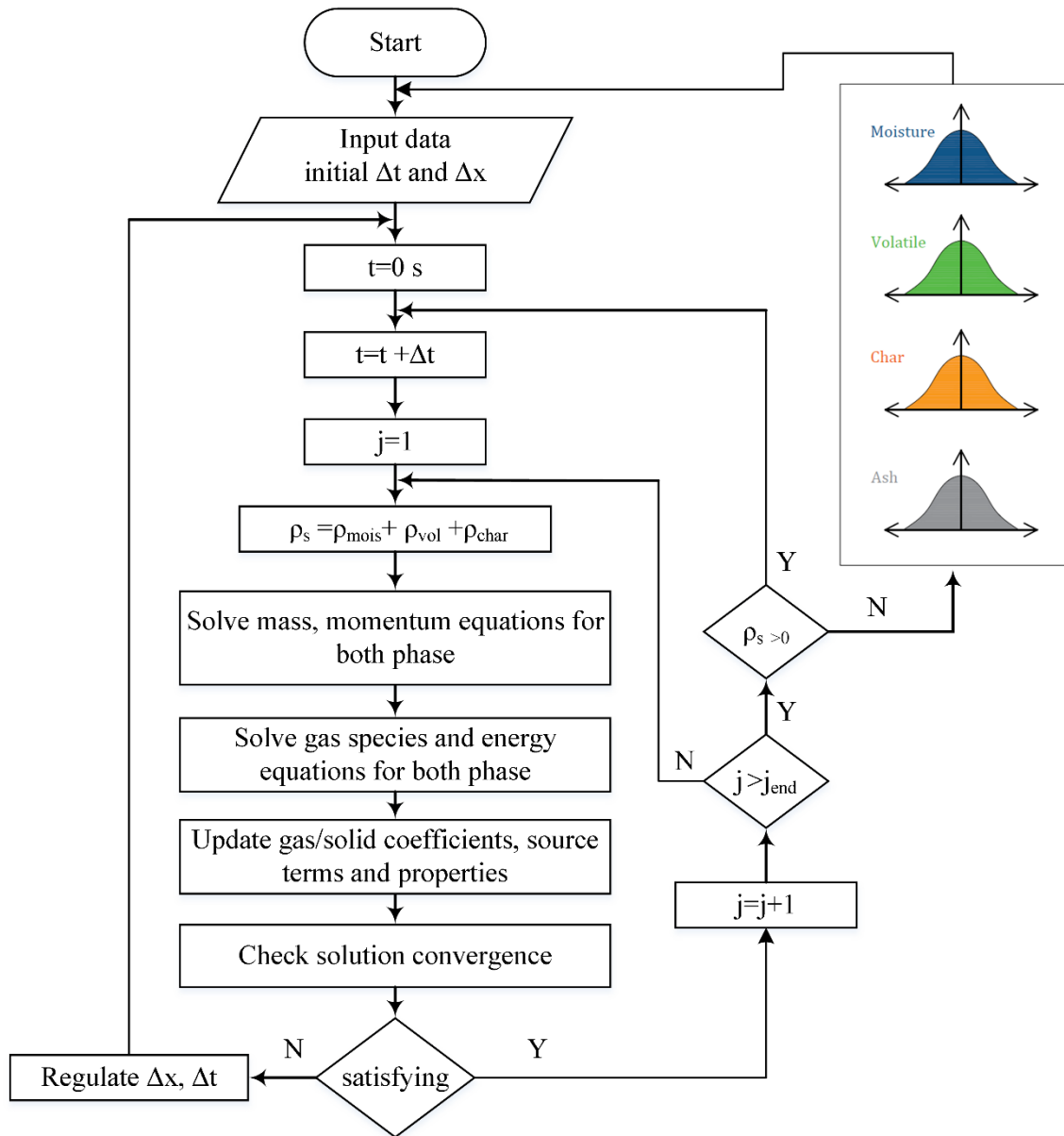


Figure 18. Solution algorithm of biomass combustion integrated with uncertainty model in terms of composition variability

5 RESULTS AND DISCUSSION

In this chapter, after validation of the model, results of the research are presented in three sections. In the first section, the model is employed to evaluate the biomass boilers operation under the three most common fuels from thermal, economic, and environmental views. In the next section, the variability of fuel composition is measured via TGA experiment, and relevant standard deviation is governed in the model to gauge combustion uncertainty for two different biomass fuels; bamboo chips and biomass pellets. In the last section, the developed Bayesian model is applied in order to take advantage of prior fuel data in addition to the measured data so that the operational system deflection from the theoretical one is addressed.

5.1 Model validation

The model was validated by practicing the temperature evolution and mass loss profile of fuel packed bed versus two earlier published experiments depicted in Figure 19. Profile of the temperature growth on the bed surface was simulated using the developed model based upon the given initial and boundary conditions of the packed bed experiment by Porteiro et al. [68]. Furthermore, the model was validated against another experimental result of mass loss presented within a work by Mahmoudi [236]. The validation results prove a quite good agreement between the developed model prediction and the experiments. The predicted temperature and mass loss profile follow the trend of the experiments results qualitatively and quantitatively well, despite small deviation which can be attributed to the inherent errors in the modeling, model assumptions as well as the measuring errors.

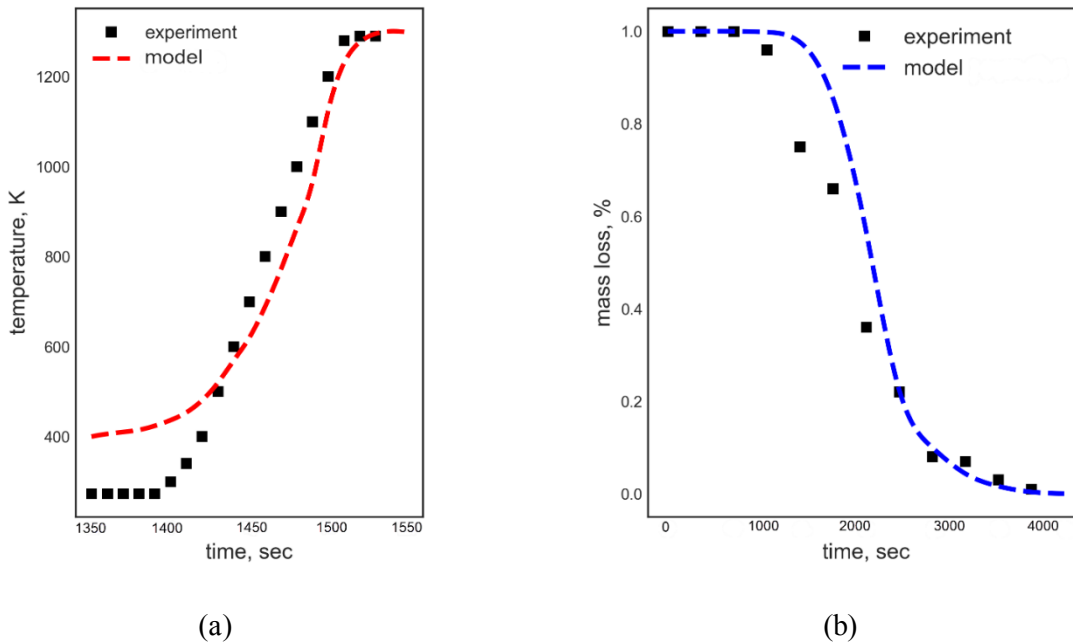


Figure 19. Validation of the model versus the experiments; (a) Ref [68], (b) [236]

The dispersion between temperature profile of the experiments and model prediction can be interpreted as in reality the fuel moisture resided inside the particle pores absorbs the most of heat coming from the overbed zone. In this situation the inside particle temperature increases while outer surface temperature which the thermocouple measures that does not increase at the same rate as inside. However, our continuous medium approach as shown in Figure 15, models the solid and gas phase of particles as a separate homogenous medium which evenly reflects temperature evolution even in the drying step.

5.2 Summary of the results

The results of the thesis are demonstrated in a paper-based format within four variant sections. In the first section, a comprehensive analysis of a moving grate boiler fed by three routine waste-based fuels, namely biomass pellet, wood waste, and refuse-derived fuel (RDF), is conducted. In the second section, the standard deviation of bamboo chips and biomass pellets composition obtained directly from TGA experiment is deployed in order to evaluate the combustion properties' uncertainty. Thirdly, the measured data are trained in the developed Bayesian model to generate a massive data set of fuel compositions, then biomass boiler operation under the uncertainty condition would be investigated. Lastly, an optimal availability-based maintenance plan regarding a vibrating-grate biomass boiler is proposed to cut the number of maintenance tasks down whereas the system availability remains in the desired region.

5.2.1 Comparative analyses of variant types of biomass in grate bed boiler

A version of this section was submitted as: "Hosseini Rahdar, M.; Nasiri, F.; Lee, B. Comparative Thermo-economic and Environmental Analysis of Biomass pellet, Wood Waste and Refuse Derived Fuel in Grate Bed Biomass Boilers. Sustainable Energy Technologies and Assessments, 2020."

Background

Within the literature, heat generation from biomass boilers is almost always accounted via simplified empirical equations in a black-box mode while this approach only provides a weak estimation without identifying detail of the process. Heat generation from a moving grate biomass boiler fed with three routine waste-based fuels, namely biomass pellet, wood waste, and refuse-derived fuel (RDF), is carefully determined via a developed one-dimensional transient numerical model. This comparative study not only comprehensively dissects the system performance under each working fuel condition but facilitates adjustment of system setups regarding each fuel scenario. Furthermore, to illustrate the long-term environmental and economic impact of system operation with each fuel, Life Cycle Analysis (LCA) and Life Cycle Costing (LCC) are conducted. It should be highlighted that grate firing boilers can concurrently burn different fuel types such as what is applied in this study, in consequence, the results of this article can practically help boiler users to regulate their system for different fuel types.

Thermochemical analysis

variant biomass fuel types including biomass pellets, wood waste, and RDF are examined in a grate firing biomass boiler. Fuel composition characteristics together with corresponding stoichiometric air ratio and particle density are represented in Table 23 [197,237,238]. A biomass boiler with a bed height of 20 centimetres, a grate length of 2 metres, and an initial overbed temperature of 1250 K were applied in this study. This overbed temperature is an initial estimation of overbed temperature and would be updated during the calculation. It would also converge to the actual value as combustion proceeds. The primary air temperature was set on 100°C to accelerate drying.

Table 23. Fuel properties and stoichiometric air-fuel ratio

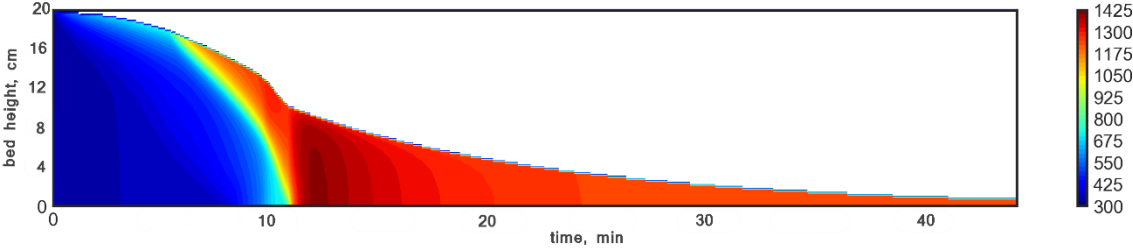
	Biomass pellet	Wood waste	RDF
C, %wt	44.49	33.32	43.00
H, %wt	5.25	4.09	5.30
O, %wt	42.4	41.3	32.68
N, %wt	1.28	1.39	-
Fixed carbon, %wt	22	11.99	6.9
Volatiles, %wt	67	47.44	61.8
Moisture, %wt	9	26.1	17.9
Ash, %wt	2	14.47	13.4
Density, kg/m ³	1000	714	810
Stoichiometric air	5.51	4.38	6.59
Bed height, cm	20	20	20
HHV, MJ/kg	18.72	13.58	14.60

The fuel properties are used within the developed model in order to compare the combustor's properties under different feeding fuel conditions. The temperature contour of the fuel bed conversion for each fuel is shown in Figure 20. The reaction front in moving grate boilers with cross-current flow regime propagates from bed surface downward the grate (the first phase), and then inversely from the grate toward the surface of the bed until the fuels would be completely burned (the second phase). The first phase of reaction front for the system fed with biomass pellets finished earlier, by 11 minutes, compared to other fuel options by 15 and 18 minutes for wood waste and RDF respectively. This can be attributed to the fact that biomass pellets contain less moisture content than the other two fuels. In the second phase, however, fuel with less fixed carbon content experiences a shorter conversion time. Furthermore, it can be concluded that the maximum

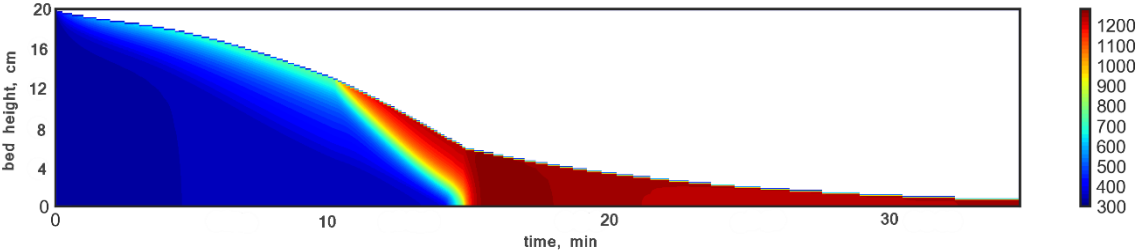
temperature inside the fuel bed has a direct correlation with the fixed carbon content of the fuel. From the system adaptation view, since the complete combustion of biomass pellets, wood waste, and RDF requires 42.8, 35.23, and 34.56 minutes correspondingly, for a grate length of 2 metres, the grate velocity must be regulated by 0.77 mm/s, 0.94 mm/s, and 0.96 mm/s respectively. Moreover, as drying, pyrolysis and char oxidation happen in different lengths of the grate, the primary air distribution should be updated by the wind-box mechanism under the grate in order to speed up the conversion process inside the fuel bed. According to Yin et al. [17,193], about 40% of primary air is injected to the fuel bed from grate opening until complete volatile decomposition, and the rest of air is distributed between middle and last zone with a ratio of 2:1. In the utilized biomass combustor, three equal wind-boxes are equipped under the grate in which the primary air is distributed for efficient conversion. Here Table 24. is proposed in order to adapt the primary air distribution of biomass bed regarding each waste fuel.

Table 24. Primary air distribution of biomass combustor for different fuels

	Zone 1	Zone 2	Zone 3
Biomass pellets	40%	40%	20%
Wood waste	25%	50%	25%
RDF	20%	55%	25%



(a)



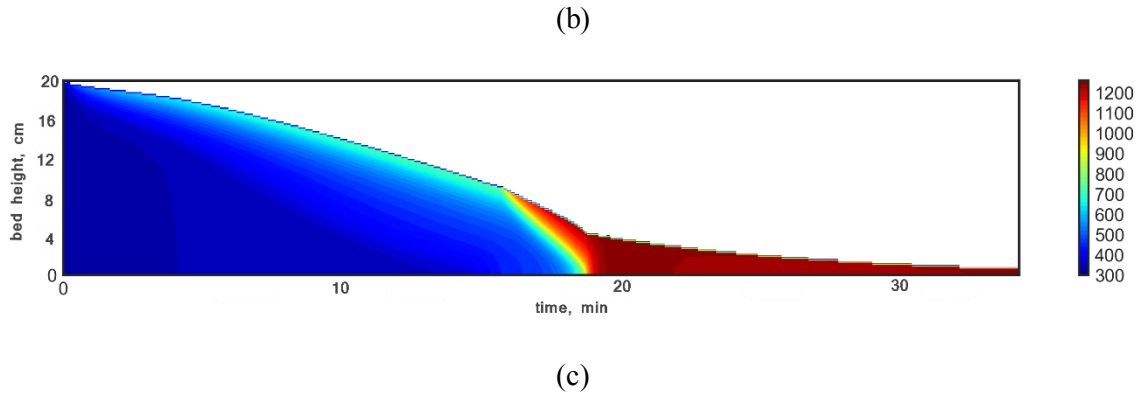


Figure 20. Contour of solid temperature for combustion of: (a) biomass pellets, (b) wood waste, (c) RDF

To elaborate on the mass loss of each proposed fuel during the combustion process, dashed-line profiles in Figure 21. are referred to. From the figure, it is clear that despite the lack of similarity between the bed decay of wood waste and RDF, the mass loss behavior is quite similar, while the biomass pellet shows a different trend. The mass-loss rate of wood waste and RDF in drying stage outperform biomass pellet because of less fuel particle density, nevertheless, as the moisture content of biomass pellet is far less than others, its devolatilization stage is triggered earlier and consequently, its mass loss dominates two other ones for a few minutes. In the final stage that char starts to burn out, again, wood waste and RDF mass loss surpass the biomass pellet, owing to less density and fixed carbon content.

Solid particle temperature profiles of bed surface regarding each biomass fuel are shown in Figure 21., in which it demonstrates the decelerating effect of moisture content on temperature evolution. Due to the fact that biomass pellets include less moisture and more char content, the temperature rise takes place in the shorter grate length and results in higher heat generation per grate length for pellets which will be quantified later on.

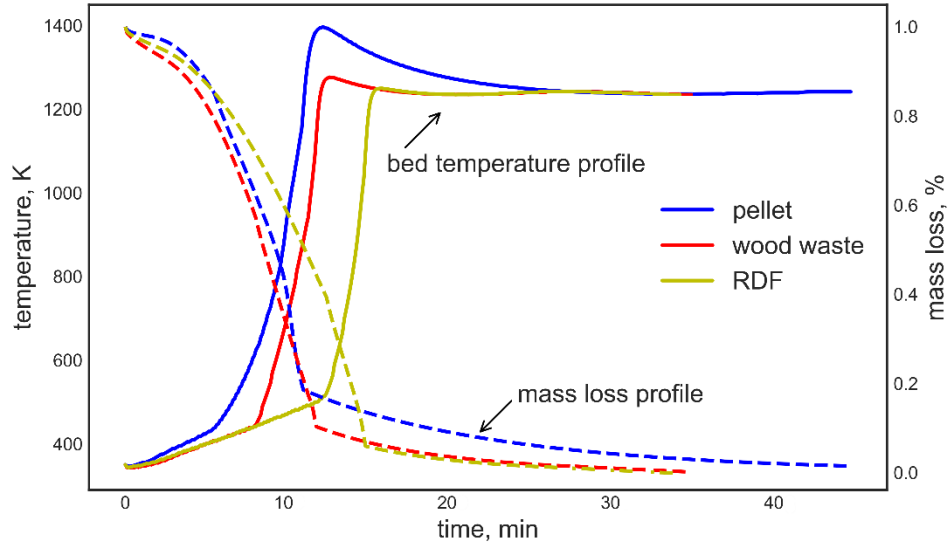


Figure 21. Mass loss (dashed-line) and temperature evolution (solid line) profiles of the three fuels

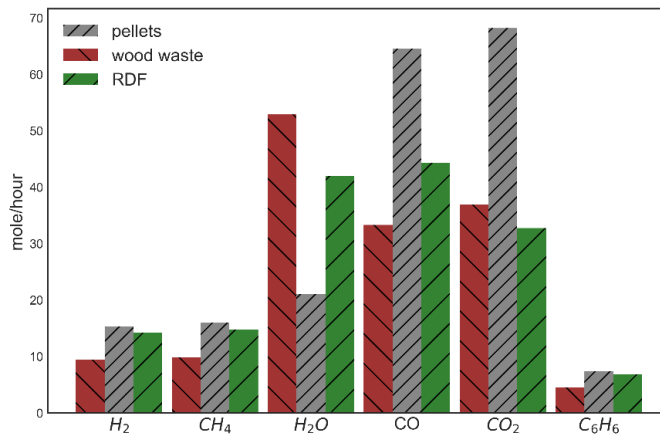


Figure 22. Volumetric concentration of emitting gases from fuel bed

Volumetric concentration in terms of mole per hour for all emitting gas from the moving fuel bed is illustrated as Figure 22. Higher water vapor of the wood waste and RDF than the pellets was expected due to more moisture content in the fuel. Carbon monoxide outflowing rate for RDF dominates one for wood waste which can be interpreted by higher volatile matter whereas carbon dioxide rate originating from fixed carbon content was inversely higher for wood waste. Among the emitting gas species from fuel bed conversion, CO_2 and H_2O remain neutral and other combustible gases react with oxygen and together with heat flux from char oxidation form the heat source in the system. It is assumed that flue gases leave the stack at the temperature 400 K.

According to the outcomes, the useful heat flux per kg of the wet biomass pellets was obtained 15.282 MJ while it lowered by 32% and 30% for wood waste and RDF respectively. It must be noted that water vapor

is not condensed within the combustor which wastes a notable amount of heat. Taking the conversion rate of each fuel into the account given in Table 25., annual heat generation from the proposed system was attained at 548 GJ for biomass pellets, contrasted with 48% and 35% lower in terms of wood waste and RDF. It was similarly concluded that for complete combustion of biomass pellets, a residence time of 42.8 minutes must be accounted for, and it must be updated when wood waste or RDF are deployed.

Gas species concentration emitted from the bed reactions are taken to find flame temperature of overbed zone via a black-box method. For a stoichiometric combustion, adiabatic flame temperature is presented for each fuel in Table 25. Due to the high air infiltrations rate in moving bed biomass boilers, flame temperature is much lower than stoichiometric condition in practice. According to the literature [202,239], excess air coefficient usually changing between 1.2-3 for such systems, the total excess air ratio of 2 is utilized here. This unwanted excess air causes significant heat loss through the combustion chamber. Although applying a screw feeder can mitigate this, it still poses a great challenge against moving bed combustor. Less flame temperature of pellets to other fuels can be attributed to higher CO/H₂ ratio because the hydrogen flame temperature is almost 200°C higher.

Table 25. Operational characteristics of the heating system for each fuel

	biomass pellets	wood waste	RDF
Heat generation, MJ/kg	15.282	10.379	10.569
Conversion rate, kg/h	4.10	3.107	3.84
Annual energy generation, GJ/annual	548.868	282.488	355.524
Maximum bed temperature, K	1396	1276	1249
Residence time, min	42.8	35.23	34.56
Stoichiometric flame temperature, K	1900	1915	1970
Flame temperature with 100% total excess air, K	1477	1490	1537

Economic analysis

Economic analysis with a focus on the annual cost (AC) and internal rate of return (IRR) for the proposed system in terms of each fuel scenario is carried out. Cost of producing heat from the proposed fuels depends on system capital cost (C_c), installation cost (C_{in}), fuel storage cost (C_{st}), fuel cost (C_f), electricity cost (C_{el}), maintenance cost (C_m), unseen cost (C_{un}), and salvation cost (C_s) which is the income at the end of system lifetime associated with equipment disposal. Table 26 displays the relevant values regarding the foregoing parameters for the 25 kW biomass boiler which can be updated via Eq. (55) for variant system size [240–243].

Table 26. List of breakdown costs for biomass boiler heating system

cost type	description	cost (\$)
Capital cost, C_c	25 kW biomass boiler and accessories	13800-15300
Installation cost, C_{in}	pipings, pumps, valves, and labors, etc.	9000-11500
Fuel storage cost, C_{st}	outdoor storage room	1000-2000
Fuel cost, C_f	biomass pellet	150/ton
	wood waste	90/ton
	RDF	70/ton
Electricity cost, C_{el}	boiler electricity usage	40/month
Maintenance cost, C_m	cleaning and non-technical maintenance	0.01* ($C_c + C_{in} + C_{st}$)
Unseen cost, C_{un}	system design and loss risks, etc.	0.01* ($C_c + C_{in} + C_{st}$)
Salvation cost, C_s	system disposal	0.05* C_c

$$C = C_0 \left(\frac{N}{N_0} \right)^g \quad (55)$$

where C and C_0 are the capital cost of the new system and base system, and N and N_0 are system capacity correspondingly along with factor g , ranging from 0.4-0.8 for process equipment. Hence, the life cycle cost (C_{LCC}) of energy generation during system lifespan which is accounted for 25 years will be as follows:

$$C_{LCC} = C_c + C_{in} + C_{st} - C_s + \sum_{p=1}^n \frac{(1+c)^p}{(1+i)^p} (C_f + C_{el} + C_m + C_{un}) \quad (56)$$

where c and i are escalation rate 4% and interest rate 2% respectively. In this way, the annualized cost (C_a) can be obtained from Eq. (57) which is a function of capital recover factor (e) achieved from interest rate (i) and equipment lifespan (n) as pointed out via Eq. (58). Eventually, the cost of heat (COH) using annual generated heat Q_{ann} and the annualized cost is calculated by Eq. (59). Additionally, the IRR, which is the interest rate at which the NPV of every cash flows during the lifespan of a project becomes zero, is counted via Eq. (60) where CF means annual cash flow.

$$C_a = e \cdot C_{LCC} \quad (57)$$

$$e = \frac{i(1+i)^n}{(1+i)^n - 1} \quad (58)$$

$$COH = \frac{C_a}{Q_{ann}} \quad (59)$$

$$\sum_{p=0}^n \frac{CF_p}{(1 + IRR)^p} = 0 \quad (60)$$

Table 27. Economic analysis conclusion for the system under different fuel conditions

	Biomass pellet	Wood waste	RDF
C_{LCC} , \$	224758	162295	154199
C_a , \$	12198	8808	8369
COH , ¢/kWh	8.56	9.203	7.408
IRR	33%	22%	29.5%

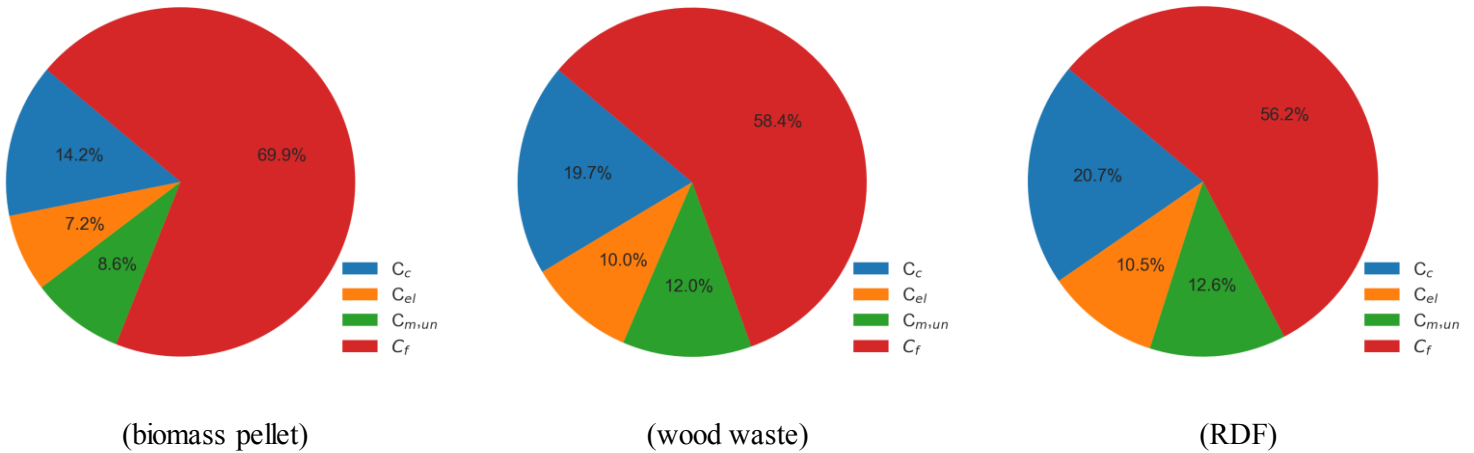


Figure 23. Life cycle cost contribution for 30 kW biomass boiler; C_c : capital cost, C_{el} : electricity cost, C_{mun} : maintenance+unseen cost, C_f : fuel cost

The results of the economic analysis are presented in Table 27. Levelized COH reveals that RDF has lowest heat price by 7.408 ¢/kWh compared to 8.56 and 9.203 ¢/kWh for pellet and wood waste correspondingly, which can be attributed to lower fuel cost of RDF. Although the annualized cost of heat from the pellet-fueled system is about 38% more than other ones, because of the corresponding higher annual heat production, the related COH factor has the marginal difference with two other options. Taking wood waste heat price into the account which is the highest reported value between all options in Table 27, still, it outperforms the US national average residential rate of 11.88¢/kWh, regardless of the potential government incentives supporting the energy generation from cleaner resources [244]. The LCC breakdown for each

particular scenario, as demonstrated in Figure 23, reveals the sway of fuel cost over the total life cycle cost of the system followed by system capital cost invested in the first year. Here in Figure 23, the capital and installation costs are aggregated in capital cost term which is roughly 14% for biomass pellet and 19% and 20% for wood waste and RDF consecutively. Finally, higher IRR of pellet to RDF in spite of lower COH of RDF is explained by the fact that the boiler generates higher annual heat under pellet feeding condition.

Environmental Life Cycle Analysis (LCA)

An LCA approach is applied in this section in order to compare the environmental impacts of each alternative fuel. The LCA boundary from fuel preparation until the heat generation for proposed fuels is depicted in Figure 24. Since it is aimed to compare the impact of each fuel utilization on the ecosystem, the same energy production is assumed for all scenarios. Table 28 lists the main input data employed in the LCA. SimaPro database for North America (TRACI 2.1) was employed for pollutant indices calculation. It must be mentioned that fuels originated from wood resources are deemed neutral CO₂ and therefore, no carbon dioxide emission is counted during the combustion process in LCA calculation while RDF as a mixture of biogenic and inorganic materials, oppositely emits CO₂ in the combustion process.

Table 28. Input data for LCA respecting biomass pellet, wood waste and RDF individually

	biomass pellet	wood waste	RDF
System load, GJ/yr	512	512	512
Transportation, tkm	5194	7754	7731
Boiler electricity use, kwh/yr	4576	4576	4576
Treatment process	✓	✓	✗
CO ₂ emission kg/ton	N/A	N/A	650

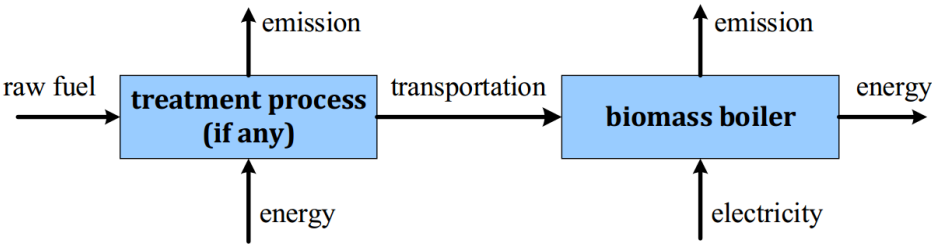


Figure 24. System boundary for the LCA implementation

Global warming impact probably is the most concerning factor among all sorted items in Table 29. From the results, the RDF has 3 times more negative impact on global warming than biomass pellets mainly caused

by emitted CO₂ in combustion. In order to elaborate on the contribution of each particular subprocess on emitting greenhouse gases, Figure 25 is displayed which is only curbed to the top three substantial affecting contributors. By switching between alternative fuels from biomass pellets to wood waste and RDF the key contributor to the greenhouse emission is the pelletizing process, electricity use by the boiler, and pollutant emission from RDF combustion correspondingly.

Table 29. Results of life cycle impact analysis for the heating system fed with proposed fuels

Impact category	Unit	Biomass pellet	Wood waste	RDF
Ozone depletion	kg CFC-11 eq	0.001522529	0.000922053	0.000869097
Global warming	kg CO2 eq	11646.90648	4720.676333	37993.95694
Smog	kg O3 eq	3633.392563	1660.603144	3622.097337
Acidification	kg SO2 eq	148.7873245	66.24748127	213.5752426
Eutrophication	kg N eq	52.86016311	4.737583662	7.979050593
Carcinogenics	CTUh	0.000368746	5.549E-05	4.48904E-05
Non carcinogenics	CTUh	0.0022399	0.000330273	0.000270265
Respiratory effects	kg PM2.5 eq	8.869188507	2.109161827	2.506143909
Ecotoxicity	CTUe	64572.91424	10768.19211	8865.587757
Fossil fuel depletion	MJ surplus	21370.00448	11928.03796	11449.94358

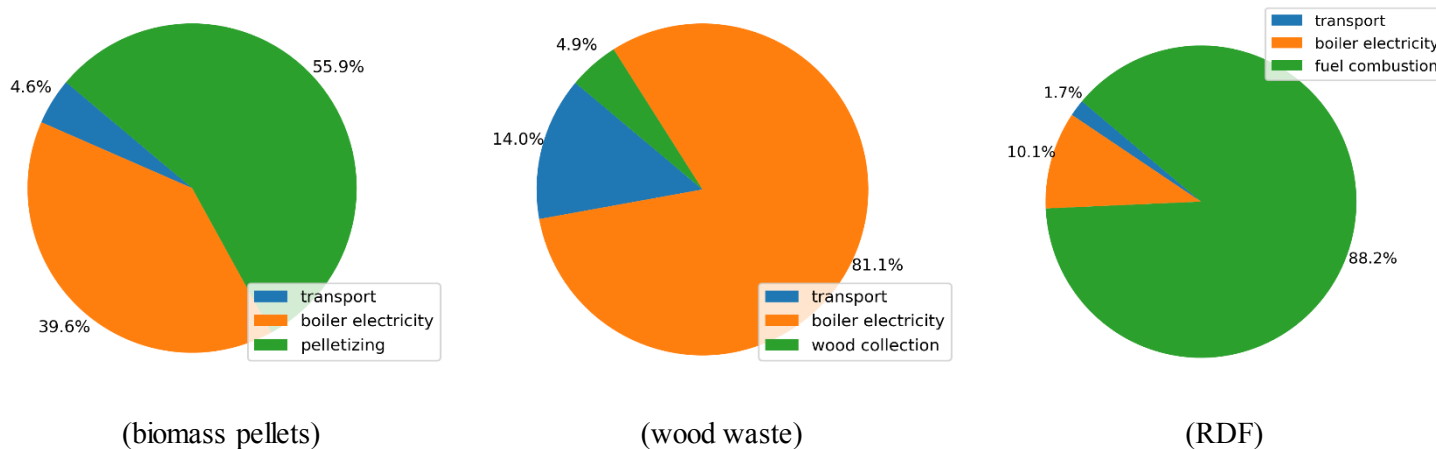


Figure 25. Proportion of three key contributors to the greenhouse gases for each feeding fuel

5.2.2 Experiment-based analysis of composition variability effects on biomass combustion

A version of this section was published as: “Hosseini Rahdar, M.; Lee, B.; Nasiri, F. Uncertainty Quantification of Biomass Composition Variability Effect on Moving Grate Bed Combustion: An Experiment-based Approach. Energy & Fuels, 2020.”

Background

Overlooking the uncertainty in biomass feeding compositions results in fluctuating operation and consequently a source of deficiency in the system. Up to now, fuel composition variability is almost always discounted in the biomass combustion analyses, while it has been quantified in some other types of fuel combustion such as biogas and nuclear fuel [245,246]. In this section, the fuel compositions mean value and corresponding standard deviation obtained from the TGA proximate analysis of a set of wood pellets and bamboo chips are deployed in the combustion study of the grate firing biomass boiler. The model runs for 250 times with random compositions value chosen from the Gaussian distribution for each fuel and stores biomass combustion characteristics in each iteration [247].

Table 30. Statistical analysis of bamboo chips and wood pellets

	Bamboo chips			Wood pellet		
	mean	range	SD	mean	range	SD
MC, %	9.95	3.091	0.92	11.37	3	0.68
VM, %	69.96	8.53	1.93	63.87	6.56	1.56
FC, %	17.85	6.37	1.53	22.74	6	1.25
A, %	2.27	3.080	0.57	2.02	3.25	0.7
Density, kg/m ³		750			1000	

The mean, range, and standard deviation (SD) of both proposed fuels are shown in Table 30. From the reported value in Table 30, it can be intuitively concluded that the pelletizing process can efficiently help to diminish composition uncertainty.

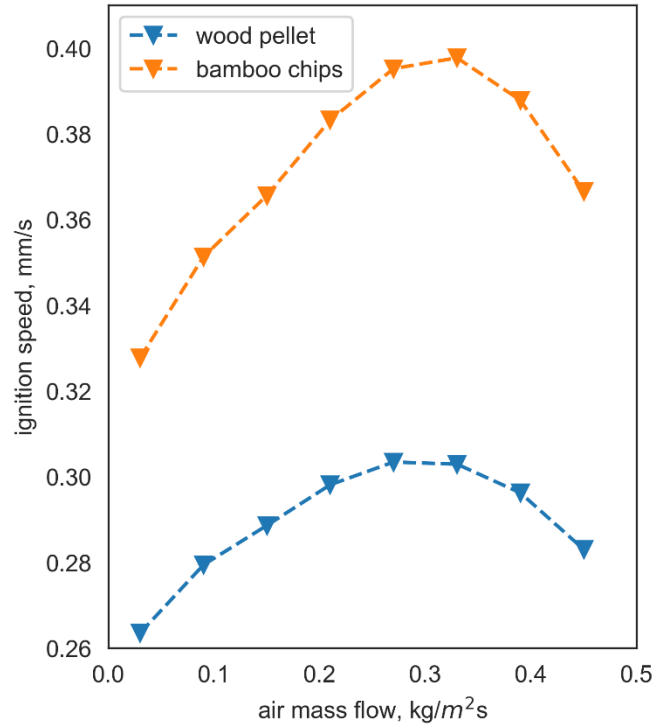


Figure 26. Ignition speed versus different amount of air flow rate for bamboo and wood pellet

The reaction front speed in various air flow rate is evaluated for both fuels in Figure 26. Air flow rate is of the most influential parameters on combustion so that it limits the amount of oxygen inside the bed, and consequently governs the rate of the combustion process. In the low air flow (lean reaction), the reaction is restricted by inadequate oxygen, and the proceeding of reaction front is governed by competitive mechanisms amongst volatile light hydrocarbons and char combustion. While the air flow rate reaches in the vicinity of the stoichiometric ratio, a sufficient amount of oxygen is available for volatiles and char oxidation so that the ignition front propagates faster. As soon as the air flow exceeds the stoichiometric condition, the extra air causes cooling down the bed temperature using a convective heat transfer mechanism and in a certain amount of excess air, it can completely extinguish the bed combustion. The reference temperature of 973 K was factored in for ignition rate calculation in this study [68,248]. Ignition speed indicates how fast the temperature varies alongside the bed. In experimental studies, the ignition rate is accounted via metering the two consecutive thermocouples distance over the measured time of transient of high-temperature fuel conversion between that zone. A similar method is employed in modeling by dividing the vertical distance between two points in the bed by the time interval taken for each point to reach the 973 K. The higher ignition front propagation for bamboo chips than wood pellets in Figure 26 is attributed mainly to less particle density of bamboo while higher volatile content can have an accelerating effect as well.

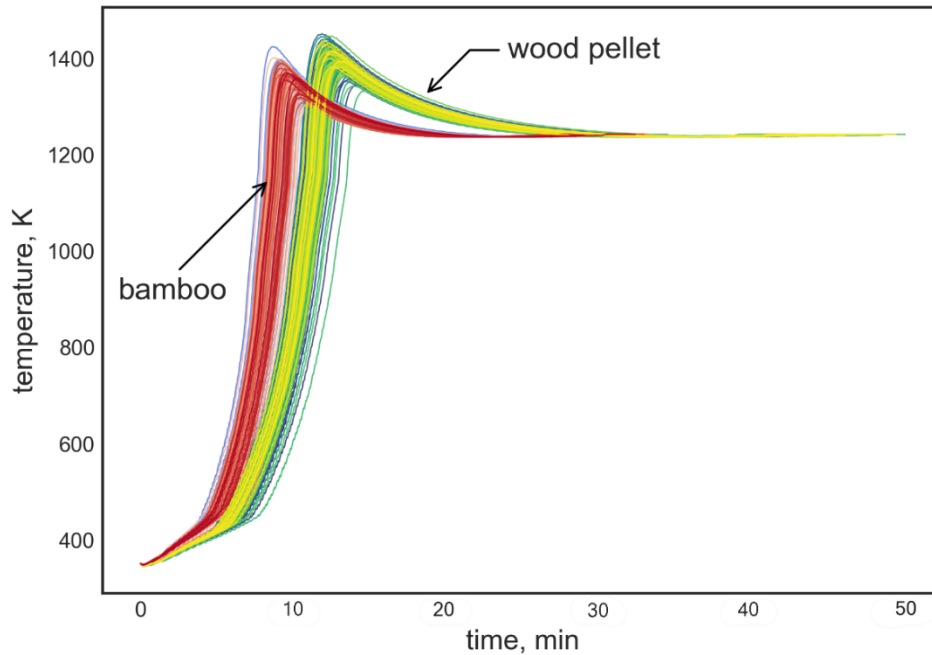


Figure 27. Solid temperature evolution versus composition variability over the fuel bed conversion process

Until here, the combustor operation was inspected using fuel compositions mean value to show how the system functions on an average basis regardless of fuel variability. In practice, however, the system does not always operate on these average values due to random composition which causes system operation deflection. Hence, the standard deviation of fuel compositions is taken into account in order to simulate what occurs within the combustion system in practice. Solid temperature evolution for both fuels under composition variability is shown in Figure 27 which was distinguished in red and yellow theme corresponding to bamboo and wood pellet. As the solid phase temperature is a key parameter in the fixed-bed biomass combustors operation, the illustrated variation in temperature profile high likely to make fluctuation in the operation. In doing so, the heat generated from the proposed combustor under composition variability for each studying fuels is monitored and the obtained values form a distribution as shown in Figure 28. Despite higher moisture of pellets compared to bamboo, pellets averagely produce 1 MJ/kg higher energy mainly owing to higher char content. Moreover, because of a slightly higher deviation in composition values regarding the bamboo, the corresponding interval of possible heat production is 3.2 MJ/kg opposed to 2.7 MJ/kg in terms of pellets.

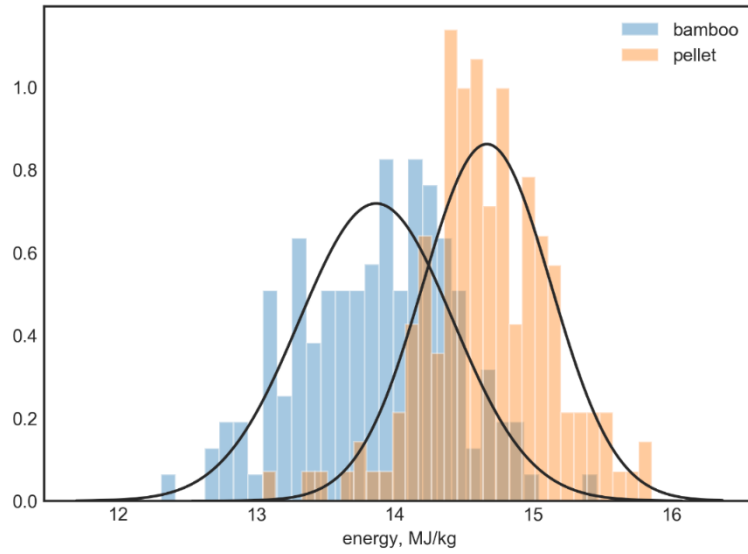


Figure 28. Distribution of heat production under fuel composition variability

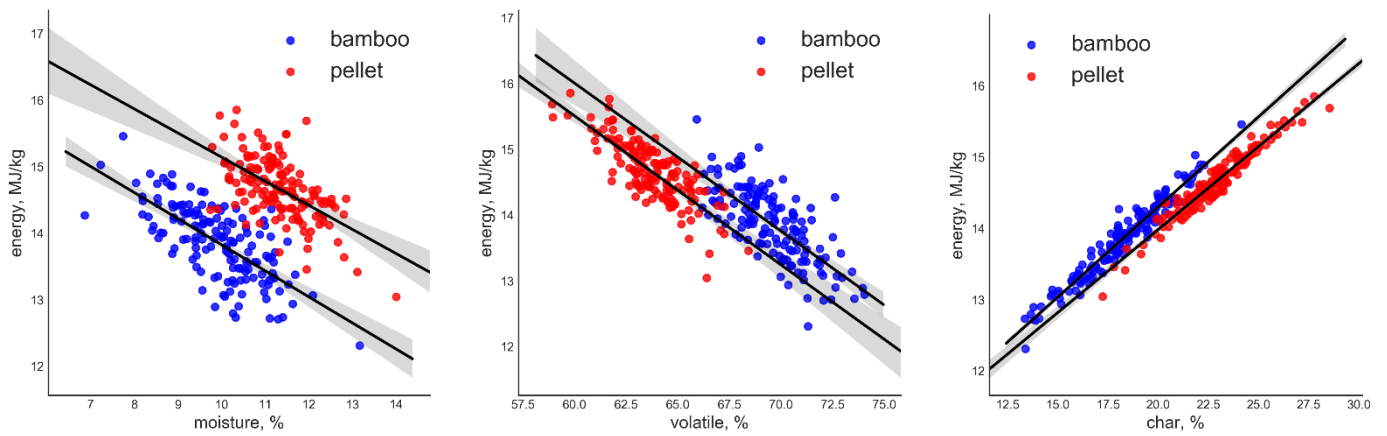


Figure 29. Effect of fuel composition variability on the heat generation for bamboo chips and wood pellet combustion

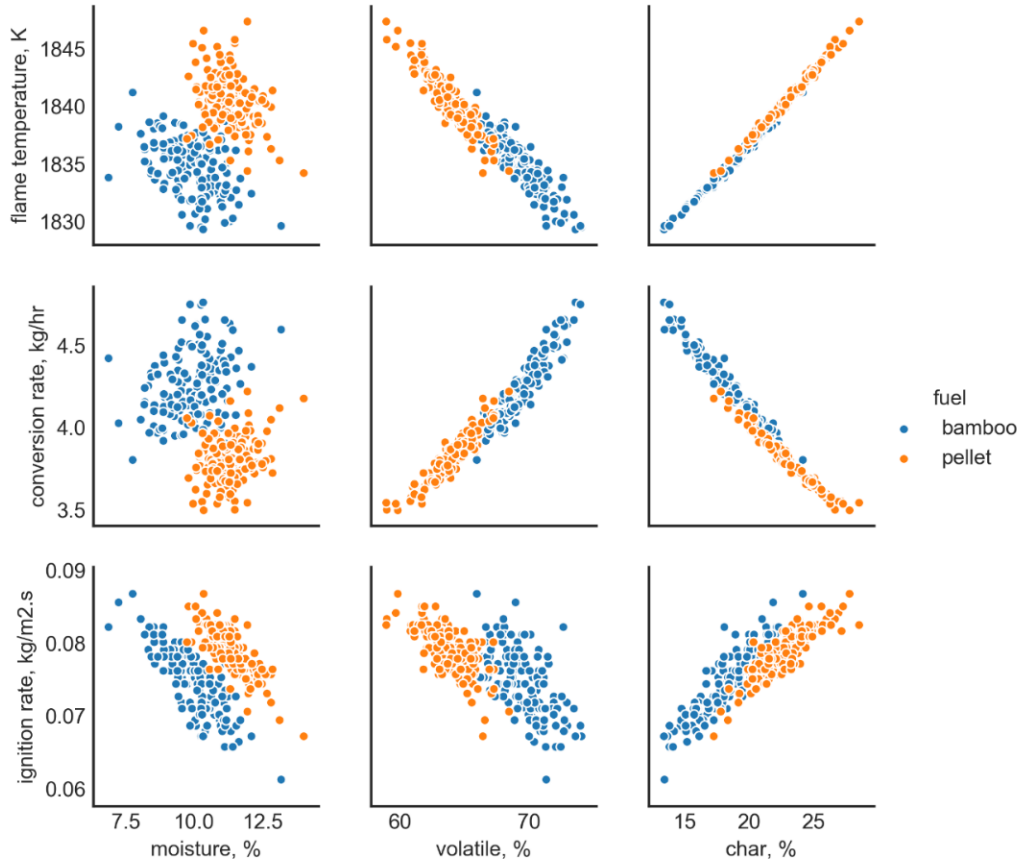


Figure 30. Effect of fuel composition uncertainty on the flame temperature, mass conversion rate, and ignition rate

In order to elaborate on the impacts of composition variability on heat generation in detail, uncertainty in produced heat associated with fuel compositions is individually displayed in Figure 29. Results revealed that while the moisture is the most detrimental contributor to the heat production uncertainty, reaching a higher heat generation level with less uncertainty strongly depends on the higher char content of the fuel. The heat variability originated from volatiles uncertainty even though is fewer than moisture, still not negligible because of the key impact of combustion of volatile gases in the overbed zone. The range of heat generation uncertainty is wider for bamboo than pellets because of higher fuel composition variability. Therefore, it can be intuitively concluded that thermal performance improvement can be achieved using biochar pellets in grate firing biomass boilers.

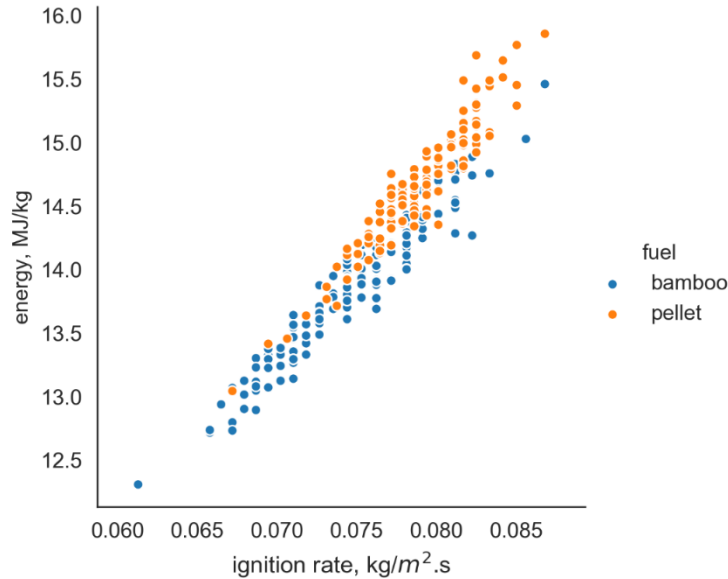


Figure 31. Straight correlation of ignition rate and heat generation in the biomass combustion

Results from this study also reveal this fact that the sensitivity analysis of fuel composition alone can be misleading to some extent. The normal approach in sensitivity analysis is to change one single independent parameter while other independent parameters are fixed and then output features of the system are dissected. Using this approach in the course of biomass fuel compositions (moisture, volatile and char) is far from reality as, for example, reduction of moisture content changes the fraction of volatile and char content. Thus, the effect of moisture reduction on the system outputs might be intensified or offset by other compositions variation. Therefore, sensitivity analysis is not always correct with respect to fuel compositions, and uncertainty analysis is required. Correlation between fuel compositions and mass conversion rate in Figure 30 confirms the latter expression where moisture shows an almost neutral impact on the mass conversion rate, and even slightly direct impact. This can be explained by this fact that moisture reduction probably results in higher char content which elongates the whole process. More volatile matters and less char content certainly accelerate biomass conversion rate as it was expected while moisture content causes great uncertainty in continuing reaction. In the course of wood pellets, the conversion rate can deviate about 13% percent, and it is even more for bamboo by 20%. Flame temperature, however, is less affected by composition variability so that it can fluctuate up to 15 °C which is negligible for high temperatures such as 1840 K. Less flame temperature uncertainty can be explained due to the fact that the main contributor in overbed combustion is CO which is released in devolatilization and char burnout. Since volatile matters increase is likely to cause char content decrease, they offset each other's effect.

Ignition of solid particles can competitively start either by char ignition on the particle surface or via volatile ignition in the fuel boundary depends on convective and radiative heat transfer rate to the particle, particularly on the bed surface. If radiation flux is high enough for the surface to quickly heat up to ignition temperature threshold of the carbon 973 K, fuels ignite instantly. On the other hand, if the surface heating is low, and the convective rate is high enough for the surface to quickly heat up, then the particle may ignite although volatiles is usually moved away from the bed zone before enough accumulation to satisfy combustion requirements. From the results, the ignition front rate develops by increasing char content and decreasing moisture and volatile content, and vice versa. Moreover, from Figure 30, it is noted that the ignition rate is highly sensitive to fuel composition uncertainty, especially for fuel with lower density. Also, a strong direct correlation between ignition front rate and energy generation of the biomass bed conversion was detected taking the composition variability into the account as shown in Figure 31.

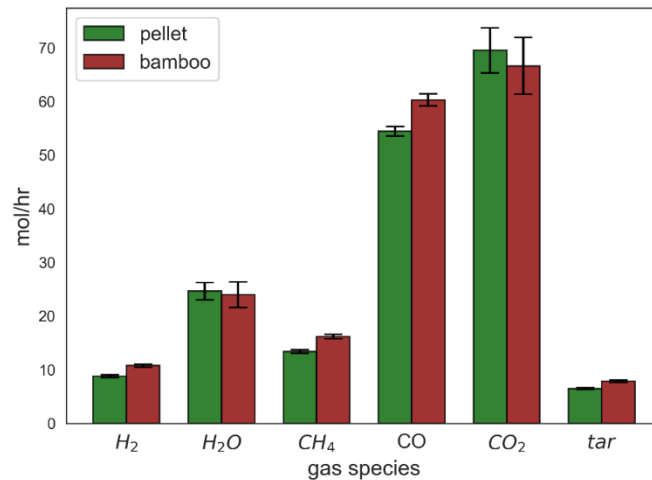


Figure 32. Mole fraction of outflowing gas species from biomass bed conversion

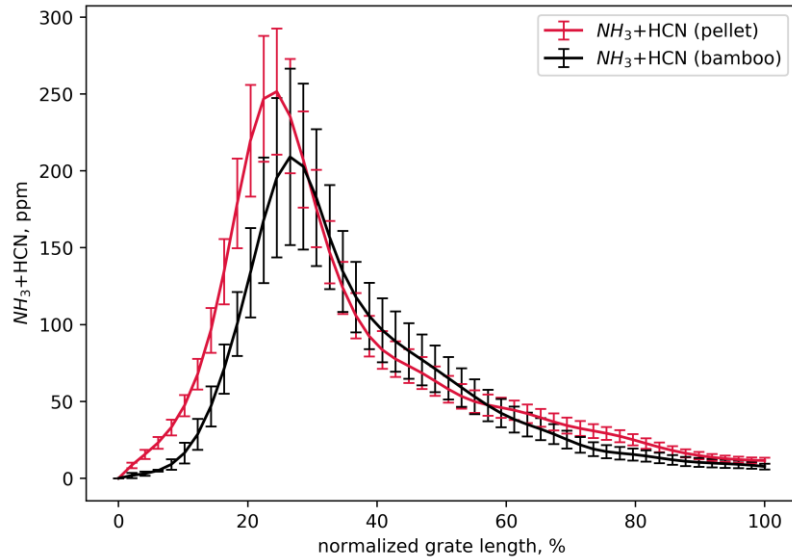
During the combustion process, biomass decomposes to combustible and non-combustible gases [249] displayed in Figure 32. Apart from H₂O evaporation in the drying phase, gas species including carbon dioxide and carbon monoxide are dominantly emitted in char burnout while hydrogen, methane, and tar in the devolatilization step. From Figure 32, uncertainty associated with the number of mole of hydrogen, methane, and tar is limited to a very short range versus the considerable uncertainty range of carbon dioxide and carbon monoxide. In this way, low fluctuation of flame temperature and high fluctuation of energy generation can rationally be interpreted so that the first one has a strong dependency on combustible gases variability, e.g., H₂, CH₄, CO, and tar, whereas the second one extremely involves with pure carbon oxidation.

Table 31. Reactions used in modeling of NO_x precursor formation

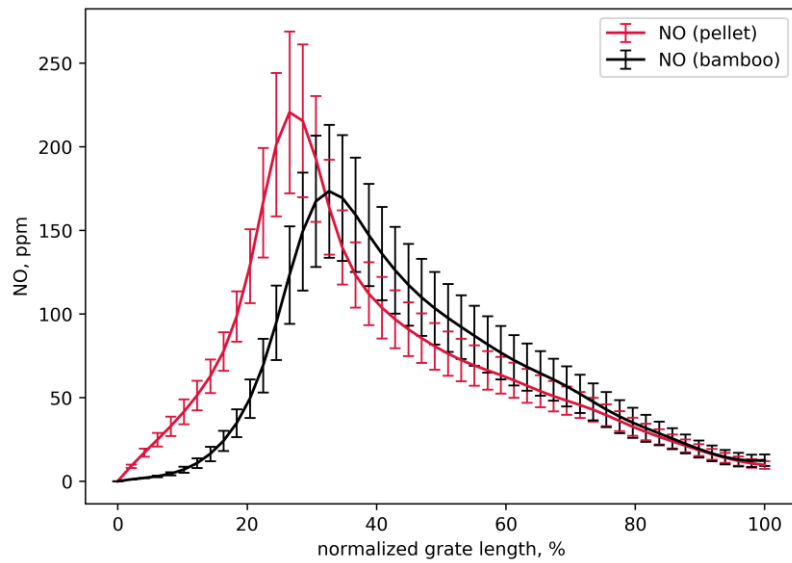
Reaction	Rate expression	Ref.
$NH_3 + O_2 = NO + H_2O + 0.5H_2$	$1.21e8 T^2 \exp\left(-\frac{8000}{T}\right)[NH_3][O_2]^{0.5}[H_2]^{0.5}$	[250]
$NH_3 + NO = N_2 + H_2O + 0.5H_2$	$8.73e17 T^{-1} \exp\left(-\frac{8000}{T}\right)[NH_3][NO]$	[250]
$HCN + 0.5O_2 = CNO$	$k[O_2][HCN]$	[251]
$CNO + 0.5O_2 = NO + CO$	$k[O_2][HCN] * (k_1 / ((k_1 + k_2[NO])))$	[251]
$CNO + NO = N_2 + 0.5O_2 + CO$	$k[O_2][HCN] * (k_2 / ((k_1 + k_2[NO])))$	[251]
	$k = 2.14e5 \exp\left(-\frac{10000}{T}\right)$	
	$\frac{k_1}{k_2} = 1.02e9 \exp\left(-\frac{25460}{T}\right)$	
$char - N + 0.5O_2 = NO$	$[char - N] \frac{d(char)}{dt}$	[251]

NO_x precursors in the combustion process are created in the three variant paths including thermal-NO, which is resulted from atmospheric nitrogen oxidation, prompt-NO, is formed from the reaction of atmospheric nitrogen with hydrocarbon radicals in fuel-rich regions, and finally, fuel-NO, which is produced from the oxidation of the fuel nitrogen bound. Since the combustion temperature in biomass furnace is not enough high for thermal-NO formation plus this fact that solid biomass fuel-N is relatively high, the focus here is paid on fuel NO generation from biomass conversion. During the pyrolysis, fuel-N is emitted in terms of NH₃ and HCN and the rest of fuel-N remains in char element which in reaction with oxygen directly converts to NO_x. The released NH₃ and HCN in a series of oxidation and reduction processes transform into NO_x and N₂. The deployed fuel-N reactions yielding to NO_x precursors are catalogued in Table 31.

In the combustion chamber within the air-rich condition, NO is the main agent amongst all NO_x element and conversely, NH₃ contributes as a predominant precursor under fuel-rich condition. Since nitrogen elements react into an oxidizing atmosphere, fuel nitrogen is significantly expected to be formed, while the evolution of fuel nitrogen in an environment with lack of oxygen can result in more N₂ instead of NO. Accordingly, caring about the timing of nitrogen evolution is essential in the combustion chamber so, in order to lessen NO_x formation in the vicinity of the bed, early touch between nitrogen and oxygen should be evaded. Fuel NO is the dominant mechanism of NO_x evolution into the combustion flame and routinely is responsible for about 80% of the entire NO_x produced in the system [70]. Nitrogen content of 0.16 wt% is factored in regarding wood pellets and bamboo chips in the calculations.



(a)



(b)

Figure 33. Nitrogen precursors yield over the biomass combustion in the moving grate bed boiler; (a) NH_3 and HCN (b) NO generation

Figure 33 displays NOx precursors profiles detected above the fuel bed and that of uncertainty resulted from fuel composition variability. With respect to the high ratio of volatile yields to char yields hence, it can be reasonably observed that NH_3 and HCN peaked while devolatilization rate is maximum, and NO formation,

which is the product of NH₃ and HCN conversion, follows the profile of NH₃ and HCN with a short delay. This signifies the required time of NO generation over the bed. After the peak then the NO_x precursors gradually decline during char burnout. Concurrent with NO_x precursors evolution in process, the uncertainty magnitude directly adheres to the trend. A maximum uncertainty of 22% and 17% were detected for NH₃+HCN and NO respectively. By comparison of wood pellets and bamboo chips, more uncertainty in bamboo is detected. Regarding the fact that the highest uncertainty in raw fuels was found in volatile matters and that of the highest proportion in total fuel mass, the sway of volatile content can be rationally interpreted. Hence, here the substitution of biochar for the wood pellets or chips can be put forward as a solution to restrain NO formation and relevant uncertainty.

5.2.3 Bayesian approach to composition variability effect on biomass combustion

A version of this section was published as:” Hosseini Rahdar, M.; Nasiri, F.; Lee, B. Effect of Fuel Composition Uncertainty on Grate Firing Biomass Combustor Performance: A Bayesian Model Averaging Approach. Biomass Conversion and Biorefinery 2020.”

Background

Following the last section, here a Bayesian-based data generator is applied to quantify biomass compositions variability effect on the uncertainty of combustion system properties. It can provide us plenty of similar data to the measured fuel composition data, and improves the reliability of inputs. The Bayesian model was generated in combination with prior fuel data and measured data with respect to TGA experiment on 30 samples of biomass pellets. Finally, an LCA is conducted to show the long-term environmental effect of using a regular biomass boiler, a modified one, and a coal-fueled boiler in an off-grid location.

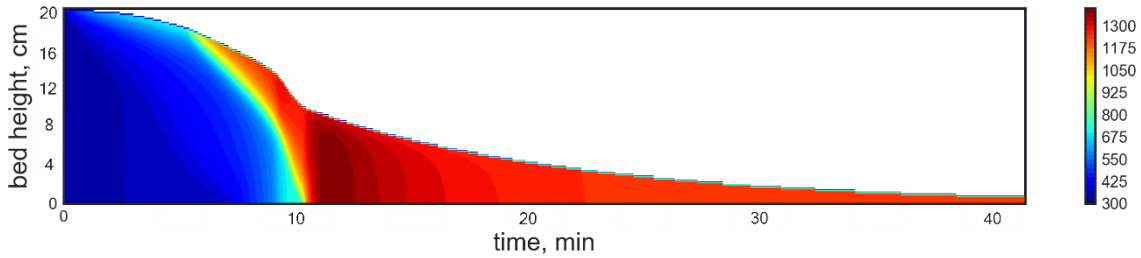
Table 32. Scenarios of system performance evaluation

First scenario	Idealistic approach factoring in the fuel composition as given by the supplier
Second scenario	Feasible scenario using obtained mean value for compositions by Bayesian model
Third scenario	System operation under fuel composition uncertainty condition

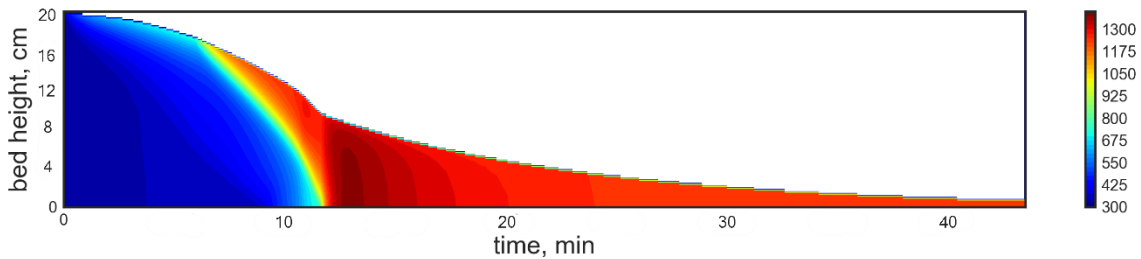
As shown in Table 32, biomass combustor is evaluated in three different scenarios. In the first scenario, grate-bed biomass combustor is ideally assumed to work under the predefined fuel composition situation which was assigned by the fuel supplier. Then in the second scenario, the mean value of Bayesian-derived fuel composition regardless of fuel uncertainty is respected, and lastly, the third scenario analyzes the combustor under fuel composition uncertainty which puts forward what occurs in practice. Within these three scenarios, it is argued how biomass combustion system performance can differ under 1. unlikely

presumed fuel compositions, 2. expected mean value fuel compositions and 3. completely realistic fuel compositions.

Uncertainty results



(a)



(b)

Figure 34. Temperature contour of the biomass fuel bed in (a) 1st scenario (b) 2nd scenario

Evaluating fuel bed temperature contour for the base scenario (a) and modified scenario (b) reveals some visual differences between system operation under these two circumstances (Figure 34). Counter-current reaction front develops from bed surface toward the grate and generated heat from reaction front moves against reaction front, as result evaporation and devolatilization of particles accelerate. The heat of the reaction front cannot move far from the reaction front owing to the opposing direction of heat and air flow. In doing so, the reaction front touches the grate surface almost 11 mins and 13 mins after the beginning of fuel conversion for the first scenario and second scenario correspondingly. At this point, another reaction zone is generated from grate to bed surface to complete char combustion. From Figure 34(a), the char combustion zone reaches a higher temperature and biomass fuel conversion is finished within 41 mins, while for the second scenario it needs more than 2 mins further to complete the conversion. Figure 35 illustrates more details of bed temperature evolution for all the first, second, and third scenarios simultaneously. The second scenario's temperature profile is in the middle of temperature profiles respecting compositions uncertainty which meets our previous expectation.

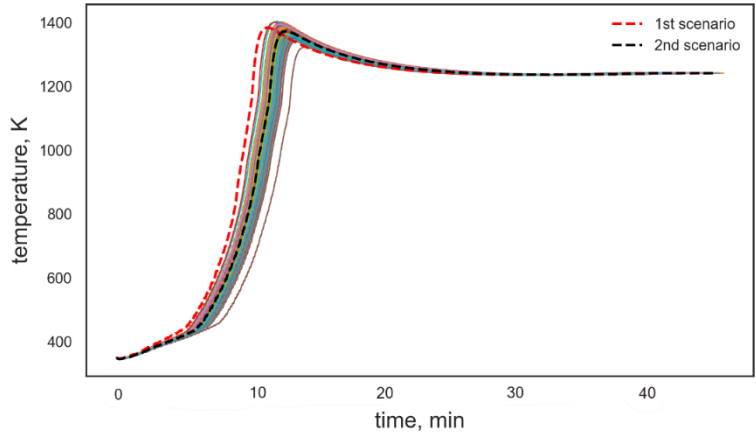


Figure 35. Bed surface temperature evolution over the fuel bed conversion process

By comparing the combustion system for the first and second scenarios, it is generally concluded that if the system is set on the first scenario’s fuel composition basis, it cannot deliver the designed tasks thoroughly. This can be attributed to the fact that the conversion rate of the system from almost 4.2 kg/hr for the first scenario, which is an imagined scenario, lowers to 3.96 kg/hr for the second scenario, which is the actual condition, and a complete pellet fuel conversion time on the grate increases from 41 mins to 43 mins respectively.

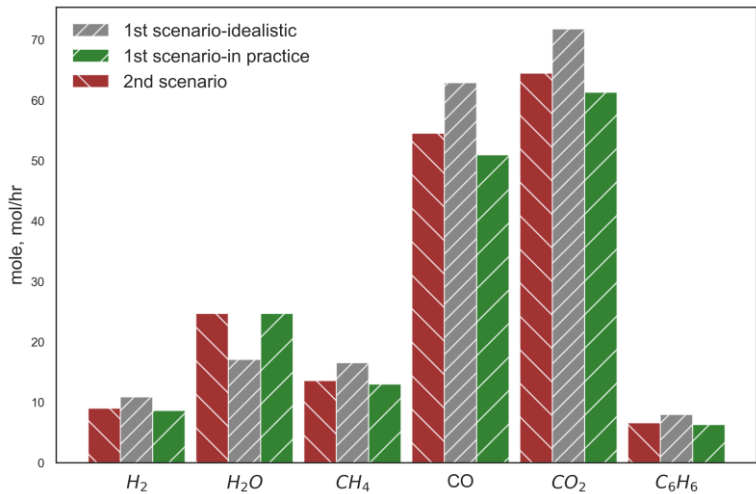


Figure 36. Molar mass of emitting gases from particle conversion for first and second scenarios

The number of moles of hourly emitting gas species from the solid fuels conversion for the first and second scenarios shown in Figure 36. Although it discloses higher moisture and less CO , H_2 , CO_2 , etc. for the second scenario than the idealistic scenario, the green column is what the first scenario will end up in practice. The higher char results in more CO_2 and CO while a significant amount of CO is formed in pyrolysis reaction as

well. On the other hand, higher moisture content decelerates temperature growth and causes a slower ignition rate and conversion rate. As a result, the first scenario makes an overestimation on system output that can cause a shortage of demand delivery.

Since the most grate-type biomass combustors are in small to medium scale systems and usually are used for applications such as district heating systems, independent heating system in an off-grid area, etc., they lack a sophisticated control system to be able to monitor the system continuously and adjust the system to perform corresponding to the feeding fuel properties deviation. In doing so, such systems are usually set on the fixed grate speed based on the presumed values for fuel composition, thus, a deviation between preset fuel composition and what is fed to the system in practice will result in system deficiency. In other words, the combustor underestimates or overestimates expected heat generation, along with incomplete particle's combustion within the furnace.

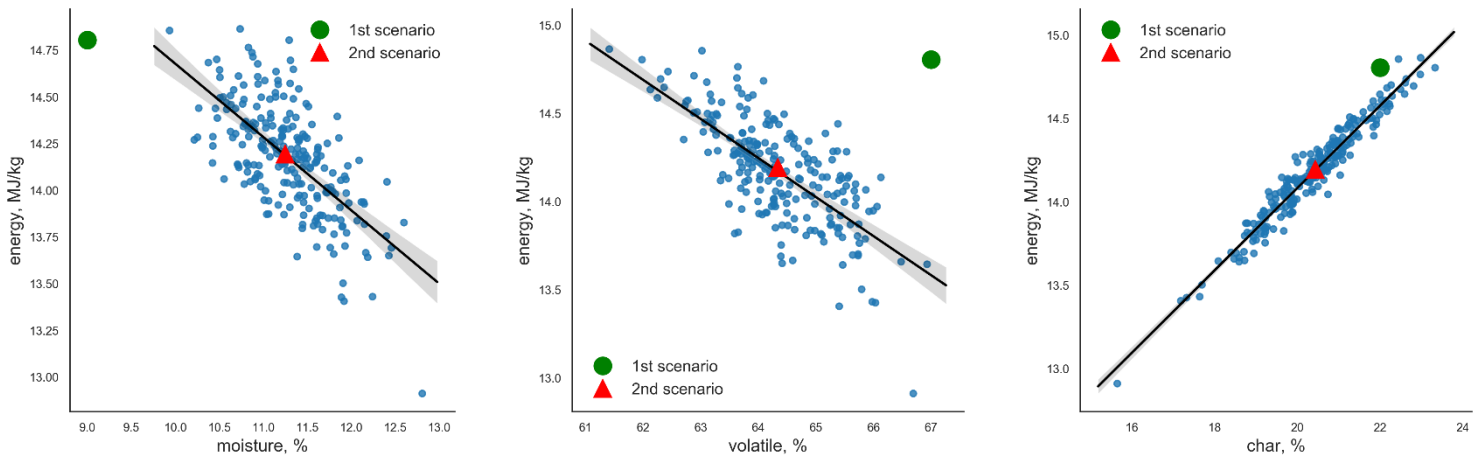


Figure 37. Produced heat fluctuation respect to fuel composition uncertainty in biomass boiler

Figure 37 shows heat generation in the system with respect to fuel compositions variability. It is important to note that a small amount of composition uncertainty can remarkably change energy generation by almost 1.5 MJ/kg. char content has the dominating role to energy generation among all compositions and causes less uncertainty in operation. Energy output from combustor reduces while moisture and volatile matter content increase. More volatile content is likely to cause less char and moisture content simultaneously. Less moisture results in higher heat generation while less char causes lower one. This can, therefore, demonstrate that char content outperforms moisture in the determination of biomass fuel quality. From Figure 37, it can be also observed that the first scenario is at the border of the expected range of system operation and unlikely to be met.

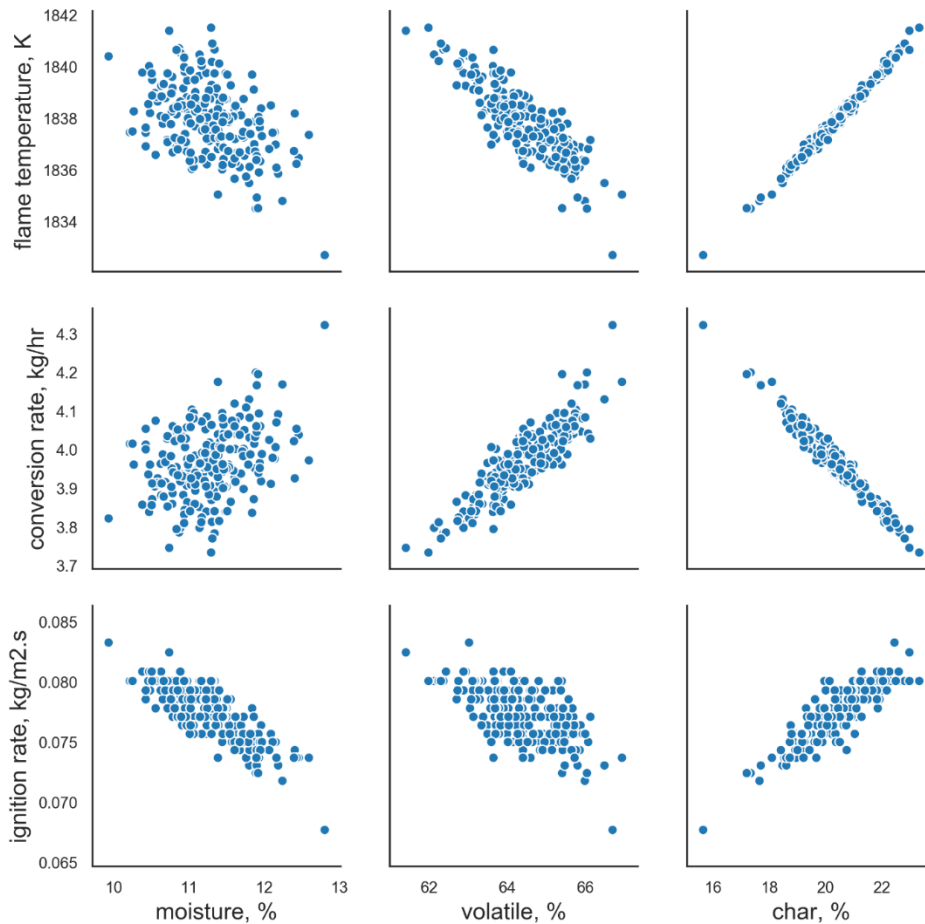


Figure 38. correlation between fuel compositions variability and ignition rate, conversion rate and flame temperature

Correlation between moisture, volatiles, and char variability with flame temperature, solid fuel conversion rate and ignition rate shown in Figure 38, identify valuable facts in terms of fuel bed combustion. Moisture uncertainty has an unbiased effect on flame temperature and fuel conversion but a strong negative impact on the ignition rate. Meanwhile, the flame temperature would not fluctuate significantly with composition variability as it is slightly dependent on volatile matter and char content in which emitting gases converted from these two compositions are the key determinants in overbed combustion. Volatiles would accelerate conversion in bed however it has a minor impact on ignition rate. Finally, char content in which its combustion is a slow reaction and makes the conversion time longer has an opposite impact on the flame temperature so as more char content means less volatile matter. The direct relation between char content and ignition rate can be interpreted based on solid combustion fundamental pointing that the ignition of fuel starts mainly in char reaction.

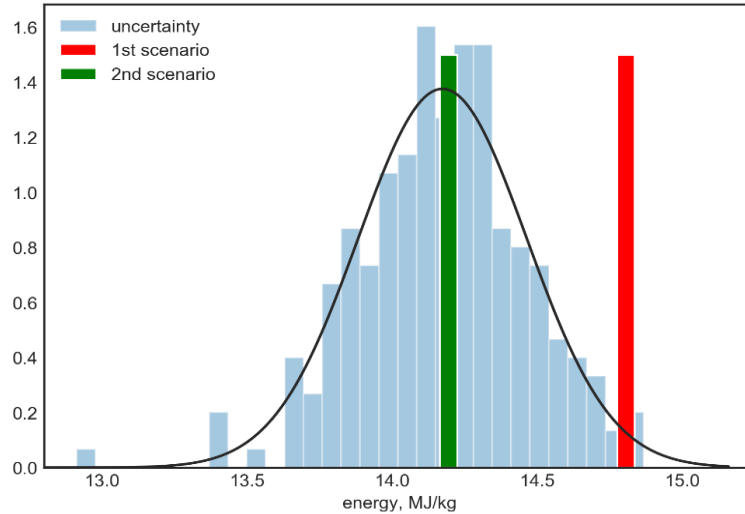


Figure 39. Heat generation from biomass combustion in the grate-firing combustor for various scenarios

Distribution of heat generation regarding fuel composition uncertainty together with that of first and second scenario in Figure 39 shows that the heat of system can deviate in a range of 13 to 15 MJ/kg while in average the expected value is around what is obtained in the second scenario by 14.2 MJ/kg. From the results, the boiler is predetermined to annually produce 512 GJ based upon idealistic scenario while it will practically generate 481 GJ on average, in other words, system setting on the first scenario causes 8.3% overestimation in system output.

Life cycle analysis (LCA)

A Life Cycle Analysis (LCA) on the proposed biomass boiler using both first and second scenarios conditions as well as a coal firing boiler on the same energy generation load is conducted. As a case study, a grate-firing boiler located in Alma town in Quebec province is selected for system installation [252]. The boundary of LCA is limited to fuel transportation from a source location to the wholesale distributor and then to the operation site, and facility operation for both coal and biomass systems along with biomass pellet production for biomass scenarios.

Major data deployed for LCA are shown in Table 33. It must be noted that the proposed distance was counted upon nearest wholesale fuel distributors for both biomass pellets and coal fuel.

Table 33. Input data for LCA analysis; first, second biomass scenario and coal-fueled case

	First scenario	Second scenario	Coal-fueled scenario
Distance from fuel supplier (km)	161	161	180
System load (Gj/year)	492	492	492

Fuel consumption (kg/year)	36,300	34,689	18,945
Transportation type	road	road	road
Fuel waste	✓	✗	✗

While there has been yet some controversial idea of whether biomass is a neutral CO₂ or not, the authors strongly believe that CO₂ emission resulted from biomass combustion should not be deemed. CO₂ amount fed in biomass resources from the atmosphere during growth is closely equal to what is emitted back to the atmosphere from combustion or degradation over the life cycle. Therefore, CO₂ emission is overlooked in biomass scenarios, and only particulate matter (PM), NO_x, SO_x are counted while CO₂ is the main pollutant in terms of coal plus those regarded to biomass fuel [253].

Table 34. LCA results of proposed scenarios based upon characterization indicator

Impact category	Unit	First scenario	Second scenario	Coal
Ozone depletion	kg CFC-11 eq	0.000138	0.000134	0.000548
Global warming	kg CO ₂ eq	1961.406	1937.524	48410.67
Smog	kg O ₃ eq	3498.394	3456.845	499.5801
Acidification	kg SO ₂ eq	91.93243	91.70835	31.87388
Eutrophication	kg N eq	11.59707	11.58003	9.957723
Carcinogenics	CTUh	7.74E-05	7.71E-05	8.78E-05
Non-carcinogenics	CTUh	0.000412	0.000409	0.000474
Respiratory effects	kg PM _{2.5} eq	2.059332	2.048117	3.156442
Ecotoxicity	CTUe	8706.071	8642.604	11078.96

Global warming impacts might be the most important factor among all, at least nowadays. As Table 34 illustrates, the coal system scenario has by far the highest influence on climate change owing to mainly coal fuel combustion and slightly from fuel transportation. In terms of biomass scenarios, the source of greenhouse gases originates from transportation and then marginally from pellet production. The breakdown of GHG contributors for all scenarios is elaborately presented in Figure 40.

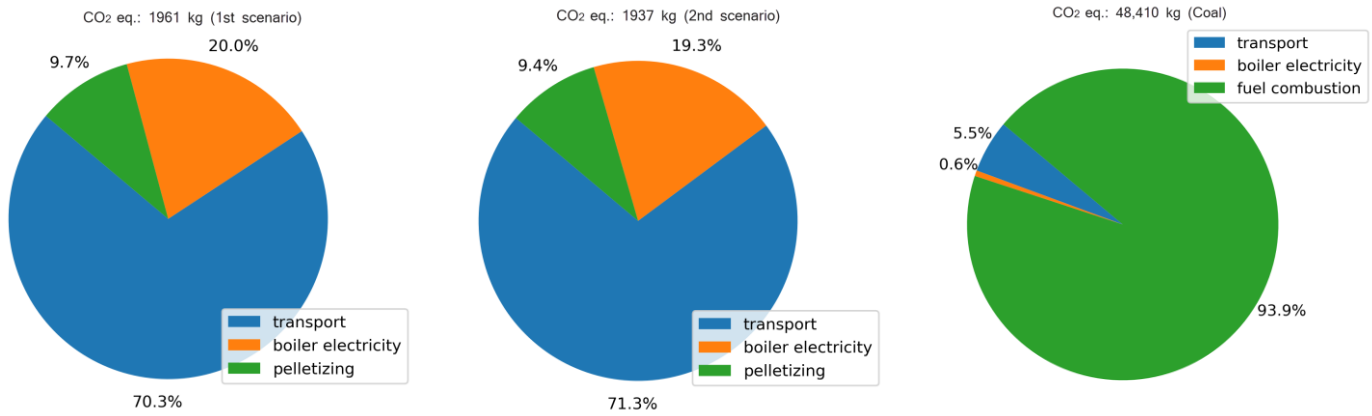


Figure 40. GHG contributors' breakdown for each scenario

Acidification mainly caused by SO_x and CO₂ emissions again is more intense for the biomass boiler due to higher sulfur content in biomass. Comparing two biomass scenarios, the first scenario partially causes more acidification than another one predominantly sourced from biomass combustion pollutants. On the other hand, ecotoxicity, which is originated from toxic materials like brake wear and tire wear emissions, and causes social health problems, is worse for the coal scenario due to further distance from mining sites than the other two scenarios. Other environmental impacts also can be observed for the proposed scenarios in Table 34.

5.2.4 An improved predictive maintenance plan for a vibrating-grate biomass boiler

A version of this section was published as: "Hosseini Rahdar M, Nasiri F, Lee B. Availability-based Predictive Maintenance Scheduling for Vibrating-grate Biomass Boilers. Safety and Reliability 2020."

Background

Apart from importance of suitable biomass particle conversion inside combustor affecting the combustor operation efficiency, a reliable maintenance plan of the whole system is another key factor mitigating the possibility of the system downtime which is put in higher priority order than combustion efficiency. Biomass boilers are particularly beneficial for remote areas where there is no access to the electricity grid with enough agricultural or forestry waste resources in the vicinity. In such circumstances, the availability of boiler systems is a critical factor due to some reasons. Access to most of the remote areas would be restricted particularly during the harsh winter owing to bad weather conditions along with their far distance from the cities. In this way, the supportability of such a system is fewer than a city-located system. This condition results in the difficulty of the maintenance arrangement when any breakdown occurs.

There are different methodologies of maintenance analysis for industrial assets such as Reliability-Availability-Maintainability (RAM), risk-based maintenance (RBM), and Bayesian network. While Reliability-Availability-Maintainability (RAM) model has served a well-established approach for product and asset management so far, nowadays rising complexity of systems requires more comprehensive approaches to deal with other aspects of management such as supportability, economics, environment, and politics [254].

In this section, a novel maintenance model for vibrating-grate biomass boilers is presented. The model aims to schedule the maintenance such that to minimize the number of maintenance tasks while the system availability remains intact. The reliability distribution parameters of the system and its components are estimated using regression analysis. A typical obstacle against using fault tree for the maintenance planning optimization is that with a simple breakdown of the system associated with a high number of components, the results are unlikely to be truly practical. Here authors recommend an approach to overcome this challenging issue by means of fault tree reconfiguration in a sophisticated way so that the maintenance of some components is integrated into a single practice to avoid over-maintenance. Finally, the optimization results for the biomass boiler maintenance would be verified by the expert judgment method.

The given system is a biomass boiler burning wood chips or pellets to produce heat for district heating and has several subsystems consists of feeding, combustion, boiler unit, ash gathering, flue gas and finally controlling part schematically disclosed in Figure 41.

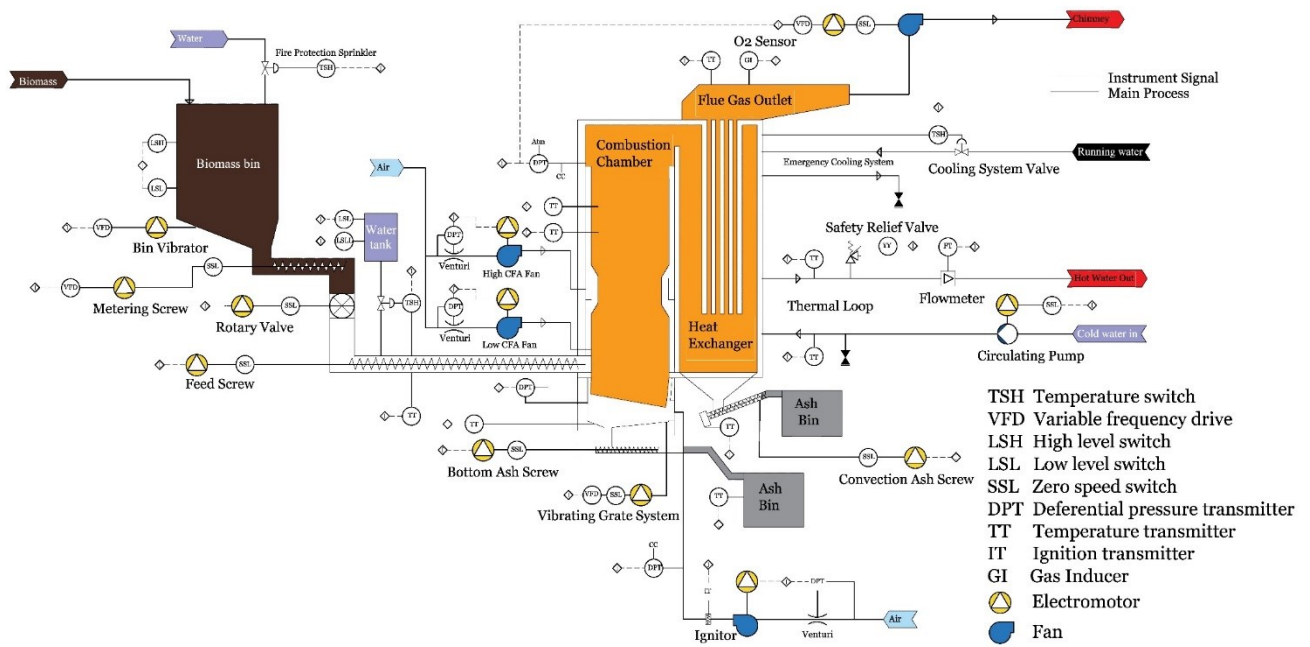


Figure 41. System configuration and instrument diagram of a 750 kW vibrating grate biomass boiler

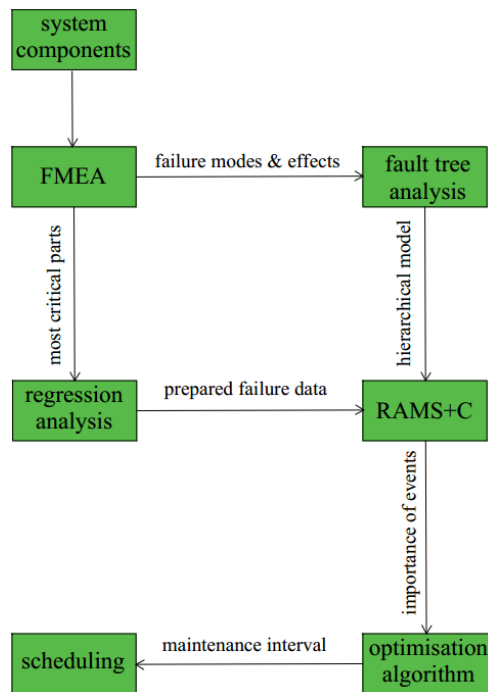


Figure 42. The model overview and interface of tools

Materials and methodology

A conceptual scheme of methodology deployed in this section is demonstrated in Figure 42. The asset components are delivered to Failure Modes and Effects Analysis (FMEA) to specify components failure modes, potential failure effects and their priority. The selected components are used in fault tree analysis and their relative failure data are gathered. In this article a RAMS+C approach is employed in order to address Reliability, Availability, Maintainability, Supportability, and implicitly Cost factors correspondingly for the proposed asset. The proposed optimization model provides us with optimal maintenance intervals and subsequently, the maintenance plan is assigned for expert judgment and final decision making. Following the system is being broken down, 33 unique critical components were recognized in consultation with experts. Failure incidents are defined as what physically occurs to equipment where a repair task is issued. Table 35 presents more common failure modes and possible effects of some critical components of the asset [255].

Table 35. failure modes and potential failure effects of asset components

part	common failure modes	potential effects of failure
sensor	insulator breakdown; high temperature; leakage current; dirt	<ul style="list-style-type: none"> • inaccurate sampling • loss of data recording
belt	belt wear; cracks in cog; breakage	<ul style="list-style-type: none"> • poor-efficient operation • vibration • loss of operation
relief valve	seal leakage; thermal effect on spring	<ul style="list-style-type: none"> • pressure change • loss of operation
mixing valve	seal leakage; pilot malfunctioning	<ul style="list-style-type: none"> • impaired operation • pressure loss
pulley	deformation; seat fracture; hub fracture	<ul style="list-style-type: none"> • vibration • noise • belt degradation
fan	impeller damage; shaft and bearing deterioration	<ul style="list-style-type: none"> • poor airflow • noise • vibration • loss of operation
water tank	leakage; corrosion; blockage	<ul style="list-style-type: none"> • inadequate water supply • damage to water pump
flowmeter	display panel; seal leakage; board hardware fault	<ul style="list-style-type: none"> • losing data reading • inaccurate operation
switch	high electricity field; dielectric breakdown; thermal aging	<ul style="list-style-type: none"> • intermittent operation • loss of operation
expansion joint	deformation; corrosion; thermal creep; cyclic fatigue	<ul style="list-style-type: none"> • vibration on system
bearing	local fatigue; wear damage; surface fatigue	<ul style="list-style-type: none"> • poor operation of attached system

transformer	insulation failure; thermal aging; winding failure	<ul style="list-style-type: none"> • loss of operation
pipe fitting	leakage; reduced wall thickness	<ul style="list-style-type: none"> • heat & pressure loss
gearbox	seal leakage; teeth fracture; bearing defect	<ul style="list-style-type: none"> • impaired operation • damaging electromotor • loss of operation
PLC	I/O modules; ground integrity; short circuit; power supply issue; heat	<ul style="list-style-type: none"> • moderate to very-high asset malfunctioning • loss of operation
VFD	high voltage; blown capacitor	<ul style="list-style-type: none"> • imperfect electric motor operation
pump	seal leakage; impeller fracture; bearing deterioration; corrosion; erosion; shaft fracture & deformation	<ul style="list-style-type: none"> • pressure loss • shortage in hot water supply
wiring	overload field fracture; failing of solder; wire melting; insulation damage; loss of continuity	<ul style="list-style-type: none"> • danger for staff • intermittent operation • loss of operation
motor	bearing defect; insulation fracture; wiring melting; current overload; overheating; dirt & moisture	<ul style="list-style-type: none"> • higher electricity consumption • poor output • loss of operation

The principal portion of the failure events in the given references originates from the useful lifetime which is occasionally known as a critical failure, where the rate of failure is approximately constant. A time-independent failure rate does not fit in the modified failure density function and a process of regression would be imperative to turn the equipment failure density function to the Weibull distribution function which can reflect the effect of the maintenance.

The failure density function of repairable components after maintenance needs to be modified concerning maintenance interval time (T), which seizes the frequency of preventive maintenance. Thereby, if $f(t)$ would be the current failure density function of a component, the modified failure density function of the component after maintenance would be represented as follow [256]:

$$f_T^*(t) = \sum_{k=0}^{\infty} f(t - kT)R^k T \quad (61)$$

where k is operation period and is equal to 0 in the first operational period, 1 in the second operational period and so on. T is maintenance interval time and $R^k T$ is a scaling factor which means the lower effect of maintenance over the life of the component. Likewise, the modified reliability function of Weibull distribution would be:

$$R_T^*(t) = \sum_{k=0}^{\infty} \exp \left[- \left(\frac{t - kT}{\alpha} \right)^{\beta} \right] R^{kT} \quad (62)$$

Since the failure rates are constant over operating time, it is deemed a hindrance against using the failure rate in our mathematical equations as the maintenance effect cannot be reflected in the system reliability. One solution to overcome this issue is to map the exponential function as the failure distribution on a Weibull function, and subsequently, the Weibull distribution parameters are extracted. In doing so, a regression task is carried out to determine the Weibull density function parameters (α and β) which provide the possibility of indication of maintenance impact mathematically respecting inconstant hazard function over time. Firstly, the failure data over the lifetime of each component were generated by virtue of the corresponding failure rate then, the regression regarding the Weibull distribution was performed to fit a Weibull distribution function to the data [257]. The α and β accompanying this fitted function were chosen as the new failure parameters for each component separately. Deviation of the fitted function came out in a reasonable range with reference data so that the goodness of fit resulted in a range of 0.022-0.035 for Kolmogorov Smirnov test. The results of the regression analysis can be found in Table 35 through Appendix I.

The proposed method in this study is based on the impact of the component's availability on the system availability which is so-called *maintenance impact*. It is aimed to reduce the number of maintenance tasks, which implicitly results in the lower maintenance cost while the system availability remains above its primary value. The fixed-interval preventive maintenance is often adopted to ensure high system availability coming up with the over-maintenance in most cases. The advantage of the optimal maintenance method to the traditional one is not only suggesting more reliable scheduling but also diminishing the maintenance cost. The reliability is generally referred to present a specific degree of assurance that the components of a system will stay successfully in working conditions over a certain period.

Maintenance impact plays a key role in the optimal maintenance scheduling, which is quantitatively described as the change in the system availability caused by the change in component's availability through the vicinity of average maintenance-interval types, and can be expressed as follow:

$$\Delta A_{j,k_j} = A(a_{j,k_j}) - A(a_{j,k_{j+1}}) \quad (63)$$

where $A(a_{j,k_j})$ and $A(a_{j,k_{j+1}})$ are system availability influenced by component j with k_j th average maintenance-interval type and (k_j+1) th average maintenance-interval type respectively. It has been assumed that k_j th is shorter maintenance period than (k_j+1) th. To achieve a precise optimal maintenance scheduling,

the accurate element availability calculation is vitally needed. The availability of component j with k th average maintenance-interval type can be obtained as follows:

$$a_{j,k_j} = \frac{M_{j,k_j}}{M_{j,k_j} + M_{r+s,k_j}} \quad (64)$$

where M_{j,k_j} is the mean time to failure (MTTF) of component j with the k th average maintenance-interval type, and $M_{r+s,j}$ summation of mean time to repair (MTTR) and mean time to supply (MTTS) of the component j in the system. Fault tree analysis of the system shown in figure 43.

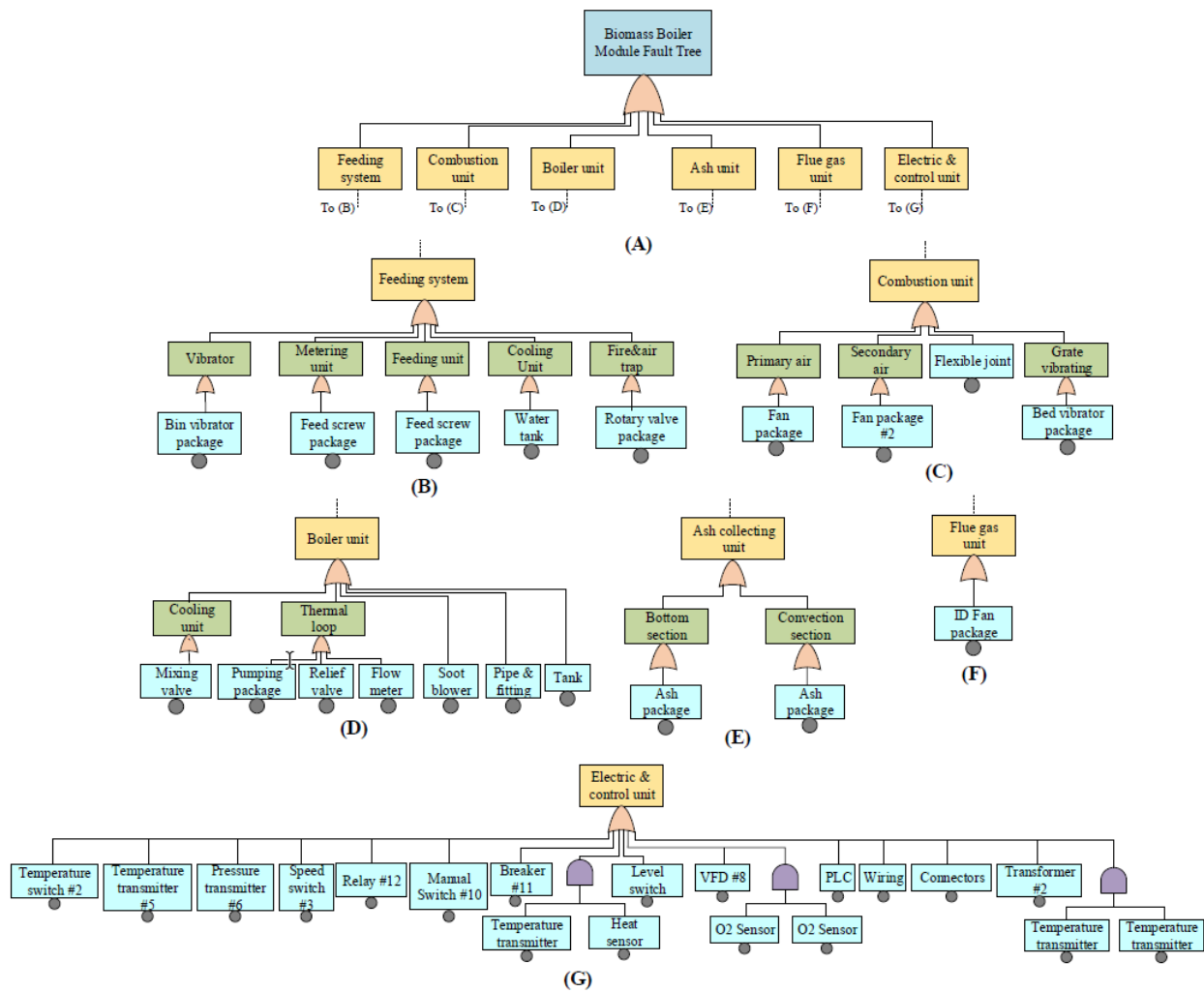


Figure 43. The fault tree analysis of serious incident of the vibrating biomass boiler

The MTTF is defined as working hours of the component during the life cycle prior to probable failure and mathematically defined as the integration of reliability of a component, while the MTTR+S depicts the demanded time for repair or replace a component merged with the logistic required time which was dug up from relative references and by consulting with a manufacturer to come up with more rational results.

$$MTTF^* = \int_0^{\infty} t f_T^*(t) dt \quad (65)$$

The initial service time interval for all elements has been assumed to be 12 months except for O₂ sensor which is 6 months due to the negative effect of ash deposition arising from bed combustion.

The optimization problem has one objective (Ω) implying the total number of maintenance effort over the life of the system which must be minimized given that the updated system availability (A_s^*) would never be under the initial system availability (A_s).

Optimization problem

Minimize Ω (overall number of maintenance task)

Subject to

$$A_s^* > A_s$$

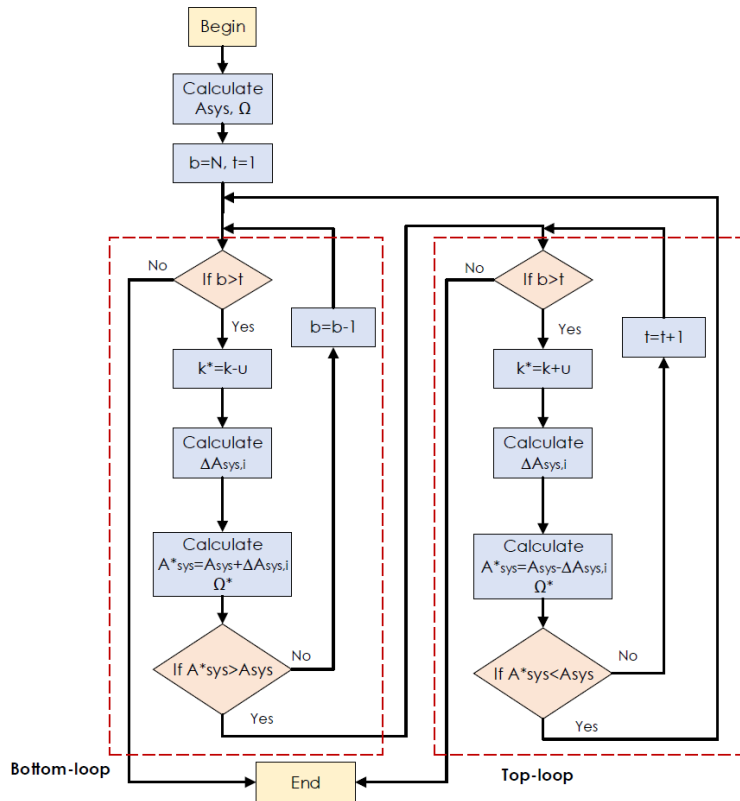


Figure 44. Optimization algorithm including two separate loops (Bottom-loop and Top-loop) for maintenance scheduling

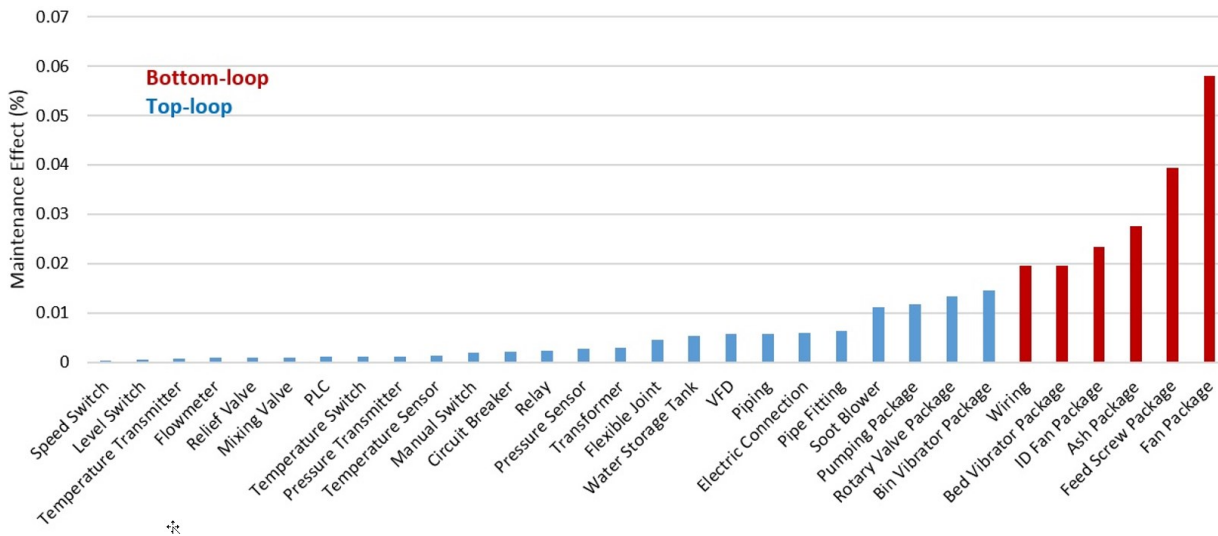


Figure 45. List of components based upon the maintenance effect corresponding to the fault tree analysis

The optimal maintenance plan schedules the periodic maintenance with respect to the maintenance impact of each component. In other words, components having a higher effect on the system availability should be

served higher consideration when periodical service is intended. Accordingly, it is indispensable to establish a sorted list of parts showing how they pertain to the availability of the system if the maintenance interval shift for a few months. To examine maintenance impact, the maintenance interval of all elements is changed from 12 to 16 months one-by-one, and the system availability deviation is measured for each element individually.

The optimization algorithm utilized to determine the optimal maintenance planning is displayed in Figure 44. First of all, the whole number of maintenance tasks in the lifetime of system as well as the current availability of the system, with the equal maintenance interval (every 12 months unlike O₂ sensor which is 6 months) is calculated. The latter system availability is pondered as the threshold criterion so that the modified system availability must never go down the threshold. Then, the six elements with the highest maintenance impact are called bottom-loop and the rest of them are called top-loop. Start with the element from the bottom-loop with the highest maintenance impact among the sorted list, and decrease its maintenance interval one unit of time (1 month) followed by system availability calculation. Thereafter, the process would be transferred to the top-loop of the algorithm initiating with a component having the lowest maintenance impact. The respective maintenance impact would be extended one unit of time and keep going to the next component through the top-loop list again followed by system availability computation in each step prior to the system availability goes under the threshold. It would move on to bottom-loop once more and the second element would be selected. This practice goes over and over up to the maintenance impact of all the components from bottom-loop would be shortened few months so that the top-loop could rationally compensate for the decreasing effect of bottom-loop on the system availability. Since the last element in bottom-loop interfaces with the last element of the top-loop, the stop criterion would be triggered and the process of optimization after the last step goes to the end where the optimal maintenance scheduling has been acquired and the number of service tasks could be counted to find out how many maintenance tasks have economized.

Results and discussion

The aforementioned mathematical modeling was implemented within a developed code by MATLAB to obtain the optimal maintenance schedule. The maintenance impact of components is illustrated in Figure 45, exposing the higher effect of the fan package, feed screw package, ash package, and ID fan package along with inversely the small impact of temperature transmitter and level switch, and flowmeter on the system availability. Comparison between maintenance impact and the failure rate of elements reveals that there is not necessarily a direct relationship between these two factors.

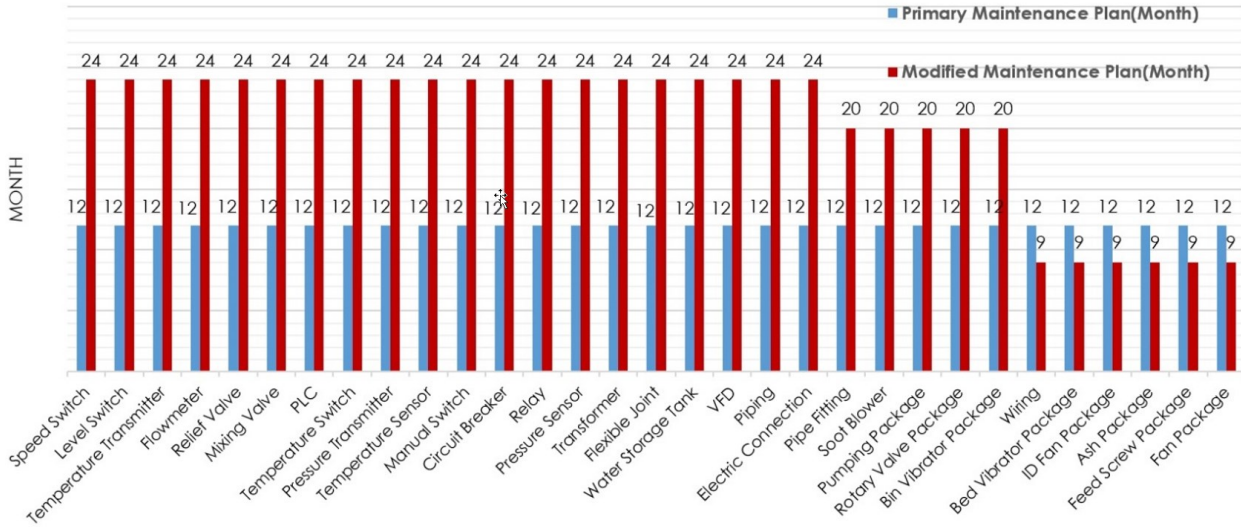


Figure 46. Optimal maintenance plan of the biomass boiler components

The results of maintenance optimization are presented in Figure 46. In accordance with this optimal maintenance scheduling, a significant reduction through the maintenance task has been achieved for the biomass boiler. In this course, the initial maintenance plan stipulates 310 service tasks for 10 years while in the optimal version of maintenance plan 210 tasks would be accomplished whereas the system availability remains over the initial availability. The results notify that if the maintenance of the subsystems/components in bottom-loop would be performed every 9 months instead of 12 months, despite the growth of maintenance actions from 60 to 80 in the bottom-loop, nevertheless, the maintenance efforts in the top-loop would decrease from 250 to 130 over 10 years. The optimal scheduling in comparison with the conventional one can reduce the number of maintenance tasks by 32.26% over 10 years. From the industrial aspect, this value is appreciated as a significant amount of cost-saving.

6 CONCLUSION AND FUTURE WORKS

The main conclusions of this research are highlighted here together with achievements and contributions by this study. Some possible improvements in this work as well as potential research areas in this field are recommended for future works.

6.1 Summary

In this study, practical aspects of moving bed biomass combustors were investigated by means of numerical modeling of biomass combustion and fuel particles experiment. The main focus of this study was on the thermal operation of biomass combustors while the environmental, economic, and reliability of systems were also addressed. The proposed methodology can be deemed a preventive control strategy to help biomass combustion improvement and to reduce incomplete solid combustion, especially inside the fuel bed.

6.2 Contributions

In this PhD thesis, experimental data of biomass pellets compositions were collected and trained to be integrated into the developed numerical model of moving bed biomass combustion. The aim was to quantify the effect of fuel composition variability on the biomass combustion properties. The following accomplishments have been made in this research:

- A TGA experiment was set up in order to measure the biomass particle compositions. 30 samples of biomass pellets were randomly gathered from different fuel bags, and moisture, volatile, char, and ash content of each particle were determined under the standard condition of the TGA experiment. The TGA experiment is accounted a micro-scale test that provides results with higher resolution than a furnace-based proximate analysis which is a macro-scale one. In order to assure repeatability of the experiment, the first pellet sample was tested twice.
- A Bayesian data generator model was created to populate data with the help of measured fuel compositions and the prior knowledge of fuel compositions claimed by the supplier. Then, a Gaussian distribution was mapped over the generated data, and subsequently the mean and standard deviation of each fuel composition were determined. Since there was an independency condition in fuel's sampled attributes, Gaussian distribution properly fits the problem.
- A 1D transient numerical model of biomass combustion on the moving grate was developed using the walking column approach. The model was properly regulated to be deployed for fuel composition variability analyses. Implicit schemes were governed for discretization so that a larger time step was possible.

- The Bayesian model and combustion model were integrated through a developed Python code in order to solve and visualize combustion properties under the uncertainty conditions.
- A comprehensive analysis of a small-scale biomass boiler was performed under different biomass fuels conditions. Required readjustments for system operation regarding each fuel were recommended and expected system outputs were obtained. Followed by expected operation, economic and environmental impacts for using each fuel in the proposed system were represented.
- An availability-based maintenance model for a vibrating-grate biomass boiler was conducted to improve the preventive maintenance condition of the proposed boiler. The RAMS+C approach was employed to count the component's availability.

6.3 Key Findings

Based upon the above contributions, several practical conclusions were achieved throughout this study, and here the most significant ones are briefly highlighted.

From this study, some practical conclusions were drawn for specialists and system owners. This work firstly delivers a useful tool for system operation readjustment when switching between various biomass waste fuels. The results of the simulation propose how air flow rate, primary air flow distribution, and fuel feeding rate should be readjusted for efficient system operation. Secondly, the feeding rate in moving bed biomass combustor must be counted using the actual fuel composition and relevant uncertainty instead of routine predefined composition so that avoiding the shortage of heat generation and waste of unburnt fuel in such systems. Last but not least, an availability-based preventive maintenance strategy was recommended in order to mitigate the cost of the maintenance program for a vibrating grate biomass boiler while system availability remains above initial availability. This maintenance model is quite practical for mid-scale moving bed boilers.

Significant biomass composition variability was realized for solid biomass even for the preprocessed fuel, such as biomass pellets. Repeatability examination of the first fuel particle experiment revealed that TGA analyzer provides high-resolution sampling. 30 biomass pellets samples sufficed the minimum amount of measured data, based on the fact that T-distribution, which is used for small data, becomes quite similar to Gaussian distribution for 25 samples above. Bayesian model properly used two sets of data: predefined fuel compound and measured fuel compound, in order to estimate fuel composition variability. The contribution of this variability on the combustion properties led to a remarkable variance in system outputs respecting the conversion rate inside the fuel bed and heat generation at overbed zone. In this way, the numerical modeling was found to be a robust tool for biomass combustion analyses, yet

it is far cheaper and more flexible than experimental analysis. Validation of model versus experiment data obtained from the packed beds proved that deploying one-dimensional transient model in place of two-dimensional steady-state model can sufficiently picture the fuel bed combustion in a less computational cost.

By comparison between the results of the current study and previous literature, it was concluded that fuel composition sensitivity analysis on combustion characteristics is not necessarily valid. For example, uncertainty analysis revealed that the fuel conversion rate had an unknown correlation with moisture content which is not in line with sensitivity analysis. Flame temperature showed a negligible sensitivity to fuel composition variability, while attributes such as ignition rate and conversion speed remarkably diverge especially for moisture and volatile content. Output heat flux as the most important parameter of the boilers showed a high sensitivity to fuel composition variability so that overlooking the biomass pellets composition variability caused a considerable overestimation in system output. In the course of char content, heat generation variability is limited to a small range, whereas this variation significantly increases concerning the moisture and volatile content. Hence, output heat generation uncertainty can be mitigated by using fuel with higher char content and lower moisture and volatile for example, biochar.

From the point of environmental impact, deploying biomass in the combustion system can significantly mitigate GHG emissions, although it has a minor impact on some other environmental terms such as Acidification and Eutrophication. Based on the results, switching from wood waste to biomass pellets, and from biomass pellets to biochar pellets, not only are the effective steps in order to restrain the biomass combustion uncertainty but improve the system thermal efficiency to a significant degree. Since the biomass conversion inside the bed is a very slow process, even systems equipped with a control unit can only improve the gas-phase combustion and it is not able to guarantee better solid-phase combustion. This study proposed a passive control strategy for moving bed biomass combustors which generally outperform the baseline operations.

From the economic aspect, it was concluded that the cost of heat from the biomass boiler in terms of various biomass fuels is at a competitive rate with the grid rate for North America. Respect to the fact that the boiler under the proposed biomass pellets feeding annually generates more heat than the proposed wood waste and RDF, higher revenue can be achieved using the pellets. From the maintenance viewpoint, taking the availability effect of each subsystem maintenance into the account, the proposed optimal maintenance schedule could reduce the maintenance cost of the biomass boiler by about 30%.

6.4 Future works

Since this research focused on the biomass composition variability, the combustion model was developed in a way to meet research requirements. It is recommended to survey the effect of particle size and shape uncertainty on the biomass combustion by applying required modifications to the combustion model. In this course, since the sampling of particle size and shape is relatively easy, the uncertainty model can be reliably created using a high number of data.

In this research, it was concluded that using biomass pellets instead of biomass chips can mitigate operation uncertainty mainly because of higher char content and less moisture of fuel. A comprehensive evaluation of grate biomass boiler under biochar pellets feeding is recommended.

Apart from grate biomass boilers, fluidized bed biomass boilers are widely used in big power plants. A similar approach to the current study can be extended for fluidized bed furnaces.

With engaging the explicit maintenance cost of each component individually, a multi-objective model could be developed to find the feasible scenarios between maximum system availability and minimum total maintenance cost. Similarly, the system availability would be the lower constraint for the system availability and upper and lower restriction of service actions could be speculated in consultation with manufacturers and experts as well.

Data science development has provided a wide range of research areas in recent years, thus, the application of data science should be vigorously developed in biomass combustion studies. For example, a high-speed infrared imaging tool is able to deliver pure and accurate data during the biomass combustion, and these data could be analyzed and learned using deep learning techniques to construct data-driven models.

One interesting research topic around biomass fuels could be a feasibility study of the use of left-overs from cargo ships as fuel in biomass combustor. Carrying garbage is a challenging issue for cargo ships while most of the garbage can be burned on the ships for heating purposes. A comprehensive study of benefits, challenges, and feasibility of a garbage-fueled combustor on a cargo ship is recommended.

REFERENCES

- [1] Bridgwater T. Biomass for energy. *J Sci Food Agric* 2006;86:1755–68. doi:10.1002/jsfa.
- [2] Bryden KM, Ragland KW. Numerical Modeling of a Deep, Fixed Bed Combustor. *Energy and Fuels* 1996;10:269–75. doi:10.1021/ef950193p.
- [3] Demirbas A. Potential applications of renewable energy sources, biomass combustion problems in boiler power systems and combustion related environmental issues. *Prog Energy Combust Sci* 2005;31:171–92. doi:10.1016/J.PECS.2005.02.002.
- [4] Mason PE, Darvell LI, Jones JM, Pourkashanian M, Williams A. Single particle flame-combustion studies on solid biomass fuels. *Fuel* 2015;151:21–30. doi:10.1016/J.FUEL.2014.11.088.
- [5] Biswas AK, Umeki K. Simplification of devolatilization models for thermally-thick particles: Differences between wood logs and pellets. *Chem Eng J* 2015;274:181–91. doi:10.1016/j.cej.2015.03.131.
- [6] Heidari M, Dutta A, Acharya B, Mahmud S. A review of the current knowledge and challenges of hydrothermal carbonization for biomass conversion. *J Energy Inst* 2018. doi:10.1016/J.JOEL.2018.12.003.
- [7] Yung MM, Jablonski WS, Magrini-Bair KA. Review of Catalytic Conditioning of Biomass-Derived Syngas. *Energy & Fuels* 2009;23:1874–87. doi:10.1021/ef800830n.
- [8] Zhang J, Wu R, Zhang G, Yu J, Yao C, Wang Y, et al. Technical Review on Thermochemical Conversion Based on Decoupling for Solid Carbonaceous Fuels. *Energy & Fuels* 2013;27:1951–66. doi:10.1021/ef400118b.
- [9] Goyal HB, Seal D, Saxena RC. Bio-fuels from thermochemical conversion of renewable resources: A review. *Renew Sustain Energy Rev* 2008;12:504–17. doi:10.1016/J.RSER.2006.07.014.
- [10] Heidari M, Salaudeen S, Dutta A, Acharya B. Effects of Process Water Recycling and Particle Sizes on Hydrothermal Carbonization of Biomass. *Energy and Fuels* 2018;32:11576–86. doi:10.1021/acs.energyfuels.8b02684.
- [11] Heidari M, Garnaik PP, Dutta A. 11 - The Valorization of Plastic Via Thermal Means: Industrial Scale Combustion Methods. In: Al-Salem SMBT-P to E, editor. *Plast. Des. Libr.*, William Andrew Publishing; 2019, p. 295–312. doi:https://doi.org/10.1016/B978-0-12-813140-4.00011-X.
- [12] Farokhi M, Birouk M, Tabet F. A computational study of a small-scale biomass burner: The influence of chemistry, turbulence and combustion sub-models. *Energy Convers Manag* 2017;143:203–17. doi:10.1016/j.enconman.2017.03.086.
- [13] Klason T. Modelling of Biomass Combustion in Furnaces. Lund university, 2006.
- [14] Bhuiyan AA, Karim MR, Naser J. Modeling of Solid and Bio-Fuel Combustion Technologies. Elsevier Inc.; 2015. doi:10.1016/B978-0-12-802397-6.00016-6.
- [15] Scharler R, Benesch C, Neudeck A, Obernberger I. CFD based design and optimisation of wood log fired stoves. 17th Eur Biomass Conf Exhib From Res to Ind Mark 2009;113:207–21.
- [16] Karim MR, Naser J. CFD modelling of combustion and associated emission of wet woody biomass in a 4 MW moving grate boiler. *Fuel* 2018;222:656–74. doi:10.1016/J.FUEL.2018.02.195.
- [17] Yin C, Rosendahl L, Kær SK, Clausen S, Hvid SL. Mathematical Modeling and Experimental Study of Biomass Combustion in a Thermal 108 MW Grate-Fired Boiler. *Energy and Fuels* 2008;22:1380–90.
- [18] Pepiot P, Dibble CJ, Foust TD. Computational fluid dynamics modeling of biomass gasification and pyrolysis. *ACS Symp Ser* 2010;1052:273–98. doi:10.1021/bk-2010-1052.ch012.
- [19] Li H. Cfd Modelling Study of Sprays and Combustion of Gasoline and Dmf in Direct Injection Gasoline Engines 2013:205.
- [20] Zhang J, Prationo W, Zhang L, Zhang Z. Computational fluid dynamics modeling on the air-firing and oxy-fuel combustion of dried victorian brown coal. *Energy and Fuels* 2013;27:4258–69. doi:10.1021/ef400032t.
- [21] Walsh AR. CFD Modeling of Waste-Fuel Boiler Combustion Systems n.d.:2.
- [22] Nasserzadeh V, Swithenbank J, Scott D, Jones B. Design optimization of a large municipal solid waste incinerator. *Waste Manag* 1991;11:249–61. doi:10.1016/0956-053X(91)90072-D.
- [23] Nasserzadeh V, Swithenbank J, Jones B. Effect Of High Speed Secondary Air Jets On The Overall Performance Of A Large MSW Incinerator With A Vertical Shaft. *Combust Sci Technol* 1993;92:389–422. doi:10.1080/00102209308907680.

- [24] Users FS. CFD Guides Design of Biomass Boiler Retrofit to Increase Capacity by 25 % and Decrease Ash Carryover by 60% 2004:1–5.
- [25] Farokhi M, Birouk M. A hybrid EDC/Flamelet approach for modelling biomass combustion of grate-firing furnace. *Combust Theory Model* 2019;7830. doi:10.1080/13647830.2019.1587177.
- [26] Kim S, Shin D, Choi S. Comparative evaluation of municipal solid waste incinerator designs by flow simulation. *Combust Flame* 1996;106:241–51. doi:10.1016/0010-2180(95)00190-5.
- [27] Scharler R, Obernberger I. Les excursions glycémiques: Etat des connaissances - Editorial. *Diabetes Metab* 2000;26:5. doi:10.1016/j.ica.2008.07.007.
- [28] Stubenberger G, Scharler R, Zahirović S, Obernberger I. Experimental investigation of nitrogen species release from different solid biomass fuels as a basis for release models. *Fuel* 2008;87:793–806. doi:10.1016/J.FUEL.2007.05.034.
- [29] Razmjoo N, Sefidari H, Strand M. Characterization of hot gas in a 4 MW reciprocating grate boiler. *Fuel Process Technol* 2014;124:21–7. doi:10.1016/J.FUPROC.2014.02.011.
- [30] Goerner K, Klason T. Modelling, simulation and validation of the solid biomass combustion in different plants. *Prog Comput Fluid Dyn* 2006;6:225–34. doi:10.1504/PCFD.2006.010031.
- [31] Weissinger A, Fleckl T, Obernberger I. In: *Proceedings of the 1. Energy 2000*;II:2–5.
- [32] Anca-Couce A, Sommersacher P, Evic N, Mehrabian R, Scharler R. Experiments and modelling of NO_x precursors release (NH₃ and HCN) in fixed-bed biomass combustion conditions. *Fuel* 2018;222:529–37. doi:10.1016/J.FUEL.2018.03.003.
- [33] Weissinger A, Fleckl T, Obernberger I. In situ FT-IR spectroscopic investigations of species from biomass fuels in a laboratory-scale combustor: the release of nitrogenous species. *Combust Flame* 2004;137:403–17. doi:10.1016/J.COMBUSTFLAME.2004.02.010.
- [34] Dong W, Blasiak W. CFD modeling of ecotube system in coal and waste grate combustion. *Energy Convers Manag* 2001;42:1887–96. doi:10.1016/S0196-8904(01)00048-6.
- [35] Blasiak W, Yang WH, Dong W. Combustion performance improvement of grate fired furnaces using Ecotube system. *J Energy Inst* 2006;79:67–74. doi:10.1179/174602206X103530.
- [36] Griselin N, Bai X-S. Particle dynamics in a biomass fired furnace predictions of solid residence changes with operation. *IFRF Combust J* 2000;October.
- [37] Klason T, Bai XS. Combustion process in a biomass grate fired industry furnace: a CFD study. *Prog Comput Fluid Dyn An Int J* 2006;6:278. doi:10.1504/PCFD.2006.010581.
- [38] Ström H, Thunman H. A computationally efficient particle submodel for CFD-simulations of fixed-bed conversion. *Appl Energy* 2013;112:808–17. doi:10.1016/J.APENERGY.2012.12.057.
- [39] Bryden KM, Ragland KW, Rutland CJ. Modeling thermally thick pyrolysis of wood. *Biomass and Bioenergy* 2002;22:41–53. doi:10.1016/S0961-9534(01)00060-5.
- [40] Xu Y, Zhai M, Jin S, Zou X, Liu S, Dong P. Numerical simulation of high-temperature fusion combustion characteristics for a single biomass particle. *Fuel Process Technol* 2019;183:27–34. doi:10.1016/J.FUPROC.2018.10.024.
- [41] González WA, Pérez JF, Chapela S, Porteiro J. Numerical analysis of wood biomass packing factor in a fixed-bed gasification process. *Renew Energy* 2018;121:579–89. doi:10.1016/J.RENENE.2018.01.057.
- [42] Rajh B, Yin C, Samec N. Advanced modelling and testing of a 13 MW th waste wood-fired grate boiler with recycled flue gas. *Energy Convers Manag* 2016;125:230–41. doi:10.1016/j.enconman.2016.02.036.
- [43] Karim MR, Naser J. Numerical study of the ignition front propagation of different pelletised biomass in a packed bed furnace. *Appl Therm Eng* 2018;128:772–84. doi:10.1016/J.APPLTHERMALENG.2017.09.061.
- [44] Khodaei H, Yeoh GH, Guzzomi F, Porteiro J. A CFD-based comparative analysis of drying in various single biomass particles. *Appl Therm Eng* 2018;128:1062–73. doi:10.1016/J.APPLTHERMALENG.2017.09.070.
- [45] Zhou H, Jensen AD, Glarborg P, Jensen PA, Kavaliuskas A. Numerical modeling of straw combustion in a fixed bed. *Fuel* 2005;84:389–403. doi:10.1016/J.FUEL.2004.09.020.
- [46] Wurzenberger JC, Wallner S, Raupenstrauch H, Khinast JG. Thermal conversion of biomass: Comprehensive reactor and particle modeling. *AIChE J* 2002;48:2398–411. doi:10.1002/aic.690481029.
- [47] Porteiro J, Patiño D, Moran J, Granada E. Study of a fixed-bed biomass combustor: Influential parameters on ignition front propagation using parametric analysis. *Energy and Fuels* 2010;24:3890–7. doi:10.1021/ef100422y.
- [48] Ranzi E, Pierucci S, Aliprandi PC, Stringa S. Comprehensive and detailed kinetic model of a traveling grate combustor of biomass. *Energy and Fuels* 2011;25:4195–205. doi:10.1021/ef200902v.

- [49] Thunman H, Leckner B. Influence of size and density of fuel on combustion in a packed bed. *Proc Combust Inst* 2005;30:2939–46. doi:10.1016/J.PROCI.2004.07.010.
- [50] Anca-Couce A, Zobel N, Jakobsen HA. Multi-scale modeling of fixed-bed thermo-chemical processes of biomass with the representative particle model: Application to pyrolysis. *Fuel* 2013;103:773–82. doi:10.1016/J.FUEL.2012.05.063.
- [51] Johansson R, Thunman H, Leckner B. Influence of intraparticle gradients in modeling of fixed bed combustion. *Combust Flame* 2007;149:49–62. doi:10.1016/J.COMBUSTFLAME.2006.12.009.
- [52] Shin D, Choi S. The combustion of simulated waste particles in a fixed bed. *Combust Flame* 2000;121:167–80. doi:10.1016/S0010-2180(99)00124-8.
- [53] Hallett W, Green B, Machula T, Yang Y. Packed bed combustion of non-uniformly sized char particles. *Chem Eng Sci* 2013;96:1–9. doi:10.1016/J.CES.2013.02.070.
- [54] Peters B, Schröder E, Bruch C, Nussbaumer T. Measurements and particle resolved modelling of heat-up and drying of a packed bed Biomass and Bioenergy 2002;23:291–306. doi:10.1016/S0961-9534(02)00052-1.
- [55] Yang Y Bin, Ryu C, Khor A, Yates NE, Sharifi VN, Swithenbank J. Effect of fuel properties on biomass combustion. Part II. Modelling approach—identification of the controlling factors. *Fuel* 2005;84:2116–30. doi:10.1016/J.FUEL.2005.04.023.
- [56] Johansson R, Thunman H, Leckner B. Sensitivity analysis of a fixed bed combustion model. *Energy and Fuels* 2007;21:1493–503. doi:10.1021/ef060500z.
- [57] Yang Y Bin, Ryu C, Khor A, Sharifi VN, Swithenbank J. Fuel size effect on pinewood combustion in a packed bed. *Fuel* 2005;84:2026–38. doi:10.1016/j.fuel.2005.04.022.
- [58] Karim MR, Naser J. Numerical Modelling of Solid Biomass Combustion: Difficulties in Initiating the Fixed Bed Combustion. *Energy Procedia* 2017;110:390–5. doi:10.1016/J.EGYPRO.2017.03.158.
- [59] Mehrabian R, Shiehnejadhesar A. Numerical modelling of biomass grate furnaces with a particle based model. 10th Eur Conf Ind Furn Boil – Porto, Port 2015:1–14.
- [60] Lans RP Van Der, Pedersen LT, Jensen A, Glarborg P. Modelling and experiments of straw combustion in a grate furnace. *Biomass and Bioenergy* 2000;19:199–208.
- [61] Gómez MA, Porteiro J, Patiño D, Míguez JL. Eulerian CFD modelling for biomass combustion. Transient simulation of an underfeed pellet boiler. *Energy Convers Manag* 2015;101:666–80. doi:10.1016/j.enconman.2015.06.003.
- [62] Zhang X, Chen Q, Bradford R, Sharifi V, Swithenbank J. Experimental investigation and mathematical modelling of wood combustion in a moving grate boiler. *Fuel Process Technol* 2010;91:1491–9. doi:10.1016/J.FUPROC.2010.05.026.
- [63] Yang Y Bin, Newman R, Sharifi V, Swithenbank J, Ariss J. Mathematical modelling of straw combustion in a 38 MWe power plant furnace and effect of operating conditions. *Fuel* 2007;86:129–42. doi:10.1016/j.fuel.2006.06.023.
- [64] Groppi G, Tronconi E, Forzatti P, Berg M. Mathematical modelling of catalytic combustors fuelled by gasified biomasses. *Catal Today* 2000;59:151–62.
- [65] Meng X, Sun R, Ismail TM, El-Salam MA, Zhou W, Zhang R, et al. Assessment of primary air on com straw in a fixed bed combustion using Eulerian-Eulerian approach. *Energy* 2018;151:501–19. doi:10.1016/J.ENERGY.2018.03.081.
- [66] Karim MR, Ovi IRQ, Naser J. A CFD model for biomass combustion in a packed bed furnace. *AIP Conf Proc* 2016;1754. doi:10.1063/1.4958417.
- [67] Gómez MA, Comesaña R, Feijoo MAÁ, Eguía P. Simulation of the effect of water temperature on domestic biomass boiler performance. *Energies* 2012;5:1044–61.
- [68] Collazo J, Porteiro J, Patiño D, Granada E. Numerical modeling of the combustion of densified wood under fixed-bed conditions. *Fuel* 2012;93:149–59. doi:10.1016/J.FUEL.2011.09.044.
- [69] Peters B, Schröder E, Bruch C. Measurements and particle resolved modelling of the thermo- and fluid dynamics of a packed bed. *J Anal Appl Pyrolysis* 2003;70:211–31. doi:10.1016/S0165-2370(02)00133-X.
- [70] Tu Y, Zhou A, Xu M, Yang W, Siah KB, Subbaiah P. NOX reduction in a 40 t/h biomass fired grate boiler using internal flue gas recirculation technology. *Appl Energy* 2018;220:962–73. doi:10.1016/J.APENERGY.2017.12.018.
- [71] Ghabi C, Benticha H, Sassi M. Two-dimensional computational modeling and simulation of wood particles pyrolysis in a fixed bed reactor. *Combust Sci Technol* 2008;180:833–53. doi:10.1080/00102200801894091.
- [72] Ranzi E, Corbetta M, Manenti F, Pierucci S. Kinetic modeling of the thermal degradation and combustion of biomass. *Chem Eng Sci* 2014;110:2–12. doi:10.1016/J.CES.2013.08.014.
- [73] Momeni M, Yin C, Kær SK, Hansen TB, Jensen PA, Glarborg P. Experimental study on effects of particle shape and operating conditions

- on combustion characteristics of single biomass particles. *Energy and Fuels* 2013;27:507–14. doi:10.1021/ef301343q.
- [74] Haseli Y, van Oijen JA, de Goey LPH. Predicting the pyrolysis of single biomass particles based on a time and space integral method. *J Anal Appl Pyrolysis* 2012;96:126–38. doi:10.1016/J.JAAP.2012.03.014.
- [75] Haseli Y, Van Oijen JA, De Goey LPH. A quasisteady analysis of oxy-fuel combustion of a wood char particle. *Combust Sci Technol* 2013;185:533–47. doi:10.1080/00102202.2012.721035.
- [76] Fatehi M, Kaviany M. Adiabatic reverse combustion in a packed bed. *Combust Flame* 1994;99:1–17. doi:10.1016/0010-2180(94)90078-7.
- [77] Gómez MA, Porteiro J, Patiño D, Míguez JL. CFD modelling of thermal conversion and packed bed compaction in biomass combustion. *Fuel* 2014;117:716–32. doi:10.1016/J.FUEL.2013.08.078.
- [78] Collazo J, Porteiro J, Patiño D, Granada E. Numerical modeling of the combustion of densified wood under fixed-bed conditions. *Fuel* 2012;93:149–59. doi:10.1016/J.FUEL.2011.09.044.
- [79] Kumar S, Dasappa S. Modeling and analysis of single particle conversion of biomass in a packed bed gasification system. *Appl Therm Eng* 2017;112:1382–95. doi:10.1016/J.APPLTHERMALENG.2016.10.170.
- [80] Anca-Couce A, Sommersacher P, Scharler R. Online experiments and modelling with a detailed reaction scheme of single particle biomass pyrolysis. *J Anal Appl Pyrolysis* 2017;127:411–25. doi:10.1016/J.JAAP.2017.07.008.
- [81] Biswas AK, Umeki K. Simplification of devolatilization models for thermally-thick particles: Differences between wood logs and pellets. *Chem Eng J* 2015;274:181–91. doi:10.1016/J.CEJ.2015.03.131.
- [82] Ström H, Thunman H. CFD simulations of biofuel bed conversion: A submodel for the drying and devolatilization of thermally thick wood particles. *Combust Flame* 2013;160:417–31. doi:10.1016/J.COMBUSTFLAME.2012.10.005.
- [83] Gómez MA, Porteiro J, Patiño D, Míguez JL. Fast-solving thermally thick model of biomass particles embedded in a CFD code for the simulation of fixed-bed burners. *Energy Convers Manag* 2015;105:30–44. doi:10.1016/J.ENCONMAN.2015.07.059.
- [84] Lehmann R. Angiographie Beim Irreversiblen Funktionsverlust Des Gehirns. *Zentralbl Chir* 1975;100:412–20. doi:10.1016/j.fuel.2018.02.063.
- [85] Gómez MA, Porteiro J, Chapela S, Míguez JL. An Eulerian model for the simulation of the thermal conversion of a single large biomass particle. *Fuel* 2018;220:671–81. doi:10.1016/J.FUEL.2018.02.063.
- [86] Yang W, Ryu C, Choi S. Unsteady one-dimensional model for a bed combustion of solid fuels. *Proc Inst Mech Eng Part A J Power Energy* 2004;218:589–98. doi:10.1243/0957650042584348.
- [87] Khodaei H, Yeoh GH, Guzzomi F, Porteiro J. A CFD-based comparative analysis of drying in various single biomass particles. *Appl Therm Eng* 2018;128:1062–73. doi:10.1016/J.APPLTHERMALENG.2017.09.070.
- [88] Kwiatkowski K, Górecki B, Korotko J, Gryglas W, Dudyński M, Bajek K. Numerical modeling of biomass pyrolysis - Heat and mass transport models. *Numer Heat Transf Part A Appl* 2013;64:216–34. doi:10.1080/10407782.2013.779166.
- [89] Varunkumar S, Rajan NKS, Mukunda HS. Single particle and packed bed combustion in modern gasifier stoves-density effects. *Combust Sci Technol* 2011;183:1147–63. doi:10.1080/00102202.2011.576658.
- [90] Kamila B, Sadhukhan AK, Gupta P, Basu P, Acharya B. Modeling of torrefaction of small biomass particles. *Biofuels* 2017;7:269:1–10. doi:10.1080/17597269.2017.1358941.
- [91] Kamila B, Sadhukhan AK, Gupta P, Basu P, Regmi B, Dutta A, et al. Two-dimensional modeling of torrefaction of a large biomass particle. *Int J Green Energy* 2017;14:1119–29. doi:10.1080/15435075.2017.1359785.
- [92] Sousa N, Azevedo JLT. Model simplifications on biomass particle combustion. *Fuel* 2016;184:948–56. doi:10.1016/J.FUEL.2016.03.106.
- [93] Yang YB, Sharifi VN, Swithenbank J, Ma L, IL, Jones JM, et al. Combustion of a Single Particle of Biomass Combustion of a Single Particle of Biomass. *Energy* 2008;306–16. doi:10.1021/ef700305r.
- [94] Gort R, Brouwers JJH. Theoretical analysis of the propagation of a reaction front in a packed bed. *Combust Flame* 2001;124:1–13. doi:10.1016/S0010-2180(00)00149-8.
- [95] Vortmeyer D. Packed bed thermal dispersion models and consistent sets of coefficients. *Chem Eng Process* 1989;26:263–8. doi:10.1016/0255-2701(89)80026-1.
- [96] Juřena T. Vysoké učení technické v Brně, Ústav procesního a ekologického inženýrství. Numerical modelling of grate combustion = Numerické modelování spalování na roštu: zkrácená verze Ph.D. Thesis. 2012.
- [97] Mahmoudi AH, Besseron X, Hoffmann F, Markovic M, Peters B. Modeling of the biomass combustion on a forward acting grate using XDEM. *Chem Eng Sci* 2016;142:32–41. doi:10.1016/j.ces.2015.11.015.

- [98] Martinez-Garcia J, Nussbaumer T. A one-dimensional transient solid fuel conversion model for grate combustion optimization. *Combust Sci Technol* 2015;187:1208–28. doi:10.1080/00102202.2015.1027819.
- [99] Mehrabian R, Scharler R, Weissinger A, Obemberger I. Optimisation of biomass grate furnaces with a new 3D packed bed combustion model - on example a small-scale underfeed stoker furnace. 18th Eur Biomass Conf Exhib 2010:1–6.
- [100] Zhang X. Numerical modeling of biomass combustion in a stoker boiler. 2011.
- [101] Vargas WL, McCarthy J. Conductivity of granular media with stagnant interstitial fluids via thermal particle dynamics simulation. *Int J Heat Mass Transf* 2002;45:4847–56. doi:10.1016/S0017-9310(02)00175-8.
- [102] Schulze S, Nikrityuk P, Compart F, Richter A, Meyer B. Particle-resolved numerical study of char conversion processes in packed beds. *Fuel* 2017;207:655–62. doi:10.1016/J.FUEL.2017.05.071.
- [103] Mehrabian R, Shiehnejadhesar A, Scharler R, Obemberger I. Multi-physics modelling of packed bed biomass combustion. *Fuel* 2014;122:164–78. doi:10.1016/J.FUEL.2014.01.027.
- [104] Yang YB, Sharifi VN, Swithenbank J. Numerical simulation of the burning characteristics of thermally-thick biomass fuels in packed-beds. *Process Saf Environ Prot* 2005;83:549–58. doi:10.1205/psep.04284.
- [105] Hosseini Rahdar M, Nasiri F, Lee B. A Review of Numerical Modeling and Experimental Analysis of Combustion in Moving Grate Biomass Combustors. *Energy & Fuels* 2019;33:9367–9402. doi:10.1021/acs.energyfuels.9b02073.
- [106] Chen J, Yin W, Wang S, Yu G, Li J, Hu T, et al. Modelling of coal/biomass co-gasification in internal circulating fluidized bed using kinetic theory of granular mixture. *Energy Convers Manag* 2017;148:506–16. doi:10.1016/j.enconman.2017.05.080.
- [107] Miltner M, Makaruk A, Harasek M, Friedl A. Computational fluid dynamic simulation of a solid biomass combustor : modelling approaches. *Clean Technol Environ Policy* 2008;10:165–74. doi:10.1007/s10098-007-0137-0.
- [108] Bates RB, Ghoniem AF. Modeling kinetics-transport interactions during biomass torrefaction: The effects of temperature, particle size, and moisture content. *Fuel* 2014;137:216–29. doi:10.1016/J.FUEL.2014.07.047.
- [109] Li J, Paul MC, Younger PL, Watson I, Hossain M, Welch S. Prediction of high-temperature rapid combustion behaviour of woody biomass particles. *Fuel* 2016;165:205–14. doi:10.1016/j.fuel.2015.10.061.
- [110] Lu H, Robert W, Peirce G, Ripa B, Baxter LL. Comprehensive study of biomass particle combustion. *Energy and Fuels* 2008;22:2826–39. doi:10.1021/ef800006z.
- [111] Yang Y, Ryu C, Khor A, Yates N, Sharifi V, Swithenbank J. Effect of fuel properties on biomass combustion. Part II. Modelling approach—identification of the controlling factors. *Fuel* 2005;84:2116–30. doi:10.1016/j.fuel.2005.04.023.
- [112] Boriouchkine A, Zakharov A, Sirkka-liisa J. Dynamic modeling of combustion in a BioGrate furnace : The effect of operation parameters on biomass firing. *Chem Eng Sci* 2012;69:669–78. doi:10.1016/j.ces.2011.11.032.
- [113] Kurz D, Schnell U, Scheffknecht G. CFD simulation of wood chip combustion on a grate using an Euler-Euler approach. *Combust Theory Model* 2012;16:251–73. doi:10.1080/13647830.2011.610903.
- [114] Porteiro J, Granada E, Collazo J, Patino D, Moran JC. A model for the combustion of large particles of densified wood. *Energy and Fuels* 2007;21:3151–9. doi:10.1021/Ef0701891.
- [115] Simsek E, Brosch B, Wirtz S, Scherer V, Krüll F. Numerical simulation of grate firing systems using a coupled CFD/discrete element method (DEM). *Powder Technol* 2009;193:266–73. doi:10.1016/J.POWTEC.2009.03.011.
- [116] Mason PE, Darvell LI, Jones JM, Pourkashanian M, Williams A. Single particle flame-combustion studies on solid biomass fuels. *Fuel* 2015;151:21–30. doi:10.1016/j.fuel.2014.11.088.
- [117] Yang Y Bin, Newman R, Sharifi V, Swithenbank J, Ariss J. Mathematical modelling of straw combustion in a 38 MWe power plant furnace and effect of operating conditions. *Fuel* 2007;86:129–42. doi:10.1016/J.FUEL.2006.06.023.
- [118] Boriouchkine A, Sharifi V, Swithenbank J, Jämsä-jounela S. A study on the dynamic combustion behavior of a biomass fuel bed. *Fuel* 2014;135:468–81. doi:10.1016/j.fuel.2014.07.015.
- [119] Cereijo GN, Curto-risso P, Antonio W. Simplified model and simulation of biomass particle suspension combustion in one-dimensional flow applied to bagasse boilers. *Biomass and Bioenergy* 2017;99:38–48. doi:10.1016/j.biombioe.2017.01.030.
- [120] Karim MR, Naser J. Numerical modelling of biomass combustion: Solid conversion processes in a fixed bed furnace. *AIP Conf Proc* 2017;1851. doi:10.1063/1.4984658.
- [121] Peters B, Bruch C. A flexible and stable numerical method for simulating the thermal decomposition of wood particles. *Chemosphere* 2001;42:481–90. doi:10.1016/S0045-6535(00)00220-4.
- [122] Duffy NTM, Eaton JA. Investigation of factors affecting channelling in fixed-bed solid fuel combustion using CFD. *Combust Flame* 2013;160:2204–20. doi:10.1016/J.COMBUST FLAME.2013.04.015.

- [123] Zhang X, Chen Q, Bradford R, Shari V, Swithenbank J. Experimental investigation and mathematical modelling of wood combustion in a moving grate boiler. *Fuel Process Technol* 2010;91:1491–9. doi:10.1016/j.fuproc.2010.05.026.
- [124] Coker AK, Coker AK. Physical Properties of Liquids and Gases. *Ludwig's Appl Process Des Chem Petrochemical Plants* 2007;103–32. doi:10.1016/B978-075067766-0/50010-5.
- [125] Rezaei H, Sokhansanj S, Bi X, Lim CJ, Lau A. A numerical and experimental study on fast pyrolysis of single woody biomass particles. *Appl Energy* 2017;198:320–31. doi:10.1016/J.APENERGY.2016.11.032.
- [126] Ding Y, Wang C, Lu S. Modeling the pyrolysis of wet wood using FireFOAM. *Energy Convers Manag* 2015;98:500–6. doi:10.1016/J.ENCONMAN.2015.03.106.
- [127] Shafizadeh F, Chin PPS. *Wood Technology: Chemical Aspects*. *Wood Technol Chem Asp* 1977;43:57–81. doi:10.1021/bk-1977-0043.
- [128] Porteiro J, Collazo J, Patin D, Granada E, Moran JC. Numerical Modeling of a Biomass Pellet Domestic Boiler. *Energy and Fuels* 2009;23:1067–75.
- [129] Neves D, Thunman H, Matos A, Tarelho L, Gómez-Barea A. Characterization and prediction of biomass pyrolysis products. *Prog Energy Combust Sci* 2011;37:611–30. doi:10.1016/J.PECS.2011.01.001.
- [130] Karim MR, Naser J. Progress in numerical modelling of packed bed biomass combustion. *Proc. 19th Australas. Fluid Mech. Conf. AFMC* 2014, 2014.
- [131] Wagenaar BM, Prins W, van Swaaij WPM. Flash pyrolysis kinetics of pine wood. *Fuel Process Technol* 1993;36:291–8. doi:10.1016/0378-3820(93)90039-7.
- [132] Thurner F, Mann U. Kinetic Investigation of Wood Pyrolysis. *Ind Eng Chem Process Des Dev* 1981;20:482–8. doi:10.1021/i200014a015.
- [133] Shafizadeh F. *Pyrolytic Reactions and Products of Biomass BT - Fundamentals of Thermochemical Biomass Conversion*. In: Overend RP, Milne TA, Mudge LK, editors. *Fundam. Thermochem. Biomass Convers.*, Dordrecht: Springer Netherlands; 1985, p. 183–217. doi:10.1007/978-94-009-4932-4_11.
- [134] Chan W-CR, Kelbon M, Krieger BB. Modelling and experimental verification of physical and chemical processes during pyrolysis of a large biomass particle. *Fuel* 1985;64:1505–13. doi:10.1016/0016-2361(85)90364-3.
- [135] Di Blasi C. Heat, momentum and mass transport through a shrinking biomass particle exposed to thermal radiation. *Chem Eng Sci* 1996;51:1121–32. doi:10.1016/S0009-2509(96)80011-X.
- [136] Jones JM, Pourkashanian M, Williams A, Hainsworth D. A comprehensive biomass combustion model. *Renew Energy* 2000;19:229–34. doi:10.1016/S0960-1481(99)00036-1.
- [137] Di Blasi C. Combustion and gasification rates of lignocellulosic chars. *Prog Energy Combust Sci* 2009;35:121–40. doi:10.1016/J.PECS.2008.08.001.
- [138] Gómez-Barea A, Leckner B. Modeling of biomass gasification in fluidized bed. *Prog Energy Combust Sci* 2010;36:444–509. doi:10.1016/J.PECS.2009.12.002.
- [139] Laurendeau NM. Heterogeneous kinetics of coal char gasification and combustion. *Prog Energy Combust Sci* 1978;4:221–70. doi:10.1016/0360-1285(78)90008-4.
- [140] Yang YB, Lim CN, Goodfellow J, Sharifi VN, Swithenbank J. A diffusion model for particle mixing in a packed bed of burning solids. *Fuel* 2005;84:213–25. doi:10.1016/J.FUEL.2004.09.002.
- [141] Rajika JKAT, Narayana M. Modelling and simulation of wood chip combustion in a hot air generator system. *Springerplus* 2016;5:1166. doi:10.1186/s40064-016-2817-x.
- [142] Fatehi H, Bai XS, Fatehi H, Bai XS. A Comprehensive Mathematical Model for Biomass Combustion. *Combust Sci Technol* 2014;186:574–93. doi:10.1080/00102202.2014.883255.
- [143] Sankar G, Kumar DS, Balasubramanian KR. Computational modeling of pulverized coal fired boilers – A review on the current position. *Fuel* 2019;236:643–65. doi:10.1016/J.FUEL.2018.08.154.
- [144] Gómez MA, Porteiro J, de la Cuesta D, Patiño D, Míguez JL. Numerical simulation of the combustion process of a pellet-drop-feed boiler. *Fuel* 2016;184:987–99. doi:10.1016/J.FUEL.2015.11.082.
- [145] Karim MR, Bhuiyan AA, Sarhan AAR, Naser J. CFD simulation of biomass thermal conversion under air/oxy-fuel conditions in a reciprocating grate boiler. *Renew Energy* 2020;146:1416–28. doi:10.1016/j.renene.2019.07.068.
- [146] Cooper J, Hallett WLH. A numerical model for packed-bed combustion of char particles. *Chem Eng Sci* 2000;55:4451–60. doi:10.1016/S0009-2509(00)00097-X.
- [147] Li T, Ku X, Løvaås T. CFD Simulation of Devolatilization of Biomass with Shrinkage Effect. *Energy Procedia* 2017;105:505–10. doi:10.1016/j.egypro.2017.03.348.

- [148] Di Blasi C. On the influence of physical processes on the transient pyrolysis of cellulosic samples. *Int Symp Fire Safety Sci* 1994;229–40. doi:10.3801/IAFSS.FSS.4-229.
- [149] Blasi C Di. Physico-chemical processes occurring inside a degrading two-dimensional anisotropic porous medium. *Int J Heat Mass Transf* 1998;41:4139–50. doi:10.1016/S0017-9310(98)00142-2.
- [150] Grønli M. A theoretical and experimental study of the thermal degradation of biomass. The Norwegian University of Science and Technology, 1996.
- [151] Gronli MG, Melaaen MC. Mathematical model for wood pyrolysis-comparison of experimental measurements with model predictions. *Energy and Fuels* 2000;14:791–800. doi:10.1021/ef990176q.
- [152] Thunman H, Leckner B, Niklasson F, Johnsson F. Combustion of wood particles—a particle model for eulerian calculations. *Combust Flame* 2002;129:30–46. doi:10.1016/S0010-2180(01)00371-6.
- [153] Miljković B, Pešenjanski I, Vičević M. Mathematical modelling of straw combustion in a moving bed combustor: A two dimensional approach. *Fuel* 2013;104:351–64. doi:10.1016/J.FUEL.2012.08.017.
- [154] Hermansson S, Thunman H. CFD modelling of bed shrinkage and channelling in fixed-bed combustion. *Combust Flame* 2011;158:988–99. doi:10.1016/j.combustflame.2011.01.022.
- [155] Shen DK, Fang MX, Luo ZY, Cen K. Modeling pyrolysis of wet wood under external heat flux. *Fire Saf J* 2007;42:210–7. doi:10.1016/J.FIRESAF.2006.09.001.
- [156] de Souza Costa F, Sandberg D. Mathematical model of a smoldering log. *Combust Flame* 2004;139:227–38. doi:10.1016/J.COMBUSTFLAME.2004.07.009.
- [157] Mehrabian R, Zahirovic S, Scharler R, Obernberger I, Kleditzsch S, Wirtz S, et al. A CFD model for thermal conversion of thermally thick biomass particles. *Fuel Process Technol* 2012;95:96–108. doi:10.1016/J.FUPROC.2011.11.021.
- [158] Hermansson S, Thunman H. CFD modelling of bed shrinkage and channelling in fixed-bed combustion. *Combust Flame* 2011;158:988–99. doi:10.1016/J.COMBUSTFLAME.2011.01.022.
- [159] Ström H, Thunman H. CFD simulations of biofuel bed conversion: A submodel for the drying and devolatilization of thermally thick wood particles. *Combust Flame* 2013;160:417–31. doi:10.1016/J.COMBUSTFLAME.2012.10.005.
- [160] Galgano A, Di Blasi C, Ritondale S, Todisco A. Quantitative analysis of pseudoephedrine in formulation by potentiometric membrane sensor; computational investigation. *Fire Mater* 2014;38:639–58. doi:10.1002/fam.
- [161] Pozzobon V, Salvador S, Bézian JJ, El-Hafi M, Le Maout Y, Flamant G. Radiative pyrolysis of wet wood under intermediate heat flux: Experiments and modelling. *Fuel Process Technol* 2014;128:319–30. doi:10.1016/J.FUPROC.2014.07.007.
- [162] Saastamoinen J, Richard J. Drying, Pyrolysis and Combustion of Biomass Particles. In: *Conversion R in TB*, editor. *Fuel Process. Technol.*, vol. 87, Elsevier; 2006, p. 169–75. doi:10.1016/J.FUPROC.2005.08.012.
- [163] Mehrabian R, Zahirovic S, Scharler R, Obernberger I, Kleditzsch S, Wirtz S, et al. A CFD model for thermal conversion of thermally thick biomass particles. *Fuel Process Technol* 2012;95:96–108. doi:10.1016/j.fuproc.2011.11.021.
- [164] Mehrabian R, Scharler R, Obernberger I. Effects of pyrolysis conditions on the heating rate in biomass particles and applicability of TGA kinetic parameters in particle thermal conversion modelling. *Fuel* 2012;93:567–75. doi:10.1016/J.FUEL.2011.09.054.
- [165] Saastamoinen J, Richard J. Drying, Pyrolysis and Combustion of Biomass Particles. In: *Bridgwater A V, Kuester JL*, editors. *Res. Thermochem. Biomass Convers.*, Dordrecht: Springer Netherlands; 1988, p. 221–35. doi:10.1007/978-94-009-2737-7_18.
- [166] Buchmayr M, Gruber J, Hargassner M, Hochenuer C. A computationally inexpensive CFD approach for small-scale biomass burners equipped with enhanced air staging. *Energy Convers Manag* 2016;115:32–42. doi:10.1016/j.enconman.2016.02.038.
- [167] Yang YB, Goodfellow J, Nasserzadeh V, Swithenbank J. Study on the transient process of waste fuel incineration in a full-scale moving-bed furnace. *Combust Sci Technol* 2005;177:127–50. doi:10.1080/00102200590883796.
- [168] Yang YB, Ryu C, Goodfellow J, Sharifi VN, Swithenbank J. Modelling Waste Combustion in Grate Furnaces. *Process Saf Environ Prot* 2004;82:208–22. doi:10.1205/095758204323065975.
- [169] Haseli Y, Van Oijen JA, De Goey LPH. A simplified pyrolysis model of a biomass particle based on infinitesimally thin reaction front approximation. *Energy and Fuels* 2012;26:3230–43. doi:10.1021/ef3002235.
- [170] Galgano A, Di Blasi C, Horvat A, Sinai Y. Experimental validation of a coupled solid- and gas-phase model for combustion and gasification of wood logs. *Energy and Fuels* 2006;20:2223–32. doi:10.1021/ef060042u.
- [171] Galgano A, Di Blasi C. Coupling a CFD code with a solid-phase combustion model. *Prog Comput Fluid Dyn* 2006;6:287–302. doi:10.1504/PCFD.2006.010037.
- [172] Bruch C, Peters B, Nussbaumer T. Modelling wood combustion under fixed bed conditions ☆. *Fuel* 2003;82:729–38. doi:10.1016/S0016-

2361(02)00296-X.

- [173] Sabelstrom H. PhD Thesis, Aalborg, 2007. Aalborg University, 2007.
- [174] Mehrabian Bardar R. CFD Simulation of the Thermal Conversion of Solid Biomass in Packed Bed Furnaces by Ramin Mehrabian Bardar 2013.
- [175] Shiehnejadhesar A, Scharler R, Mehrabian R, Obernberger I. Development and validation of CFD models for gas phase reactions in biomass grate furnaces considering gas streak formation above the packed bed. *Fuel Process Technol* 2015;139:142–58. doi:10.1016/j.fuproc.2015.07.029.
- [176] Yang YB, Goh YR, Zakaria R, Nasserzadeh V, Swithenbank J. Mathematical modelling of MSW incineration on a travelling bed. *Waste Manag* 2002;22:369–80. doi:10.1016/S0956-053X(02)00019-3.
- [177] Bryden KM. Computational modeling of wood combustion 1998:xix, 206 leaves.
- [178] Porteiro J, Míguez JL, Granada E, Moran JC. Mathematical modelling of the combustion of a single wood particle. *Fuel Process Technol* 2006;87:169–75. doi:10.1016/J.FUPROC.2005.08.012.
- [179] Pyle DL, Zaror CA. Heat transfer and kinetics in the low temperature pyrolysis of solids. *Chem Eng Sci* 1984;39:147–58. doi:10.1016/0009-2509(84)80140-2.
- [180] Smith JM, Van Ness HC, Abbott MM. Introduction to chemical engineering thermodynamics. 7th ed. Boston: McGraw-Hill; 2005.
- [181] Hagge MJ, Bryden KM. Modeling the impact of shrinkage on the pyrolysis of dry biomass. *Chem Eng Sci* 2002;57:2811–23. doi:10.1016/S0009-2509(02)00167-7.
- [182] Harada T, Hata T, Ishihara S. Thermal constants of wood during the heating process measured with the laser flash method. *J Wood Sci* 1998;44:425–31. doi:10.1007/BF00833405.
- [183] Gupta M, Yang J, Roy C. Specific heat and thermal conductivity of softwood bark and softwood char particles☆. *Fuel* 2003;82:919–27. doi:10.1016/S0016-2361(02)00398-8.
- [184] Grieco E, Baldi G. Analysis and modelling of wood pyrolysis. *Chem Eng Sci* 2011;66:650–60. doi:10.1016/J.CES.2010.11.018.
- [185] Wakao N, Kaguei S. Heat and mass transfer in packed beds. Gordon and Breach Science Publishers; 1983.
- [186] Fjellerup J, Henriksen U, Jensen AD, Jensen PA, Glarborg P. Heat transfer in a fixed bed of straw char. *Energy and Fuels* 2003;17:1251–8. doi:10.1021/ef030036n.
- [187] Yagi S, Kunii D. Studies on Effective Thermal Conductivities in Packed Beds. *AIChE J* 1957;3:373–81.
- [188] Peeketi AR, Moscardini M, Vijayan A, Gan Y, Kamlah M, Annabattula RK. Effective thermal conductivity of a compacted pebble bed in a stagnant gaseous environment: An analytical approach together with DEM. *Fusion Eng Des* 2018;130:80–8. doi:10.1016/j.fusengdes.2018.02.088.
- [189] Simpson W, Ten Wolde A. Chapter 3 - Physical properties and moisture relations of wood. *Wood Handb Wood as an Eng Mater* 1999;3:1-3.24.
- [190] Gómez MA, Martín R, Chapela S, Porteiro J. Steady CFD combustion modeling for biomass boilers: An application to the study of the exhaust gas recirculation performance. *Energy Convers Manag* 2019;179:91–103. doi:10.1016/J.ENCONMAN.2018.10.052.
- [191] Duffy NTM, Eaton JA. Investigation of 3D flow and heat transfer in solid-fuel grate combustion: Measures to reduce high-temperature degradation. *Combust Flame* 2016;167:422–43. doi:10.1016/J.COMBUST FLAME.2015.12.032.
- [192] Silva J, Teixeira J, Teixeira S, Preziati S, Cassiano J. CFD Modeling of Combustion in Biomass Furnace. *Energy Procedia* 2017; 120:665–72. doi:10.1016/J.EGYPRO.2017.07.179.
- [193] Yin C, Rosendahl L, Clausen S, Hvid SL. Characterizing and modeling of an 88 MW grate-fired boiler burning wheat straw: Experience and lessons. *Energy* 2012;41:473–82. doi:10.1016/j.energy.2012.02.050.
- [194] Yin C, Rosendahl L, Kær SK, Clausen S, Hvid SL, Hiller T. Mathematical modeling and experimental study of biomass combustion in a thermal 108 MW grate-fired boiler. *Energy and Fuels* 2008;22:1380–90. doi:10.1021/ef700689r.
- [195] Collazo J, Porteiro J, Míguez JL, Granada E, Gómez MA. Numerical simulation of a small-scale biomass boiler. *Energy Convers Manag* 2012;64:87–96. doi:10.1016/J.ENCONMAN.2012.05.020.
- [196] Rezeau A, Diez LI, Royo J, Díaz-Ramírez M. Efficient diagnosis of grate-fired biomass boilers by a simplified CFD-based approach. *Fuel Process Technol* 2018;171:318–29. doi:10.1016/J.FUPROC.2017.11.024.
- [197] Zhou A, Xu H, Yang W, Tu Y, Xu M, Yu W, et al. Numerical Study of Biomass Grate Boiler with Coupled Time-Dependent Fuel Bed Model and Computational Fluid Dynamics Based Freeboard Model. *Energy & Fuels* 2018;32:9493–505. doi:10.1021/acs.energyfuels.8b01823.

- [198] Zhou A, Xu H, Tu Y, Zhao F, Zheng Z, Yang W. Numerical investigation of the effect of air supply and oxygen enrichment on the biomass combustion in the grate boiler. *Appl Therm Eng* 2019;156:550–61. doi:10.1016/J.APPLTHERMALENG.2019.04.053.
- [199] Tu Y, Zhou A, Xu M, Yang W, Siah KB, Prabakaran S. Experimental and numerical study on the combustion of a 32 MW wood-chip grate boiler with internal flue gas recirculation technology. *Energy Procedia* 2017;143:591–8. doi:10.1016/J.EGYPRO.2017.12.732.
- [200] Sun R, Ismail TM, Ren X, Abd El-Salam M. Numerical and experimental studies on effects of moisture content on combustion characteristics of simulated municipal solid wastes in a fixed bed. *Waste Manag* 2015;39:166–78. doi:10.1016/j.wasman.2015.02.018.
- [201] Silva J, Teixeira J, Teixeira S, Preziati S, Cassiano J. CFD Modeling of Combustion in Biomass Furnace. *Energy Procedia* 2017;120:665–72. doi:10.1016/j.egypro.2017.07.179.
- [202] Gómez MA, Comesaña R, Feijoo MA, Eguía P. Simulation of the effect of water temperature on domestic biomass boiler performance. *Energies* 2012;5:1044–61. doi:10.3390/en5041044.
- [203] Mätzing H, Gehrman H-J, Seifert H, Stapf D. Modelling grate combustion of biomass and low rank fuels with CFD application. *Waste Manag* 2018;78:686–97. doi:10.1016/J.WASMAN.2018.05.008.
- [204] Sharffi VN, Group FT. Optimization Study Of Incineration In A MSW Incinerator With A Vertical Radiation Shaft A Thesis. Thesis, Univ Sheff 1990.
- [205] Ryu C, Phan AN, Yang Y, Sharifi VN, Swithenbank J. Ignition and burning rates of segregated waste combustion in packed beds. *Waste Manag* 2007;27:802–10. doi:10.1016/J.WASMAN.2006.04.013.
- [206] Yang YB, Goh YR, Zakaria R, Nasserzadeh V, Swithenbank J. Mathematical modelling of MSW incineration on a travelling bed. *Waste Manag* 2002;22:369–80. doi:10.1016/S0956-053X(02)00019-3.
- [207] Erić A, Nemoda S, Komatina M, Dakić D, Repić B. Experimental investigation on the kinetics of biomass combustion in vertical tube reactor. *J Energy Inst* 2018. doi:10.1016/J.JOEI.2018.06.009.
- [208] Porteiro J, Patiño D, Collazo J, Granada E, Moran J, Miguez JL. Experimental analysis of the ignition front propagation of several biomass fuels in a fixed-bed combustor. *Fuel* 2010;89:26–35. doi:10.1016/J.FUEL.2009.01.024.
- [209] Markovic M, Bramer EA, Brem G. Experimental investigation of wood combustion in a fixed bed with hot air. *Waste Manag* 2014;34:49–62. doi:10.1016/J.WASMAN.2013.09.021.
- [210] Cepic Z, Nakomic-Smaragdakis B, Miljkovic B, Radovanović LZ, Djuric S. Combustion characteristics of wheat straw in a fixed bed. *Energy Sources, Part A Recover Util Environ Eff* 2016;38:1007–13. doi:10.1080/15567036.2014.922646.
- [211] Shan L, Kong M, Bennet TD, Sarroza AC, Eastwick C, Sun D, et al. Studies on combustion behaviours of single biomass particles using a visualization method. *Biomass and Bioenergy* 2018;109:54–60. doi:10.1016/J.BIOMBIOE.2017.12.008.
- [212] Razmjoo N. Characterization of conversion zones in a reciprocating grate furnace firing wet woody biomass. 2018.
- [213] Lamberg H, Sippula O, Tissari J, Jokiniemi J. Effects of air staging and load on fine-particle and gaseous emissions from a small-scale pellet boiler. *Energy and Fuels* 2011;25:4952–60. doi:10.1021/ef2010578.
- [214] Kær SK. Numerical modelling of a straw-fired grate boiler. *Fuel* 2004;83:1183–90. doi:10.1016/J.FUEL.2003.12.003.
- [215] El-Sayed SA, Khairy M. An Experimental Study of Combustion and Emissions of Wheat Straw Pellets in High-Temperature Air Flows. *Combust Sci Technol* 2018;190:222–51. doi:10.1080/00102202.2017.1381953.
- [216] Zhu Y, Yang W, Fan J, Kan T, Zhang W, Liu H, et al. Effect of sodium carboxymethyl cellulose addition on particulate matter emissions during biomass pellet combustion. *Appl Energy* 2018;230:925–34. doi:10.1016/J.APENERGY.2018.09.013.
- [217] Anca-Couce A, Sommersacher P, Evic N, Mehrabian R, Scharler R. Experiments and modelling of NO_x precursors release (NH₃ and HCN) in fixed-bed biomass combustion conditions. *Fuel* 2018;222:529–37. doi:10.1016/J.FUEL.2018.03.003.
- [218] Wang X, Hu Z, Adeosun A, Liu B, Ruan R, Li S, et al. Particulate matter emission and K/S/Cl transformation during biomass combustion in an entrained flow reactor. *J Energy Inst* 2018;91:835–44. doi:10.1016/J.JOEI.2017.10.005.
- [219] Striugas N, Sadeckas M, Paulauskas R. Investigation of K*, Na* and Ca* flame emission during single biomass particle combustion. *Combust Sci Technol* 2018;00:1–12. doi:10.1080/00102202.2018.1452408.
- [220] Yang W, Zhu Y, Cheng W, Sang H, Yang H, Chen H. Characteristics of Particulate Matter Emitted from Agricultural Biomass Combustion. *Energy and Fuels* 2017;31:7493–501. doi:10.1021/acs.energyfuels.7b00229.
- [221] Uusitalo L, Lehtikoinen A, Helle I, Myrberg K. An overview of methods to evaluate uncertainty of deterministic models in decision support. *Environ Model Softw* 2015;63:24–31. doi:10.1016/J.ENVSOFT.2014.09.017.
- [222] Jin X, Xu CY, Zhang Q, Singh VP. Parameter and modeling uncertainty simulated by GLUE and a formal Bayesian method for a conceptual hydrological model. *J Hydrol* 2010;383:147–55. doi:10.1016/j.jhydrol.2009.12.028.

- [223] Zhang D, Luh PB, Fan J, Gupta S. Chiller Plant Operation Optimization with Input and Model Uncertainties. *IEEE Int Conf Autom Sci Eng* 2018;2018-Augus:8–13. doi:10.1109/COASE.2018.8560368.
- [224] Regan HM, Colyvan M, Burgman MA. A taxonomy and treatment of uncertainty for ecology and conservation biology. *Ecol Appl* 2002;12:618–28. doi:10.1890/1051-0761(2002)012[0618:ATATOU]2.0.CO;2.
- [225] Culka M. Uncertainty analysis using Bayesian Model Averaging: a case study of input variables to energy models and inference to associated uncertainties of energy scenarios. *Energy Sustain Soc* 2016;6. doi:10.1186/s13705-016-0073-0.
- [226] Liu Z, Merwade V. Accounting for model structure, parameter and input forcing uncertainty in flood inundation modeling using Bayesian model averaging. *J Hydrol* 2018;565:138–49. doi:10.1016/J.JHYDROL.2018.08.009.
- [227] Yen H, Wang R, Feng Q, Young C-C, Chen S-T, Tseng W-H, et al. Input uncertainty on watershed modeling: Evaluation of precipitation and air temperature data by latent variables using SWAT. *Ecol Eng* 2018;122:16–26. doi:10.1016/J.ECOLENG.2018.07.014.
- [228] Zouaoui F, Wilson JR. Accounting for input-model and input-parameter uncertainties in simulation. *IIE Trans (Institute Ind Eng)* 2004;36:1135–51. doi:10.1080/07408170490500708.
- [229] Chick SE. Steps to implement Bayesian input distribution selection 2003:317–24. doi:10.1145/324138.324233.
- [230] Li C, Suzuki K. Process design and simulation of H₂-rich gases production from biomass pyrolysis process. *Bioresour Technol* 2010;101:S86–90. doi:10.1016/J.BIORTECH.2009.05.010.
- [231] Thunman H, Niklasson F, Johnsson F, Leckner B. Composition of volatile gases and thermochemical properties of wood for modeling of fixed or fluidized beds. *Energy and Fuels* 2001;15:1488–97. doi:10.1021/ef10097q.
- [232] Rath J, Wolfinger MG, Steiner G, Krammer G, Barontini F, Cozzani V. Heat of wood pyrolysis. *Fuel* 2003;82:81–91. doi:10.1016/S0016-2361(02)00138-2.
- [233] R. C. Roberts. *Molecular diffusion of gases* n.d.
- [234] Shiehnejadhesar A, Scharler R. Application of numerical modelling to biomass grate furnaces. *Therm Eng* 2015;1:550–6. doi:-.
- [235] Ragland KW, Bryden KM. *Combustion Engineering*. Taylor & Francis Group; 2011. doi:10.2307/3102126.
- [236] Mahmoudi AH. *Prediction of Heat-Up, Drying and Gasification of Fixed and Moving Beds By the Discrete Particle Method (Dpm)*. 2015.
- [237] Porteiro J, Patiño D, Collazo J, Granada E, Moran J, Miguez JL. Experimental analysis of the ignition front propagation of several biomass fuels in a fixed-bed combustor. *Fuel* 2010;89:26–35. doi:10.1016/J.FUEL.2009.01.024.
- [238] Hosseini Rahdar M, Nasiri F, Lee B. Effect of fuel composition uncertainty on grate firing biomass combustor performance: a Bayesian model averaging approach. *Biomass Convers Biorefinery* 2020;86. doi:10.1007/s13399-020-00774-2.
- [239] Houshfar E, Skreiber Ø, Løv T, Sørum L. Effect of Excess Air Ratio and Temperature on NO_x Emission from Grate Combustion of Biomass in the Staged Air Combustion Scenario. *Energy & Fuels* 2011:4643–54. doi:10.1021/ef200714d.
- [240] Wang K, Zhang Y, Sekelj G, Hopke PK. Economic analysis of a field monitored residential wood pellet boiler heating system in New York State. *Renew Energy* 2019;133:500–11. doi:10.1016/J.RENENE.2018.10.026.
- [241] Reza B, Soltani A, Ruparathna R, Sadiq R, Hewage K. Environmental and economic aspects of production and utilization of RDF as alternative fuel in cement plants: A case study of Metro Vancouver Waste Management. *Resour Conserv Recycl* 2013;81:105–14. doi:10.1016/J.RESCONREC.2013.10.009.
- [242] Nabavi V, Azizi M, Tarmian A, Ray CD. Feasibility study on the production and consumption of wood pellets in Iran to meet return-on-investment and greenhouse gas emissions targets. *Renew Energy* 2020;151:1–20. doi:10.1016/J.RENENE.2019.10.140.
- [243] Pradhan P, Gadkari P, Arora A, Mahajani SM. Economic feasibility of agro waste pelletization as an energy option in rural India. *Energy Procedia* 2019;158:3405–10. doi:10.1016/J.EGYPRO.2019.01.936.
- [244] Residential Electricity Rates and Consumption in New York. www.ElectricityLocalCom/States/New-York/ 2020.
- [245] Zhang K, Jiang X. An investigation of fuel variability effect on bio-syngas combustion using uncertainty quantification. *Fuel* 2018;220:283–95. doi:10.1016/J.FUEL.2018.02.007.
- [246] Bouloré A. Importance of uncertainty quantification in nuclear fuel behaviour modelling and simulation. *Nucl Eng Des* 2019;355:110311. doi:10.1016/J.NUCENGDDES.2019.110311.
- [247] Hosseini Rahdar M, Lee B, Nasiri F. Uncertainty Quantification of Biomass Composition Variability Effect on Moving-Grate Bed Combustion : An Experiment-Based Approach. *Energy & Fuels* 2020;34:9697–708. doi:10.1021/acs.energyfuels.0c01557.
- [248] Duffy NTM, Eaton JA. Investigation of factors affecting channelling in fixed-bed solid fuel combustion using CFD. *Combust Flame* 2013;160:2204–20. doi:10.1016/j.combustflame.2013.04.015.

- [249] He F, Behrendt F. A new method for simulating the combustion of a large biomass particle—A combination of a volume reaction model and front reaction approximation. *Combust Flame* 2011;158:2500–11. doi:<https://doi.org/10.1016/j.combustflame.2011.04.016>.
- [250] Brink A, Kilpinen P, Hupa M. A simplified kinetic rate expression for describing the oxidation of volatile fuel-N in biomass combustion. *Energy and Fuels* 2001;15:1094–9. doi:10.1021/ef0002748.
- [251] Liu H, Gibbs BM. Modeling NH₃ and HCN emissions from biomass circulating fluidized bed gasifiers. *Fuel* 2003;82:1591–604. doi:10.1016/S0016-2361(03)00091-7.
- [252] Hosseini Rahdar M, Nasiri F, Lee B. Availability-based predictive maintenance scheduling for vibrating-grate biomass boilers. *Saf Reliab* 2020;39:165–87. doi:10.1080/09617353.2020.1759261.
- [253] Benetto E, Popovici EC, Rousseaux P, Blondin J. Life cycle assessment of fossil CO₂ emissions reduction scenarios in coal-biomass based electricity production. *Energy Convers Manag* 2004;45:3053–74. doi:10.1016/j.enconman.2003.12.015.
- [254] Martinetti A, Braaksma AJJ, van Dongen LAM. Beyond RAMS Design: Towards an Integral Asset and Process Approach. In L. Redding, R. Roy, & A. Shaw (Eds.), *Advances in Through-life Engineering Services*. (Decision Eng. Springer, 2017, p. 417–28. doi:https://doi.org/10.1007/978-3-319-49938-3_25.
- [255] Tinga T. *Principles of loads and failure mechanisms; Applications in maintenance, reliability and design*. 2013.
- [256] Ramakumar R. *Engineering Reliability: Fundamentals and Applications*. 1st ed. Pearson; 1992.
- [257] Smith RL. Weibull regression models for reliability data. *Reliab Eng Syst Saf* 1991;34:55–76. doi:10.1016/0951-8320(91)90099-S.

APPENDIX I

Table 36. Components characteristics regarding failure distribution and maintenance time

Components	Failure rate (per 10 ⁶ hr)	Weibull distribution		MTTR+S (hr)	Components	Failure rate (per 10 ⁶ hr)	Weibull distribution		MTTR+S (hr)
		α	β				α	β	
<i>O2 Sensor</i>	10	85305	1.1239	171	<i>Pres Sensor</i>	5.8	96546	1.5722	26
<i>Coupling</i>	1.907	93212	1.5181	74	<i>VFD</i>	1.2	145140	1.5186	75
<i>Belt</i>	23.719	42075	1.0134	49	<i>Manual Switch</i>	0.46	150960	1.5799	25
<i>Level Switch</i>	0.273	152430	1.5962	74	<i>Flex joint</i>	14.2	57917	1.1455	174
<i>Water Storage Tank</i>	0.074	153990	1.6142	348	<i>Relay</i>	0.3	152210	1.5939	24.25
<i>Temp Switch</i>	0.228	152780	1.6002	78	<i>Bearing</i>	7.99	96638	1.1746	78
<i>Speed Switch</i>	0.48	150800	1.5781	25	<i>Piping</i>	0.03	154340	1.618	76
<i>Rotary Valve</i>	9.26	89291	1.1407	342	<i>Transformer</i>	2.5	91290	1.4889	76
<i>Relief Valve</i>	3.84	124830	1.3443	76	<i>Circuit Breaker</i>	0.2	152990	1.6027	25
<i>Temp Transmitter</i>	0.437	151140	1.5819	26	<i>Pipe Fitting</i>	3.26	129190	1.3774	52
<i>Pulley</i>	12.609	72931	1.0787	74	<i>Gearbox</i>	5	83312	1.3815	339
<i>Flowmeter</i>	3.26	129190	1.3774	76	<i>PLC</i>	5	116370	1.286	88
<i>Fan</i>	2.5	91290	1.4889	339	<i>Pump</i>	20.52	45370	1.0728	78
<i>ID Fan</i>	2.5	91290	1.4889	726	<i>Soot Blower</i>	42	34060	1.1722	171
<i>Pres Transmitter</i>	0.414	151320	1.5839	26	<i>Wiring</i>	0.627	149650	1.5656	50
<i>Mixing Valve</i>	10.06	84995	1.1227	76	<i>Motor</i>	28.44	34559	1.0315	340
<i>Temp Sensor</i>	4.57	119460	1.3065	26	<i>Electric</i>	0.145	153420	1.6075	25

APPENDIX II

FDM-based solution code for combustion model:

Finite difference method (FDM) was utilized to approximate the governing equations using the implicit technique for solving the set of equations which provides model stability regardless of the value of time step. The average parameter method was introduced to identify the unknown parameters after a specified time interval. All mass, momentum and energy equations are formulated as a function of the average mass, velocity and temperature within each cell. In this appendix, the mass, momentum and energy balance equations for the heat and mass transfer media of a complete system are presented and solved referring to the system in Section 4.2.

1- Mass equation

$$\frac{\phi(\rho_i^{t+1} - \rho_i^t)}{\Delta t} + \frac{\phi v_i (\rho_{i+1}^{t+1} - \rho_{i-1}^{t+1})}{2\Delta x} = S_{total}$$

$$\rho_i^{t+1} + \frac{v_i \Delta t}{2\Delta x} (\rho_{i+1}^{t+1} - \rho_{i-1}^{t+1}) = \rho_i^t + \frac{S_{total} \Delta t}{\phi}; \quad \alpha = \frac{v_i \Delta t}{2\Delta x}, S = \frac{S_{total} \Delta t}{\phi}$$

$$\begin{bmatrix} 1 & 2\alpha & 0 & \dots & 0 \\ -\alpha & 1 & \alpha & \ddots & \vdots \\ 0 & \ddots & \ddots & \ddots & 0 \\ \vdots & \ddots & -\alpha & 1 & \alpha \\ 0 & \dots & 0 & -2\alpha & 1 \end{bmatrix} \begin{bmatrix} \rho_0^{t+1} \\ \rho_1^{t+1} \\ \vdots \\ \rho_{n-1}^{t+1} \end{bmatrix} = \begin{bmatrix} \rho_0^t \\ \rho_1^t \\ \vdots \\ \rho_{n-1}^t \end{bmatrix} + \begin{bmatrix} S_0 \\ S_1 \\ \vdots \\ S_{n-1} \end{bmatrix}$$

2- Momentum equation

$$\frac{(v_i^{t+1} - v_i^t)\phi}{\Delta t} + \frac{(v_{i+1}^{t+1} - v_{i-1}^{t+1})\phi v_i}{\Delta x} = -\frac{P_i - P_{i-1}}{\rho_g \Delta x}$$

$$v_i^{t+1} + \frac{v_i \Delta t}{\Delta x} (v_{i+1}^{t+1} - v_{i-1}^{t+1}) = v_i^t - \frac{(P_i - P_{i-1})\Delta t}{\phi \rho_g \Delta x}; \quad \alpha = \frac{v_i \Delta t}{\Delta x}, S = \frac{-(P_i - P_{i-1})\Delta t}{\phi \rho_g \Delta x}$$

$$\begin{bmatrix} 1 & 2\alpha & 0 & \dots & 0 \\ -\alpha & 1 & \alpha & \ddots & \vdots \\ 0 & \ddots & \ddots & \ddots & 0 \\ \vdots & \ddots & -\alpha & 1 & \alpha \\ 0 & \dots & 0 & -2\alpha & 1 \end{bmatrix} \begin{bmatrix} v_0^{t+1} \\ v_1^{t+1} \\ \vdots \\ v_{n-1}^{t+1} \end{bmatrix} = \begin{bmatrix} v_0^t \\ v_1^t \\ \vdots \\ v_{n-1}^t \end{bmatrix} + \begin{bmatrix} S_0 \\ S_1 \\ \vdots \\ S_{n-1} \end{bmatrix}$$

3- Energy equation

Gas phase

$$\frac{(T_i^{t+1} - T_i^t)}{\Delta t} + \frac{v_i (T_{i+1}^{t+1} - T_i^{t+1})}{\Delta x} = \frac{\lambda_g (T_{i+1}^{t+1} - 2T_i^{t+1} + T_{i-1}^{t+1})}{\phi c_{p,i} \rho_i \Delta x^2} + \frac{hS(T_s - T_g) + S_i}{\phi c_{p,i} \rho_i}$$

$$\left(-\frac{\lambda_g \Delta t}{\phi c_{p,i} \rho_i \Delta x^2}\right)T_{i-1}^{t+1} + \left(1 - \frac{v_i \Delta t}{\Delta x} + \frac{2 \lambda_g \Delta t}{\phi c_{p,i} \rho_i \Delta x^2}\right)T_i^{t+1} + \left(\frac{v_i \Delta t}{\Delta x} - \frac{\lambda_g \Delta t}{\phi c_{p,i} \rho_i \Delta x^2}\right)T_{i+1}^{t+1} = T_i^t + \frac{hS(T_s - T_g) + S_i}{\phi c_{p,i} \rho_i} \Delta t$$

$$F = \frac{\lambda_g \Delta t}{\phi c_{p,i} \rho_i \Delta x^2}, L = \frac{v_i \Delta t}{\Delta x}, S = \frac{hS(T_s - T_g) + S_i}{\phi c_{p,i} \rho_i} \Delta t$$

$$\begin{bmatrix} 1-L+2F & 2(L-F) & 0 & 0 & \dots & \dots & 0 \\ -F & 1-L+2F & L-F & 0 & \ddots & 0 & 0 \\ 0 & -F & \ddots & \ddots & \ddots & \ddots & \vdots \\ \vdots & 0 & \ddots & \ddots & \ddots & \ddots & 0 \\ \vdots & \ddots & 0 & \ddots & \ddots & \ddots & 0 \\ 0 & 0 & \ddots & 0 & -F & \ddots & L-F \\ 0 & 0 & 0 & 0 & 0 & -2F & 1-L+2F \end{bmatrix} \begin{bmatrix} T_0^{t+1} \\ T_1^{t+1} \\ T_2^{t+1} \\ \vdots \\ \vdots \\ T_{n-1}^{t+1} \end{bmatrix} = \begin{bmatrix} T_0^t \\ T_1^t \\ T_2^t \\ \vdots \\ \vdots \\ T_{n-1}^t \end{bmatrix} + \begin{bmatrix} S_0^{t+1} \\ S_1^{t+1} \\ S_2^{t+1} \\ \vdots \\ \vdots \\ S_{n-1}^{t+1} \end{bmatrix}$$

Solid phase

$$\frac{(T_i^{t+1} - T_i^t)}{\Delta t} = \frac{\lambda_{eff} (T_{i+1}^{t+1} - 2T_i^{t+1} + T_{i-1}^{t+1})}{(1-\phi)\rho_i c_{p,i} \Delta x^2} + \frac{(hS(T_g - T_s) + S_s + S_{rad})}{(1-\phi)\rho_i c_{p,i}}$$

$$\left(-\frac{\lambda_{eff} \Delta t}{(1-\phi)c_{p,i} \rho_i \Delta x^2}\right)T_{i-1}^{t+1} + \left(1 + \frac{2 \lambda_{eff} \Delta t}{(1-\phi)c_{p,i} \rho_i \Delta x^2}\right)T_i^{t+1} + \left(-\frac{\lambda_{eff} \Delta t}{(1-\phi)c_{p,i} \rho_i \Delta x^2}\right)T_{i+1}^{t+1} = T_i^t + \frac{(hS(T_g - T_s) + S_s + S_{rad})}{(1-\phi)\rho_i c_{p,i}} \Delta t ;$$

$$F = \frac{\lambda_{eff} \Delta t}{(1-\phi)c_{p,i} \rho_i \Delta x^2}, S = \frac{(hS(T_g - T_s) + S_s + S_{rad})}{(1-\phi)\rho_i c_{p,i}} \Delta t$$

$$\begin{bmatrix} 1+2F & -2F & 0 & 0 & \dots & \dots & 0 \\ -F & 1+2F & -F & 0 & \ddots & 0 & 0 \\ 0 & -F & 1+2F & \ddots & \ddots & \ddots & \vdots \\ \vdots & 0 & \ddots & \ddots & \ddots & \ddots & 0 \\ \vdots & \ddots & 0 & \ddots & \ddots & -F & 0 \\ 0 & 0 & \ddots & 0 & -F & 1+2F & -F \\ 0 & 0 & 0 & 0 & 0 & -2F & 1+2F \end{bmatrix} \begin{bmatrix} T_0^{t+1} \\ T_1^{t+1} \\ T_2^{t+1} \\ \vdots \\ \vdots \\ T_{n-1}^{t+1} \end{bmatrix} = \begin{bmatrix} T_0^t \\ T_1^t \\ T_2^t \\ \vdots \\ \vdots \\ T_{n-1}^t \end{bmatrix} + \begin{bmatrix} S_0^{t+1} \\ S_1^{t+1} \\ S_2^{t+1} \\ \vdots \\ \vdots \\ S_{n-1}^{t+1} \end{bmatrix}$$